FINAL REPORT

FHWA-WY-15/04F

State of Wyoming
Department of Transportation

U.S. Department of Transportation
Federal Highway Administration

EVALUATING THE RISK OF ALKALI-SILICA REACTION IN WYOMING: CONTINUED EVALUATION OF FIELD SPECIMENS AND PROPOSED MITIGATION STRATIGIES

By:

Department of Civil and Architectural Engineering
University of Wyoming
1000 East University Avenue, Dept. 3295
Laramie, WY 82071

September 2015

Notice

This document is disseminated under the sponsorship of the U.S. Department of Transportation in the interest of information exchange. The U.S. Government assumes no liability for the use of the information contained in this document.

The contents of this report reflect the views of the author(s) who are responsible for the facts and accuracy of the data presented herein. The contents do not necessarily reflect the official views or policies of the Wyoming Department of Transportation or the Federal Highway Administration. This report does not constitute a standard, specification, or regulation.

The United States Government and the State of Wyoming do not endorse products or manufacturers. Trademarks or manufacturers' names appear in this report only because they are considered essential to the objectives of the document.

Quality Assurance Statement

The Federal Highway Administration (FHWA) provides high-quality information to serve Government, industry, and the public in a manner that promotes public understanding. Standards and policies are used to ensure and maximize the quality, objectivity, utility, and integrity of its information. FHWA periodically reviews quality issues and adjusts its programs and processes to ensure continuous quality improvement.

Technical Report Documentation Page

Report No.	Government Accession No.	Recipients Catalog No.
FHWA-WY-15/04F		

Title and Subtitle Evaluating the Risk of Alkali-Silica Reaction in Wyoming: Continued Evaluation of Field Specimens and Proposed Mitigation Strategies	Report Date September 2015 Performing Organization Code
Author(s) Margaret Kimble, Ryan Fertig, Darby Hacker, Jennifer Eisenhauer Tanner	Performing Organization Report No.
Performing Organization Name and Address Department of Civil and Architectural Engineering University of Wyoming, Dept 3295 Laramie, WY 82071-3295	Work Unit No. Contact or Grant No. RSO6212
Sponsoring Agency Name and Address Wyoming Department of Transportation 5300 Bishop Blvd. Cheyenne, WY 82009-3340 WYDOT Research Center (307) 777-4182	Type of Report and Period Covered Final Report Sept. 2013 – August 2015 Sponsoring Agency Code

Supplementary Notes
WYDOT Project Manager: Bob Rothwell, Assistant State Materials Engineer

Abstract

A comprehensive study was performed to evaluate the ASR reactivity of eight Wyoming aggregates. State-of-the-art and standardized test methods were performed and results were used to classify these aggregate sources. Of the eight aggregates: one is highly reactive; one is moderately/highly reactive, three are moderately reactive; one is potentially reactive and two are nonreactive. The Concrete Prism Test (CPT) and unboosted large scale field blocks provided the most accurate data.

Key Words	Distribution Statement
Wyoming, Alkali-silica reaction, concrete, durability, aggregate, expansion	Unlimited

Security Classif. (of this report)	Security Classif. (of this page)	No. of Pages	Price
Unclassified	Unclassified	211	

Form DOT F 1700.7 (8-72) Reproduction of form and completed page is authorized.

SI* (Modern Metric) Conversion Factors

Approximate Conversions from SI Units

Symbol	When You Know	Multiply By	To Find	Symbol
Length				
mm	millimeters	0.039	inches	in
m	meters	3.28	feet	ft
km	kilometers	0.621	miles	mi
Area				
mm^2	square millimeters	0.0016	square inches	in^2
m^2	square meters	10.764	square feet	ft^2
km^2	square kilometers	0.386	square miles	mi^2
Volume				
ml	milliliters	0.034	fluid ounces	fl oz
l	liters	0.264	gallons	gal
m^3	cubic meters	35.71	cubic feet	ft^3
m^3	cubic meters	1.307	cubic yards	yd^3
Mass				
g	grams	0.035	ounces	oz
kg	kilograms	2.202	pounds	lb
Temperature (exact)				
°C	Centigrade temperature	1.8 C + 32	Fahrenheit temperature	°F
Force and Pressure or Stress				
N	newtons	0.225	poundforce	lbf
kPa	kilopascals	0.145	pound-force per square inch	psi

Approximate Conversions to SI Units

Symbol	When You Know	Multiply By	To Find	Symbol
Length				
in	inches	25.4	millimeters	Mm
ft	feet	0.305	meters	M
mi	miles	1.61	kilometers	Km
Area				
in^2	square inches	645.2	square millimeters	mm^2
ft^2	square feet	0.093	square meters	m^2
mi^2	square miles	2.59	square kilometers	km^2
Volume				
fl oz	fluid ounces	29.57	milliliters	Ml
gal	gallons	3.785	liters	L
ft^3	cubic feet	0.028	cubic meters	m^3
yd^3	cubic yards	0.765	cubic meters	m^3
Mass				
oz	ounces	28.35	grams	G
lb	pounds	0.454	kilograms	Kg
Temperature (exact)				
°F	Fahrenheit temperature	5(F-32)/9 or (F-32)/1.8	Celsius temperature	°C
Force and Pressure or Stress				
lbf	pound-force	4.45	newtons	N
psi	pound-force per square inch	6.89	kilopascals	kPa

Executive Summary

Alkali-silica reactivity (ASR) is a global concrete durability problem that continues to plague concrete around Wyoming. Currently WYDOT evaluates ASR potential in aggregates using the Accelerated Mortar Bar Test (AMBT) before using them in new concrete. Although, this test is appealing because of its relatively short duration (16 days), it is a harsh test that produces both false positives and negatives. Eight aggregate sources were selected for evaluation, the results of which are included in report. Tested aggregates include: Black Rock; Devries Farm; Harris Pit; Goton Pit; Knife River; Labarge; Lamax; and Worland. Researchers classified each aggregate on the basis of both standardized and state-of-the art methods including: the Concrete Prism Test (CPT); the Accelerated Mortar Bar Test (AMBT); the Autoclaved Concrete Prism Test (ACPT); petrography; and real-time field exposure. Despite the one-year time frame to complete CPTs of standard aggregates, it is still considered the best accelerated test method because it correlates best with field performance.

A large scale, outdoor exposure, real-time field site was developed at the Civil and Architectural Engineering Research Facility. A total of 28 blocks measuring 380 x 380 x 660 mm (15 x 15 x 26 in.) specimens were built in order to measure expansions over a period of 10 years. Results from the first 5.5 years of exposure are presented in this report. Petrography was conducted on some of the field specimens to determine reactivity. While ASR exudations were found, the reaction had not progressed to the formation of microcracking or gel deposits.

All eight aggregates are classified based on the CPT and field expansions. The Knife River source is highly reactive and this is validated by observations around the state of Wyoming. Goton Pit is moderately/highly reactive. Black Rock, Lamax, and Worland sources are classified as moderately reactive. Labarge aggregate is potentially reactive. Harris Pit and Devries Farm aggregates are nonreactive. Continued testing of field exposure specimens will be conducted at the University of Wyoming (UW).

Additional testing was conducted to evaluate the effectiveness of the 25% Class F fly ash replacement baseline treatment for aggregate reactivity. This mitigation program, using the Mitigated Accelerated Mortar Bar Test (MAMBT) and Mitigated Concrete Prism Test (MCPT), was found to be effective for the eight aggregates tested.

Table of Contents

List of Tables

List of Figures

1 Introduction

Discovered in the 1940s, alkali-silica reaction (ASR) causes expansion in concrete. If unmitigated, ASR may cause premature deterioration. Since its discovery, researchers have sought an economic and rapid method for detecting the potential and presence of ASR. Though numerous methods have been developed, a rapid and accurate method to determine aggregate reactivity remains elusive.

Industry continues to seek a quick method to classify and an economic way to work with reactive aggregates. Although, the addition of lithium mitigates reactive aggregates in new concrete; its cost prohibits general use. Another alternative is to use pozzolans, such as fly ash, in new construction. As appropriate fly ash becomes more difficult to procure and more expensive, engineering fixes to mitigate ASR become more important.

1.1 Introduction to Wyoming Department of Transportation (WYDOT) Project

WYDOT funded this project to classify the ASR reactivity of eight Wyoming aggregate sources. Most of the aggregate sources center around the Big Horn Basin area with one aggregate source tested from Cheyenne and one from Rock Springs. Locations and names of the aggregate sources are shown in Figure 1 and Table 1. Black Rock aggregate was initially received as two separate shipments of Big Horn Cody (BHC) and Big Horn Powell (BHP), these aggregates were later confirmed to have originated at the single source now called Black Rock.

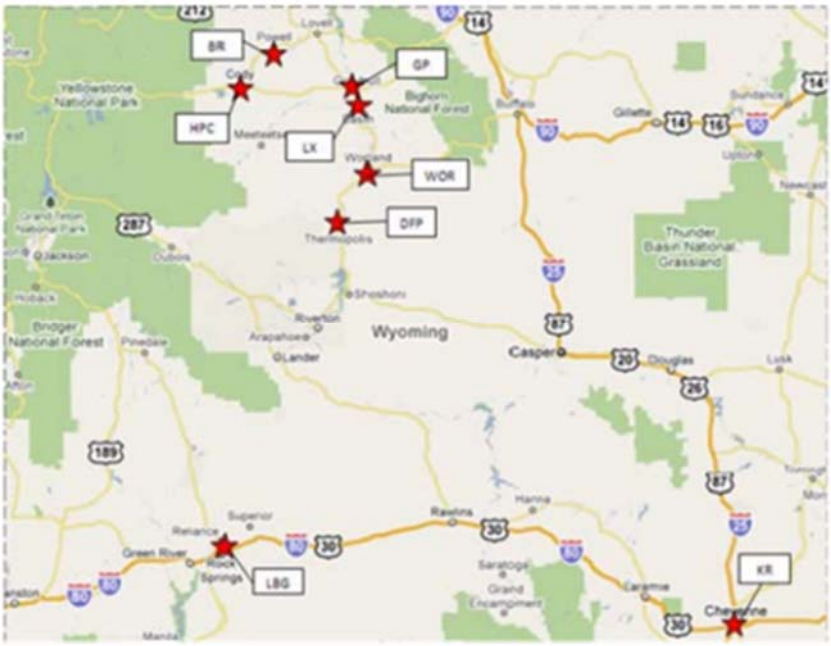

Figure 1. Wyoming map showing the location of each aggregate source.

Table 1. Aggregate abbreviations and locations.

Aggregate Name	Abbreviation	Location
Black Rock	BR	Powell, WY
Devries Farm	DFP	Thermopolis, WY
Goton Pit	GP	Greybull, WY
Harris Pit	HP	Cody, WY
Knife River	KR	Cheyenne, WY
Labarge	LBG	Rock Springs, WY
Lamax	LX	Basin, WY
Worland	WOR	Worland, WY

This research builds on work by Fertig (2010) and Jones (2011) to produce a final classification and mitigation strategy. The testing methods include the commonly used Accelerated Mortar Bar Test (AMBT) and Concrete Prism Test (CPT). Less commonly used tests include the evaluation

of both unboosted and boosted field specimens. Boosted specimens have an increased alkali content to encourage reaction, compared to concrete field blocks where all alkalis are supplied by the cement. Experimental work was conducted using the recently proposed Autoclaved Concrete Prism Test (ACPT).

The second portion of this research is the evaluation of ASR mitigation through the replacement of cement with low calcium oxide (CaO) fly ash. As appropriate fly ash sources and other mitigating agents become harder to acquire or more expensive, it has become even more important to correctly identify an aggregate's ASR potential. Adding mitigating agents when they are not needed adds considerable cost to a construction project and uses valuable resources that could mitigate more reactive aggregates. Reactive or potentially reactive aggregates were further tested with a 25 percent fly ash replacement using the Mitigated Concrete Prism (MCPT) and Mitigated Accelerated Mortar Bar (MAMBT) tests.

1.2 Report Overview

This report presents the research results for both classification testing and mitigation program evaluation. 2 provides a background of the alkali-silica reaction (ASR). Chapters 3 and 4 discuss the history of standard testing methods and findings of note by other investigators. These chapters also lay out testing methods and procedures for the classification of aggregate reactivity and the evaluation of mitigation programs. Chapter 5 discusses the materials and equipment used in this research. Test results are presented in Chapters 0 and 7. Conclusions and future work are detailed in Chapter 8.

2 Alkali-Silica Reactivity

Alkali-silica reaction (ASR) was first recognized as a concrete durability problem in California by the engineer Thomas Stanton in 1940. Since this time, ASR has been identified in countries all over the world. Stanton recognized that the reaction was dependent on several factors including the type of aggregate, type of cement, and the environmental exposure conditions. Common reactive mineral types were found to include: opal, chalcedony, cristobalite, tridymite, and cryptocrystalline quartz (Hobbs 1988). Industry's need for a rapid test for the evaluation of cement-aggregate combinations became apparent. This need for a rapid test has resulted in numerous testing methods being developed. Several existing reactivity tests are reviewed in Chapter 3.

2.1 Mechanism of Reaction

Although ASR has been tested since the 1940s, many aspects of the reaction mechanism are not well understood. While there are two schools of thought as to the progression of the ASR, both mechanisms can only proceed when three ingredients are present in the concrete:

- Reactive aggregate.
- Sufficient alkalis.
- Sufficient moisture.

The two proposed mechanisms of reaction vary slightly in the manner in which pressure and cracking develop within the concrete. The first and historically-accepted method involves the two-step development of alkali-silica gel from the pore solution (Stanton 1940); while the second involves the formation of two gel products and the growth of calcium rims around the aggregate.

In the first step of the mechanism proposed by Stanton, alkali hydroxides in the concrete pore solution react with the free silica in the aggregate, producing an alkali-silica gel product. This gel readily absorbs water, leading to expansion and cracking of the concrete. Cracking exposes new surfaces, continuing the iterative damage process as shown in Figure 2.

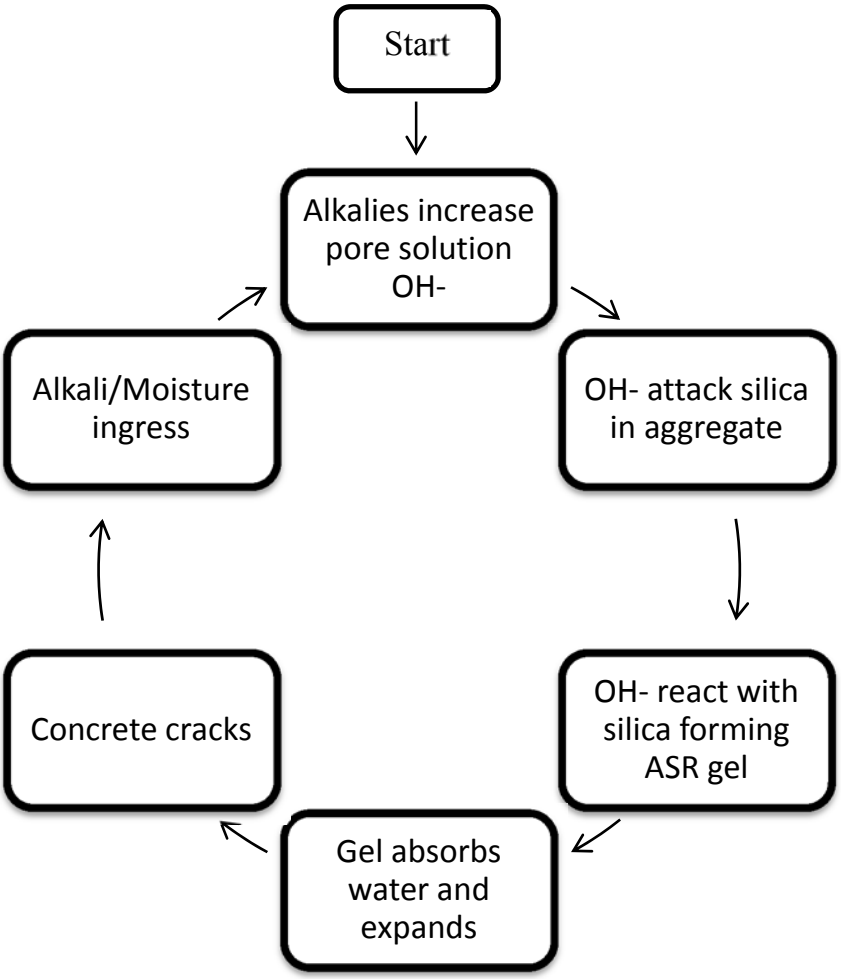

Figure 2. Schematic of reaction.

While the first mechanism suggests that deterioration is caused by the hydration of pore solution gel, Ichikawa and others proposed an alternate theory in which restrained gel causes an increase

in pressure (Aiqin et al. 1999; Bleszynski and Thomas 1998; Helmuth et al. 1993; Ichikawa 2009; Mindess et al. 2003). The reaction begins as alkali hydroxides attack the reactive aggregates, producing two layers of gel: a layer of mature alkali silicate around a layer of immature alkali silicate gel. The difference in the maturity of the gels relates to the degree of gel hydration. Part of the mature portion of the gel is extruded and dissolved in the pore solution. Consumption of hydroxide (OH^-) ions by reaction increases the calcium (Ca^{2+}) content of the pore solution which preferentially reacts with mature alkali silicate reducing permeability. This semi-permeable barrier allows the penetration of alkali hydroxide and water into the aggregate but prevents the extrusion of silicate gel due to osmotic cell pressure theory (Hobbs 1988). Expansive gel trapped within this barrier builds pressure between the aggregate and reaction rim. When the stress exceeds the tensile strength of the aggregate, a crack initiates in this aggregate. The multi-phase gel reaction cycle is shown in Figure 3. Forces produced have been measured to be twice that necessary to crack concrete. Representative cracks are shown in Figure 4. This model takes into account the role of calcium in the reaction series making this a more complete method of analyzing the reaction chemistry.

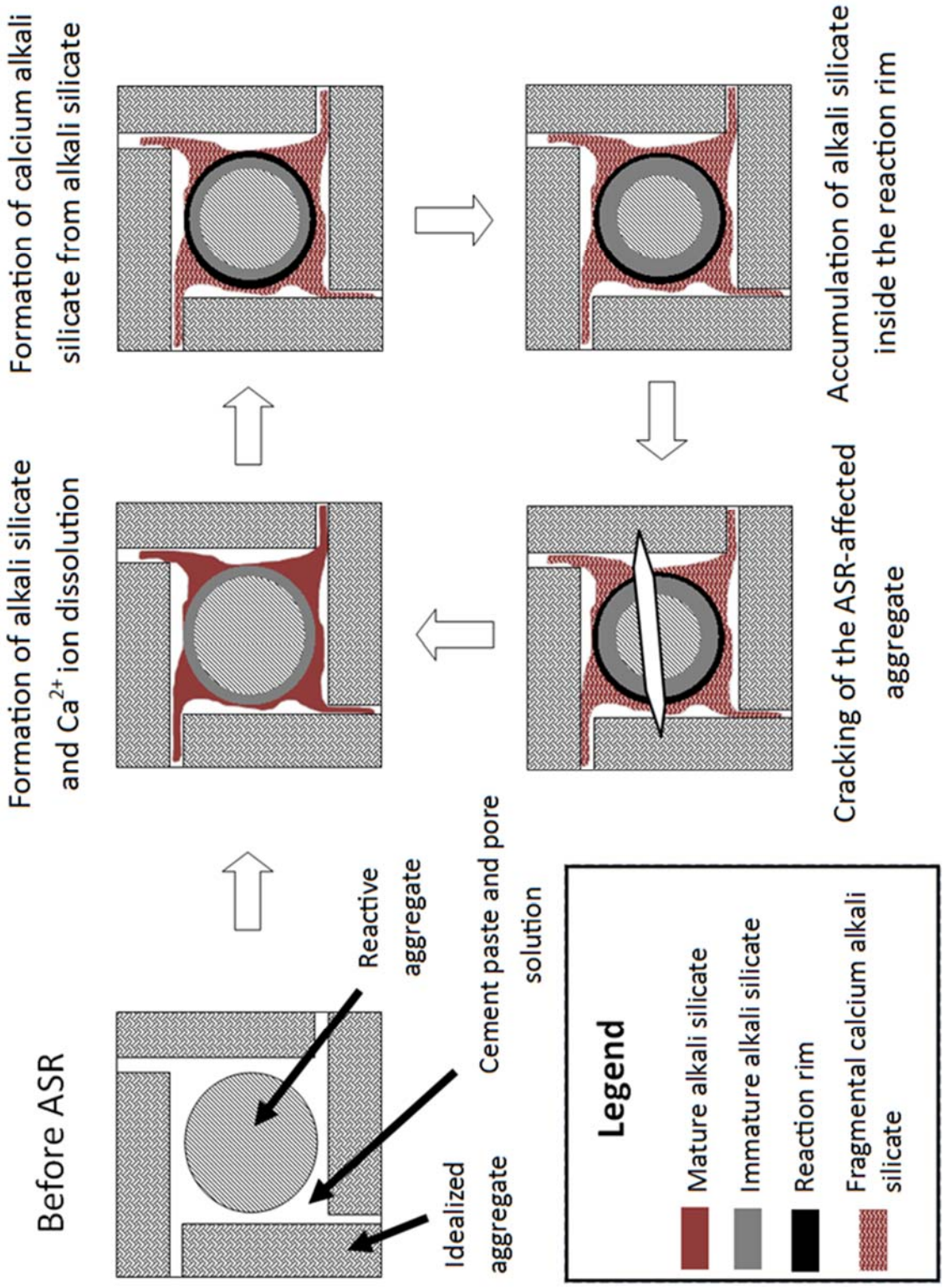

Figure 3. Schematic of alternate reaction. Modified from Ichakawa 2009.

Figure 4. Reflected light photomicrographs of polished surfaces exhibiting gel in microcracks (red arrows) on C1260 mortar bar. (Rothstein 2011).

As cracks develop, the interior of the concrete opens and receives additional water and chemicals that will continue the cycle of reaction. This cracking also exposes the concrete to other deteriorating mechanisms, including freeze-thaw.

Another issue that complicates ASR research is the pessimum effect. The pessimum proportion is the proportion of alkalis or calcium at which the maximum expansion occurs, as seen in Figure 5. The pessimum effect is the phenomenon of expansion decreasing as reactive ingredients increase. Under the pore solution mechanism, increased alkalis are attributed to limiting expansion. The multi-phase gel reaction theory associates pessimum to the consumption of calcium available to form reaction rims (Ichikawa 2009).

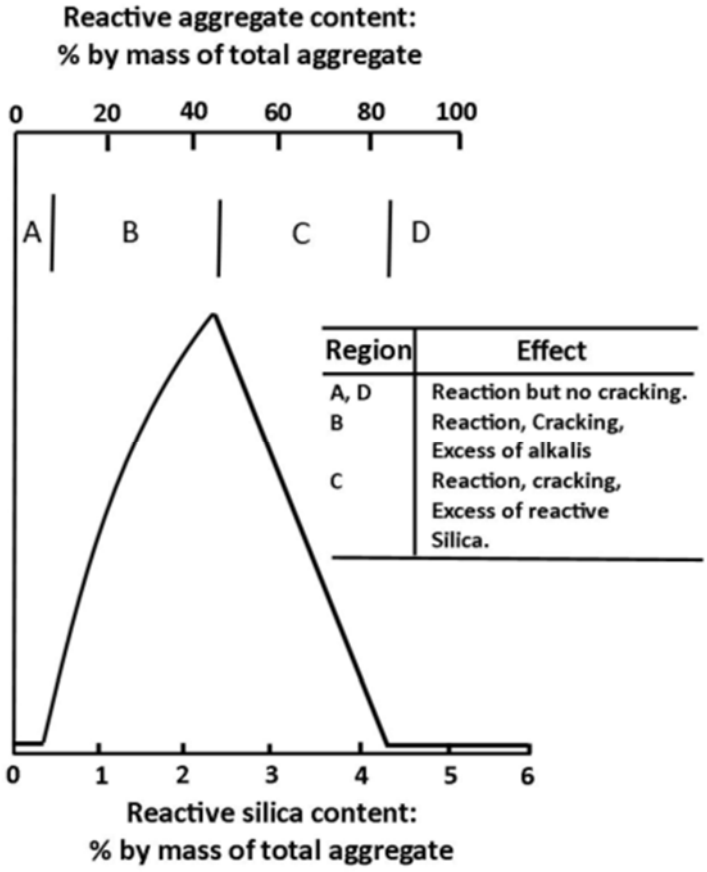

Figure 5. Pessimum effect behavior: water/cement and aggregate/cement rations 0.4 and 2.75, respectively. Alkali content 6 kg/m^3. Modified from Hobbs 1988.

It is also hypothesized that the size of the aggregate will also influence the amount of reactivity. Smaller aggregates have a greater specific surface area and therefore a larger reaction surface than that of larger aggregates. Limiting factors, such as calcium, should be more evident with an increased reaction surface. This theory is more applicable for aggregate sources that exhibit reactivity in only certain size fractions rather than a general reactivity of all aggregate. For

example, an aggregate with reactive fines will utilize more calcium initially than an aggregate in which the coarse component is reactive.

Wetting and drying cycles of the concrete have been shown to affect expansion due to ASR and the development of map cracks. As concrete is dried, the reaction is slowed because water serves as one of the constituents necessary for reaction. Rewetting the concrete decreases the pore solution alkalinity as a portion of the alkali ions become fixed in the drying process. Alkali concentrations have been reduced 34 to 61 percent by wetting and drying treatments (Rivard et al. 2003). Should the wetting process rinse the specimen, alkali-leaching will increase. Leaching at the surface causes the development of map cracks as the surface expansion fails to match subsurface expansion (Berube et al. 2002). Wetting and drying of ASR affected concrete decreases the total expansion experienced while increasing surface cracking exposing that material to other problems such as freeze-thaw.

2.2 Mitigation of the Alkali-Silica Reaction

In order to slow or stop ASR, the characteristics of the reaction must be altered. Supplementary cementitious materials (SCMs) are often used to alter this chemistry. SCMs have been suggested to influence the alkali-silica reaction by varying several characteristic mechanisms. These mechanisms include:

1. Diluting of the pore solution alkalinity.
2. Binding alkalis into an insoluble form such as converting the alkalis into salts.
3. Reducing concrete permeability.
4. Increasing the tensile strength.

5. Altering the aggregate dissolution rate.
6. Increasing the consumption of $Ca(OH)_2$ through pozzolanic reaction.

These mechanisms were investigated quantitatively by Shafaatian et al. (2013). Their work attempted to isolate the mitigation mechanisms on ASTM C1567 specimens. Their research determined that alkali dissolution and reduction of the aggregate dissolution rate were negligible mitigation mechanisms. The other four mechanisms (2, 3, 4, and 6) have a significant effect on the expansion of the concrete. This research will use fly ash to take advantage of mechanisms 2, 3, 4 and 6 to limit the deleterious effects of ASR.

While many SCMs are available for use, fly ash has been commonly selected because it is a byproduct of power generation from coal and has a lower cost than other mitigating agents. As fly ash transitions from a waste material to a valued commodity, using it efficiently becomes an important consideration. ASTM separates fly ashes into three classifications (N, C, and F) based on pozzolanic properties according to ASTM C618. The use of fly ash with these varying classifications produces different levels of mitigation. In numerous cases, Class F fly ash has shown superior mitigation characteristics (ACI Committee 221 2008; Malvar et al. 2002; Shehata 2000; Shon et al. 2002; Thomas 2007). This mitigation is largely attributed to calcium-silicate-hydrate (C-S-H) binding harmful alkalis in the pore solution. Furthermore, fly ashes with lower calcium-oxide (CaO) contents mitigate more effectively (Shafaatian 2013). Shehata (2000) plots the variation in mitigation effectiveness with respect to CaO content as illustrated in Figure 6. Although fly ashes with CaO contents less than 8 percent clearly mitigate ASR expansions, fly ashes with CaO contents between 8 and 20 percent mitigate some aggregates and do not work with other aggregate sources. Until recently, ASTM C618 included a note limiting the CaO

content to less than 10 percent for Class F fly ash produced by coal combustion. The specification currently notes that Class C fly ash generally has a higher CaO content than Class F but no longer prescribes a maximum level.

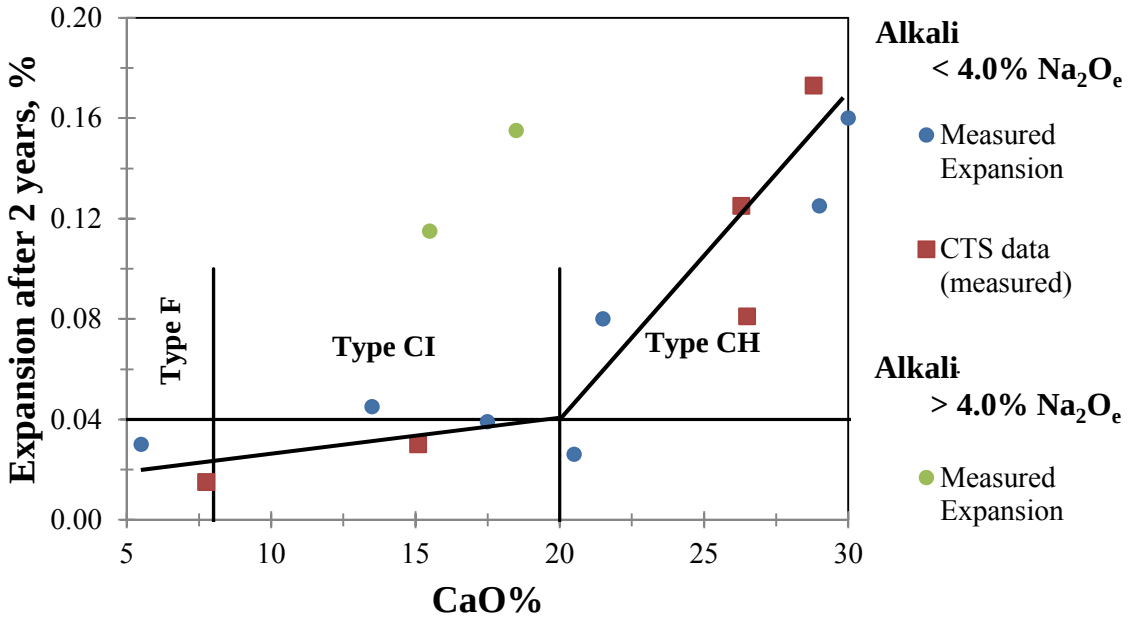

Figure 6. Effect of CaO content of fly ash on expansion of concrete containing 25 percent fly ash. Fly ash classification are based on Canadian definitions rather than ASTM designations. Modified from Shehata 2000.

The quality and characteristics of fly ash vary widely based on the source of coal from which it is produced. Coals from bituminous sources are generally lower in CaO than those produced from subbituminous coals (Portland Cement Association 2002). Wyoming has primarily subbituminous coal though areas of bituminous coal exist throughout the state. This variation in fly ash lends itself to the importance of having fly ashes chemically tested before use in

mitigation as the two classes require significantly different amounts of fly ash to produce the same levels of mitigation (Shehata 2000). Class F fly ash is used in Wyoming ASR research as the mitigating agent.

3 Classification Methods and Test Procedures

While the development of a model to predict the reactivity of a given aggregate in a specific concrete mixture would be advantageous and eliminate much of the time necessary for testing, comprehensive modeling methods do not exist due to the complexity of the chemical reaction and concrete microstructure. Factors influencing the progress of ASR include the aggregate particle size and porosity, cement alkalinity and fineness, and permeability of the hydrated cement paste (Neville, 2012). Experimental testing takes all these factors into account to provide an estimation of the reactivity of an aggregate/cement combination.

Due to the widespread occurrence of ASR, numerous testing methods have been developed to identify potentially-deleterious alkali-silica reactivity. These test methods include large-scale field exposure testing, the Concrete Prism Test (CPT), and the Accelerated Mortar Bar Test (AMBT). Exploratory work is also being conducted on the Autoclaved Concrete Prism Test (ACPT). Testing conditions are summarized in Table 2. The following section discusses the development and procedures for each method.

Table 2. Classification testing methods.

Test	Specimen Alkali-Boosting	Specimen Size	Storage Environment	Testing Duration
Large-Scale Field Exposure	Unboosted and 1.25%	380 x 380 x 660 mm (15 x 15 x 26 inch)	Outdoor	Minimum five years
CPT	1.25%	75 x 75 x 285 mm (3 x 3 x 11.25 inch)	100 percent relative humidity 38 °C (100 °F)	One year
AMBT	Unboosted	25 x 25 x 285 mm (1 x 1 x 11.25 inch)	1 N NaOH solution 80 °C (176 °F)	14 days
ACPT	3.00%	75 x 75 x 285 mm (3 x 3 x 11.25 inch)	Autoclave: 0.2 MPa	4 days

3.1 Large-Scale Field Exposure

Large-scale field tests are advantageous, providing the most accurate expansion data possible because the blocks experience real-world conditions eliminating the need to correlate normal expansions to those experienced under accelerated testing conditions. Where many accelerated tests are forced to alter the mix design to accelerate reaction, field specimens are able to test 'job' mixes, or those that are used in the field. The use of large-scale specimens also limits the leaching of alkalis, a problem common to smaller test specimens (Zhang et al. 1999).

While large-scale field specimen testing is most accurate at portraying the reactivity of a concrete mix, it is severely disadvantaged by the long time period associated with testing. Field service information is seldom taken from an existing structure until it is at least 10 years old (Thomas et al. 2006). This same rule of thumb could apply to cast-in-place field specimens. The time to classification must be long enough for the alkali-silica reaction to take place. A five-year classification period allows the progression of the reaction but limits the wait for classification results. While this test is being conducted, continued excavation of a pit may reveal new strata with varying reactivity characteristics. This limits the effectiveness of the test for industrial use as pit characteristics may change before a classification is reached. The test is important to academic research, however, as a point of comparison for the results of accelerated testing methods. Field specimens are exposed to the same thermal gradients and freeze-thaw cycles experienced in outdoor structures. Field conditions are very difficult to reproduce in a laboratory setting, and exposure testing provides a good check of laboratory test results.

Large-scale specimen testing has been limited to only a small number of field sites in the world although this number is increasing. The early sites include the Building Research Establishment

in the U.K.; CANMET in Ottawa, Canada; The University of Texas in Austin, TX; and the University of Wyoming in Laramie, WY. An additional marine exposure site exists in Treat Island, ME. The number of field sites had grown from 5 to 23 by 2012 (Ideker et al. 2012).

Due to limited testing, little work has been done and published to date on the establishment of expansion limits for reactivity classification. The Wyoming ASR research group has developed preliminary limits in the hope of providing future guidance for field classifications.

ASR expansion curves are initially linear and expansions slow with time as a field block reaches the completion of the reaction. The research group based the final classification on expansions measured at five years. Continued testing is recommended for aggregates that are believed to show increased expansion with prolonged exposure. Limits were proposed using a linear relationship between age and average percent expansion. Aggregates are divided into three classification groups: nonreactive, moderately reactive, and highly reactive. In addition to designating the reactive from the nonreactive aggregates, these classifications were designed to separate levels of reactivity to assist in mitigation programs. Moderately reactive aggregates should require less mitigation than highly reactive aggregates. This information should be used in the future to economize the use of fly ash.

To differentiate field specimen reactivity levels, limits were fit to the values of the results to date for the boosted specimens for the eight Wyoming aggregate sources because they naturally fit into three groups. In this manner proposed expansion limits are a 0.02 percent increase in expansion per year separating nonreactive from moderately reactive specimens and a 0.06 percent increase in expansion per year separating moderately reactive and highly reactive aggregates. These proposed limits are halved for unboosted specimens; 0.01 percent for

nonreactive to moderately reactive and 0.03 percent for moderately reactive to highly reactive. Boosted and unboosted limits are shown in the field exposure classification section of Chapter 6.

Natural gradation from the source was used in the field specimens, as determined by sieving material from each pit. Each field specimen was cast using the same amounts of coarse aggregate, fine aggregate, cement, and air entrainment admixture. The amount of water added to each mixture varied by a small amount depending on the workability of the concrete, and moderate amounts of superplasticizer were added to further simulate field conditions. Leeman and Lothenbach studied the effect of superplasticizer on ASR expansion and concluded that polycarboxylate superplasticizers had a negligible effect on concrete expansion due to ASR (2010).

To represent an upper-bound estimate of an aggregate's reactive potential, at least one field specimen from each aggregate source was boosted to 1.25 percent Na_2O equivalent by the addition of NaOH to the mixing water. Table 3 shows the major materials quantities for all the field specimens. Materials specific to each specimen are included in Table 43 of Appendix A. It should be noted that the BHP and BHC specimens refer to the Black Rock aggregate.

Table 3. Material quantities common to all field specimens.

Material	Quantity kg (lb)
Coarse Aggregate	138 (305)
Fine Aggregate	89 (196)
Cement	56 (124)

These blocks were then cast using procedures established by Fertig in 2008. Further details regarding the exposure site conditions, casting, measurement stud installation and labeling are included in Appendix A.

3.1.1 Measurement

To monitor expansion, twelve locations on each block were measured. There were four longitudinal measurements on the top, and two longitudinal measurements along each side. In addition, there were two transverse measurements on top and one vertical measurement on each end. All measurements had an approximate gauge length of eight inches. Figure 7 shows the typical measurement location layout for each field specimen, where 9 of the 12 measurements are shown.

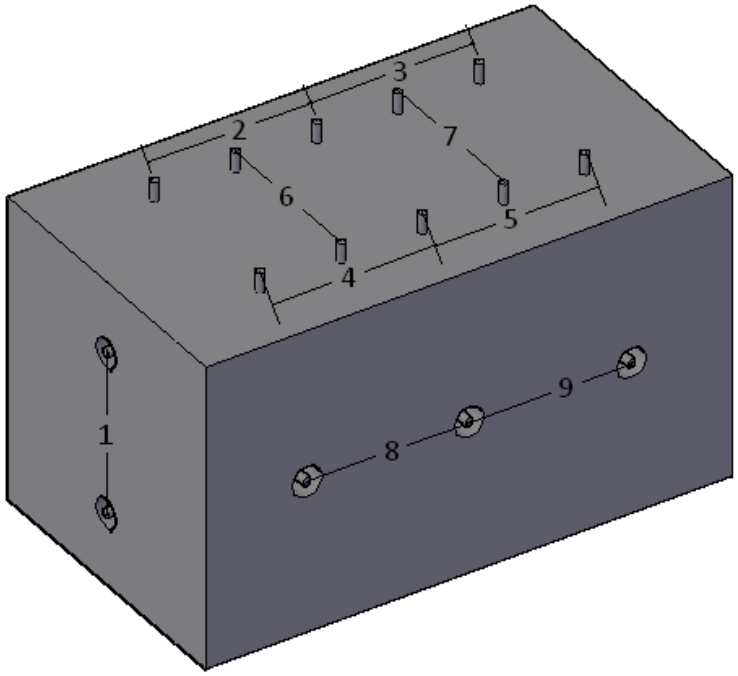

Figure 7. Field specimen diagram showing the layout of the measurement locations.

In some cases, expansion measurements did not begin for approximately two months after the specimens were cast. This was because studs were installed after placing some blocks at the field site. Although there was a delay in initial measurement, the field specimens were not expected to display reactive behavior in the early phases of exposure.

As each measurement was recorded to the nearest 0.001 mm (39 x 10^{-6} inch), the effect of variations in exposure conditions during the time of measurement was significant. Ideally, the effects of thermal expansion would be eliminated by measuring each field specimen at the same ambient temperature and under constant cloud cover to avoid direct sunlight. However, due to the erratic weather that is common in Laramie, WY it was not feasible to wait for these ideal conditions. To reduce thermal expansion effects, the surface temperature was taken at the time of measurement, and the recorded measurements were then scaled to obtain an equivalent value at 21 °C (70 °F). For preliminary results, a conservative coefficient of thermal expansion, 18.2 x 10^{-6} /°C (5.5 x 10^{-6} /°F), was used to scale the measurements.

In addition to the challenges that were introduced by measuring at different temperatures, measuring in direct sunlight instead of cloud cover introduced thermal gradients into the specimens. Initially, the effects of thermal gradients were minimized by shading the block with a 3 meter (9 foot) diameter patio umbrella for at least 20 minutes prior to measuring, to reduce temperature differences on different block faces. Later measurements were taken in the morning when the entire site was shaded.

3.1.2 Mechanical Strain Gauge Measurement Technique

A Demec mechanical strain gauge is used to measure changes in length between measurement points on the field specimens. To obtain consistent results with the Demec mechanical strain gauge system, several guidelines are provided. The points on the Demec instrument must be placed in exactly the same location in the studs every time a measurement is made, so care should be taken to make sure the gauge points are securely seated in the drilled holes. Because the angle of the instrument with respect to the block affects the measurement significantly, the axis of the instrument should be perpendicular to the block. Analysis of this error is presented in Section 5.2.

The amount of pressure that is applied to the instrument in any direction when measuring will also affect the measurement obtained. When measuring the top of the block, the instrument can be balanced on the studs with minimal force. However, it can be difficult to feel how much pressure is being applied on the four vertical sides of the block. A method to provide effective vertical measurements was to hold the instrument normally, but to resist its weight with one finger and push the points into the holes in the studs until it could be seen that they were securely seated.

A standard measurement procedure was developed to ensure that all field specimen measurements in the future are consistent with past measurements.

1. Expose the gauge instrument and the reference bar (Figure 8) to field conditions to avoid errors due to thermal changes in the measurement equipment.

2. After the instrument and reference bar have normalized to the outdoor temperature, turn on the instrument and measure the reference bar (Figure 8) to obtain the reference measurement.

Figure 8. Invar reference bar.

3. On the block, measure each distance between studs at least three times, and confirm that the difference in measurements is less than 0.005 mm (0.2 x 10^{-3} inch) each time.
4. Record the average of these three measurements.
5. Repeat steps 2 through 4. The second series of measurements should be completely independent of the first measurement series.
6. If the difference between related measurements in the two series is more than 0.015 mm (0.59 x 10^{-3} inch) (equivalent to 0.0075 percent expansion) then that location on the specimen should be measured again.

3.2 Concrete Prism Test (CPT) – ASTM C1293

The CPT was developed in the 1950s. The test arose from failure of the ASTM C227 to correctly identify both ASR and alkali-carbonate reactivity (ACR) (Thomas et al. 2006). The total alkali loading level was adjusted to better calibrate to field specimen performance until the current levels were adopted in ASTM C1293 in 1995.

The test uses 75 x 75 x 285 mm (3 x 3 x 11.25 inch) prisms with a water-to-cement ratio between 0.42 and 0.45, a specific proportion of coarse and fine aggregate, and a cement content of 420 kg/m^3 (26.2 lb/ft^3). Cement is required to have a base total alkali content of 0.9 ± 0.1 percent Na_2O equivalent, which is boosted to 1.25 percent by mass of cement through the addition of NaOH. This boosting was developed to accelerate reaction in the 100 percent relative humidity storage at 38 °C (100 °F). Specimens are stored above water to limit the potential for alkali leaching (Thomas et al. 2006). The behavior of the mix is evaluated for the period of one year to determine reactivity. Aggregates are classified as potentially reactive if the expansion at one year is equal to or greater than 0.04 percent by ASTM C1293. Additional classifications from the Federal Highway Administration will be used to define reactivity levels, Table 4.

Table 4. FHWA CPT classification limits.

Aggregate Reactivity Class	Description of Aggregate Reactivity	One Year Expansion in CPT (%)
R0	Nonreactive	≤ 0.04
R1	Moderately reactive	> 0.04, ≤ 0.12
R2	Highly reactive	> 0.12, ≤ 0.24
R3	Very highly reactive	> 0.24

CPT specimens have the advantage of testing both coarse and fines unlike mortar bar specimens. Combining both coarse and fine aggregate fractions, moderate environmental conditions, and boosting, leads to a strong correlation with field specimen results (Cornell 2002). While the test has been shown to produce accurate aggregate classifications, the one year duration makes the test impractical for evaluating construction specification conformance (Lane 1999). The test has also been shown to allow significant leaching of alkalis (Rivard et al. 2003), which can result in

a decrease in the rate of reaction and maximum value of expansion due to ASR. Despite these limitations, the CPT test is considered the most reliable accelerated test for ASR.

ASTM C1293 provides instructions for testing either coarse or fine aggregate for reactivity, and the standard also outlines the gradation requirements for both types of aggregates depending on the coarse or fine fraction to be tested. Because both fine and coarse aggregates are used together in the field, they were combined for testing. The individual specified gradations used for fine and coarse aggregates, as defined in ASTM C1293 and ASTM C33, are shown in Table 5.

Table 5. Coarse (ASTM C1293) and fine (ASTM C33) aggregate gradations.

Coarse	
Size	**% Passing**
1/2”	33
3/8”	33
#4	33

Fine	
Size	**% Passing**
# 8	80-100
#16	50-65
#30	25-60
#50	5-10
#100	0-10

Aggregates were sieved into the sizes required by the standards. Aggregate retained on sieve #30 or larger were then washed and oven dried. After drying, the unit weight of the coarse aggregate was measured and recorded using the procedure described in ASTM C29.

3.2.1 Casting

The concrete was proportioned and mixed according to ASTM C1293. The aggregates were oven dried before use in the concrete. A water-to-cement ratio of 0.42 was used resulting in 3.79 kg (8.35 lb) of water per batch. The volume of coarse aggregate per unit volume of concrete is specified as 0.70 ± 0.2 percent in ASTM C1293 meaning 70 percent of the total concrete mixture volume is occupied by coarse aggregate.

A NaOH admixture was used to bring the alkalinity of the concrete mixture to 1.25 percent Na_2O equivalent by mass of the cement as specified in ASTM C1293. The mass addition was determined by subtracting the equivalent alkali content of the cement from the required alkalis, Figure 9. Molecular weights of Na_2O and NaOH are 61.98 and 39.997, respectively. This standard was developed using cement with an alkalinity of 0.9 ±0.1 percent. The cement alkalinity is significant because high alkalinity cements have more expansion than low alkali cements whose alkalinity has been increased by the addition of alkali hydroxide (Mo et al. 2010). Cement used in this study had an alkali content which was just below the lower alkali limit of 0.8 percent. Minimal difference in test expansion results are expected with this variation in cement alkalinity. A total of 0.06 kg (0.14 lb) of NaOH were added to each batch.

$$NaOH\ addition$$

$$= (Cement\ mass\ x\ Required\ Alkali\ content$$

$$- Cement\ mass\ x\ Cement\ Na_2O\ equivalent) x\ (\frac{2 * 39.997}{61.98})$$

Figure 9. Equation. NaOH Addition. ASTM 2008.

The concrete mixture was proportioned using the absolute volume method described by the Portland Cement Association (Kosmatka et al. 2002). The specific gravities and absorptions of the aggregates were known and the specific gravity of the cement was taken to be 3.15. The amount of mixing water was adjusted for each aggregate to reflect their different absorption capacities. Enough concrete was batched to cast four 75 x 75 x 285 mm (3 x 3 x 11.25 inch) specimens and three 100 mm (4 inch) cylinders. Table 44 in Appendix A summarizes the materials used in each concrete mixture. Cylinder compressive strengths for each batch cast by Fertig and Kimble are shown in Table 45 and Table 46 of Appendix A, respectively.

An electric concrete mixer was used to mix the materials. The process of mixing was as follows:

1. Dissolve the NaOH pellets in the mixing water.
2. Add some of the coarse aggregate and the water to the mixer while stopped.
3. Start the mixer.
4. Add the remaining coarse aggregate, fine aggregate, cement and water.
5. Continue mixing for three minutes after all the materials have been added.
6. Stop the mixer for three minutes and cover the opening to prevent moisture loss.
7. Uncover the opening and mix for two more minutes.

The slump was then measured in accordance with ASTM C143, and the air content and yield were obtained following ASTM C138. Table 47 and Table 48 summarize the measurements that were taken on the concrete mixtures.

After the slump and air content were measured, the concrete was placed in the molds (Figure 10) and in 100 mm (4 inch) cylinders for later compression testing. A debonding agent was applied before the measurement gauge studs were screwed in place to avoid weakening the bond between the studs and the concrete. Concrete was placed in the molds in two equal layers and each layer was rodded 33 times. After the concrete was placed, the ends and corners of the molds were tapped with a rubber mallet to aid in the consolidation process. The surface of the mold was struck off flush and finished.

Figure 10. ASTM C1293 mold.

Immediately after the concrete was placed in the molds and cylinders, they were stored in a moist curing room for 24 hours. Plastic lids were placed on the cylinders. ASTM C511 calls for the moist curing room to be 23 ± 2 °C (73 ± 4 °F) with a relative humidity not less than 95 percent.

3.2.2 Measurement and Storage

When the concrete had cured for 24 hours, the CPT specimens were removed from their molds and measured using the comparator shown in Figure 22.

The specimen was placed in the comparator and then spun gently, and when the measurement settled on a number, it was recorded. Each specimen was labeled with a name and arrow to ensure that it was measured with the same end up each time. All specimens were measured at 1, 7, 28, and 56 days, and at 3, 6, 9 and 12 months. After each measurement the specimens were stored with a different end facing up to limit alkali migration.

Storage environment requirements are specified by ASTM C1293. In fulfillment of the standard, 1 kilogram (2.3 pound) of water was added to each 5 gallon bucket to provide slightly less than 25 mm (1 inch) of water in the bottom. Wicking material, needed to move the moisture throughout the storage container, was placed around the edge of the bucket. A rack, Figure 11, to elevate the specimens above the water was placed in the bucket.

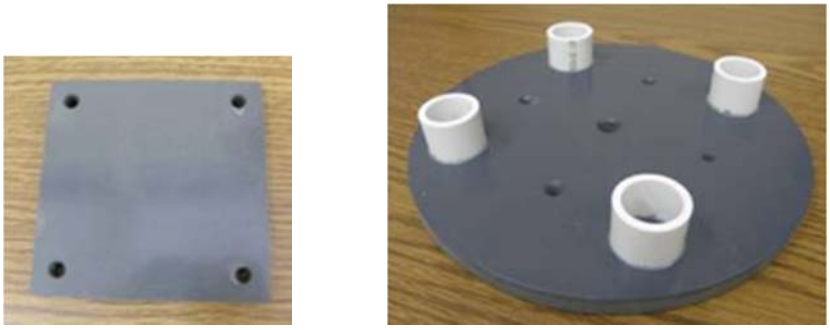

a) b)

Figure 11. a) Top portion of rack and b) bottom portion of rack shown upside-down.

Once the specimens were placed on the rack, the top piece was added to ensure constant separation between specimens. The storage environment without the lid is shown in Figure 12. Then a lid, providing an airtight seal, was screwed on and the bucket was placed in an oven at 38 °C (100 °F).

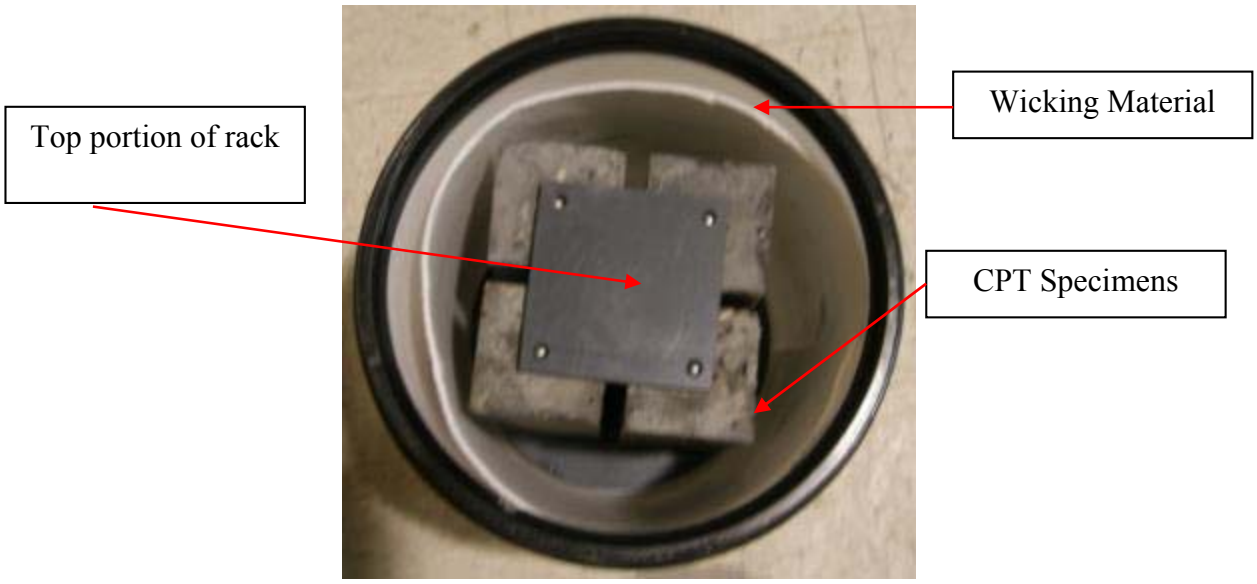

Figure 12. CPT storage environment without Lid.

ASTM C1293 states that the specimens should be removed from the storage environment for 16 ± 4 hours to allow them to cool to room temperature before "cold" measurements are taken. At the end of one year, expansion values that exceed 0.04 percent indicate reactive aggregates, while expansions less than 0.04 percent indicate a nonreactive aggregate. Reactive aggregates are further separated into moderately reactive, highly reactive, and very highly reactive according to the FHWA classification limits.

3.3 Accelerated Mortar Bar Test (AMBT) – ASTM C1260

The AMBT test was developed in South Africa in 1986 (Oberholster and Davies 1986). The methodology was created to improve on short-comings of the ASTM C277 and ASTM C289 tests. As a result the test methods were combined with ASTM C277 mortar bars being stored in the ASTM C289 soak solution. The 25 x 25 x 285 mm (1 x 1 x 11.25 inch) mortar bars have a 0.47 water-to-cement ratio. These specimens were demolded after 24 hours and immersed in tap water in an air tight container at 80 °C (176 °F) for 24 hours. Specimens were then moved to another air tight container of 1 normal (N) NaOH solution at 80 °C (176 °F) and measured periodically for a minimum of 14 days. The solution was meant to provide unlimited alkalis while producing the highest level of expansion. This method would go on to become the ASTM C1260 test that was formally adopted in 1994. The 1 N NaOH solution was confirmed to produce the highest expansion when testing quartz and silicate-bearing aggregates in 0.25 N, 0.5 N, 0.75 N, 1 N and 2 N solutions (Shon et al. 2002). ASTM C1260 indicates that expansions greater than 0.20 percent display potentially deleterious reactive aggregate, expansions between 0.10 and 0.20 percent include "both aggregates that are known to be innocuous and deleterious in field performance" (ASTM International 2001). Additional classifications from the Federal Highway Administration will be used to define reactivity levels, Table 6.

Table 6. FHWA AMBT classification limits.

Aggregate Reactivity Class	Description of Aggregate Reactivity	14-Day Expansion in AMBT (%)
R0	Nonreactive	≤ 0.10
R1	Moderately reactive	$> 0.10, \leq 0.30$
R2	Highly reactive	$> 0.30, \leq 0.45$
R3	Very highly reactive	> 0.45

This test is commonly used due to the short testing duration. It has been determined that the test has given both false negative and false positive results when compared to field performance (Fournier et al. 2006; Swenson 1958). As such, the ASTM standard recommends additional testing for difficult to classify aggregates as determined by expansions between 0.10 and 0.20 percent expansion.

AMBT aggregate gradation conformed to the ASTM standard, Table 7. Each aggregate portion was composed of 60 percent crushed coarse and 40 percent natural fine aggregate to better characterize field concrete. Coarse aggregate was crushed and then sieved into fine size gradations. Aggregates were washed and dried before being mixed into mortar.

Table 7. Aggregate gradation for the AMBT.

Passing	Retained On	Mass (%)
#4	#8	10
#8	#16	25
#16	#30	25
#30	#50	25
#50	#100	15

3.3.1 Casting

The ASTM standard specifies a cement-to-aggregate ratio of 1:2.25 and a water-to-cement ratio of 0.47 by mass. This results in quantities of materials shown in Table 8 for each mortar mixture.

Table 8. ASTM C1260 mix quantities.

Material	Quantity g (lb)
Cement	440 (1.0)
Aggregate	990 (2.2)
Water	207 (0.5)

Mixing was carried out using a Hobart mixer that conformed to ASTM C305. The mixing procedure followed ASTM C1260 and is summarized below.

1. Place all water into the dry mixer.
2. Add cement to water.
3. Allow to mix for 30 seconds at slow speed.
4. Add aggregate slowly over 30 seconds while mixing at slow speed.
5. Stop mixer and change to medium speed and mix for 30 seconds.
6. Stop the mixer scraping down any mortar that has collected on the side of the bowl. Allow to rest for 90 seconds.
7. Finish by mixing for 60 seconds at medium speed.

After mixing, the mortar was placed into the 25 x 25 x 285 mm (1 x 1 x 11.25 inch) molds (Figure 13) in two equal layers, with each layer compacted by a tamping tool. The mortar bars were then struck off and finished.

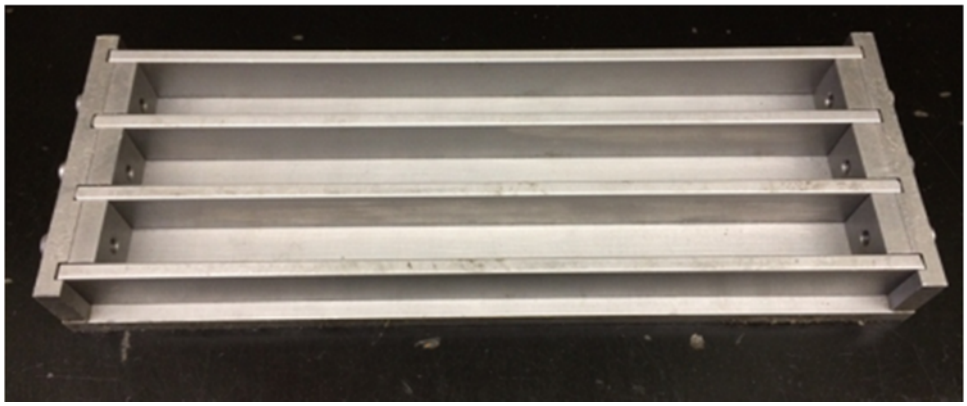

Figure 13. ASTM C1260 mold.

3.3.2 Measurement and Storage

Measurement and storage procedures follow the ASTM C1260 standard. After casting, the specimens were placed in a fog room conforming to ASTM C511 for 24 hours and initial length measurements were taken after demolding. The bars were placed in a tap water solution at 80 °C (176 °F) for 24 hours and measured again before they were placed in a 1 N NaOH solution at 80 °C (176 °F). The bars were measured periodically, in accordance with the standard, for 28 days after immersion in the NaOH solution. Testing was carried out to 28 days while ASTM C1260 requires that bars only be measured to 14 days.

Aggregate is considered innocuous if the 14 day expansion is less than 0.10 percent and potentially deleteriously reactive if the expansion exceeds 0.20 percent. The aggregate cannot be classified for expansions between 0.10 and 0.20 percent and additional testing is recommended. It should be noted, however, that some agencies use different expansion limits. For example, the FHWA and WYDOT uses a limit of 0.10 percent to indicate reactive aggregate. FHWA

classifications for moderately reactive, very reactive, and very highly reactive aggregates will be used for classification in this research.

Specimen lengths are measured using a comparator. A single bar was removed from the soak solution container and toweled dry. It is then placed in the length comparator and gently spun. The lowest reading displayed on the indicator during the spinning process is recorded. The bar is then set aside, out of the container, while the other specimens are measured. The percent expansion is calculated using a 10 inch gauge length in the equation below.

$$\%\ Expansion\ at\ Day\ (i) = \frac{Day\ (i)\ measurement - Day\ (0)\ measurement}{Gauge\ Length}$$

Figure 14. Equation. Percent expansion.

3.4 Correlation between AMBT and CPT

It is often determined that ASTM C1293 is the most accurate method for predicting potential deleterious expansion, therefore it is used as a baseline for all other tests. The effectiveness of the classifications based on ASTM C1260 has been of major concern because of the two week duration of the AMBT. As a result, the correlation between the two is of particular interest.

Lu et al. (2008) showed that when comparing AMBT and CPT results, a positive linear correlation would be expected for most aggregate types as shown in Figure 15. Expansion limits for each test are provided for reference.

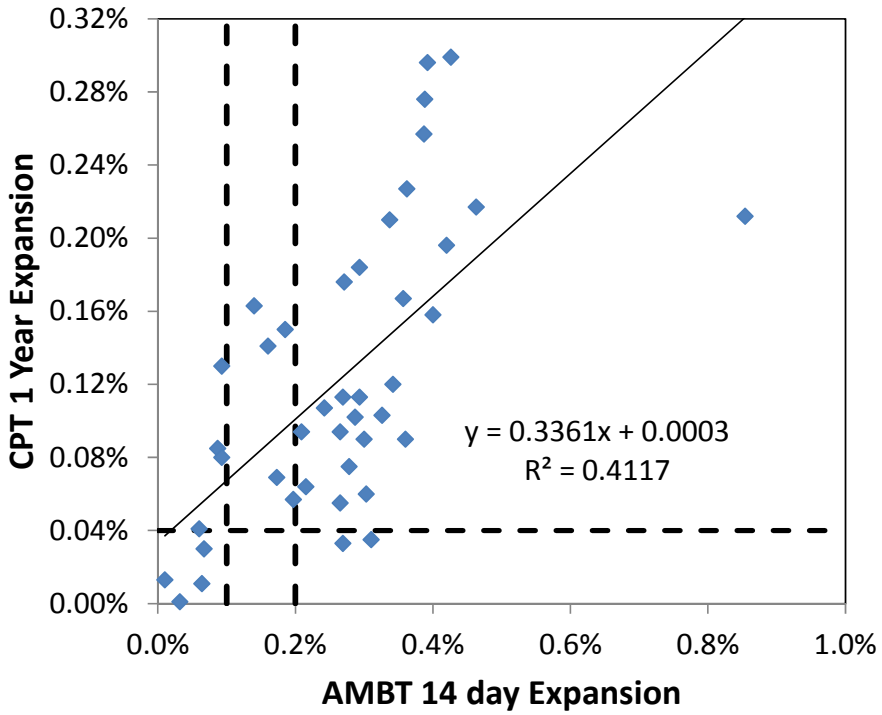

Figure 15: AMBT vs. CPT data (Lu 2008).

A poor correlation was observed between the AMBT and CPT with an R^2=0.4117. The AMBT did a poor job of estimating aggregates that would be classified as moderately reactive in the CPT. This could be explained by the single point on the right in Figure 15. However, it should be noted that there is a positively linear trend and linear regression shows that the linear coefficient is statistically significant with a p-value of 0.000 (α=0.05). This indicates that there is a direct correlation between the performance in the CPT and a projected value in the AMBT.

In recent research, AMBT and CPT results were compared for various mineralogical compositions of both fine and crushed coarse aggregates from the United States and Canada (Idecker 2012). The result for the fine aggregate is shown in Figure 16 and the coarse aggregate in Figure 17.

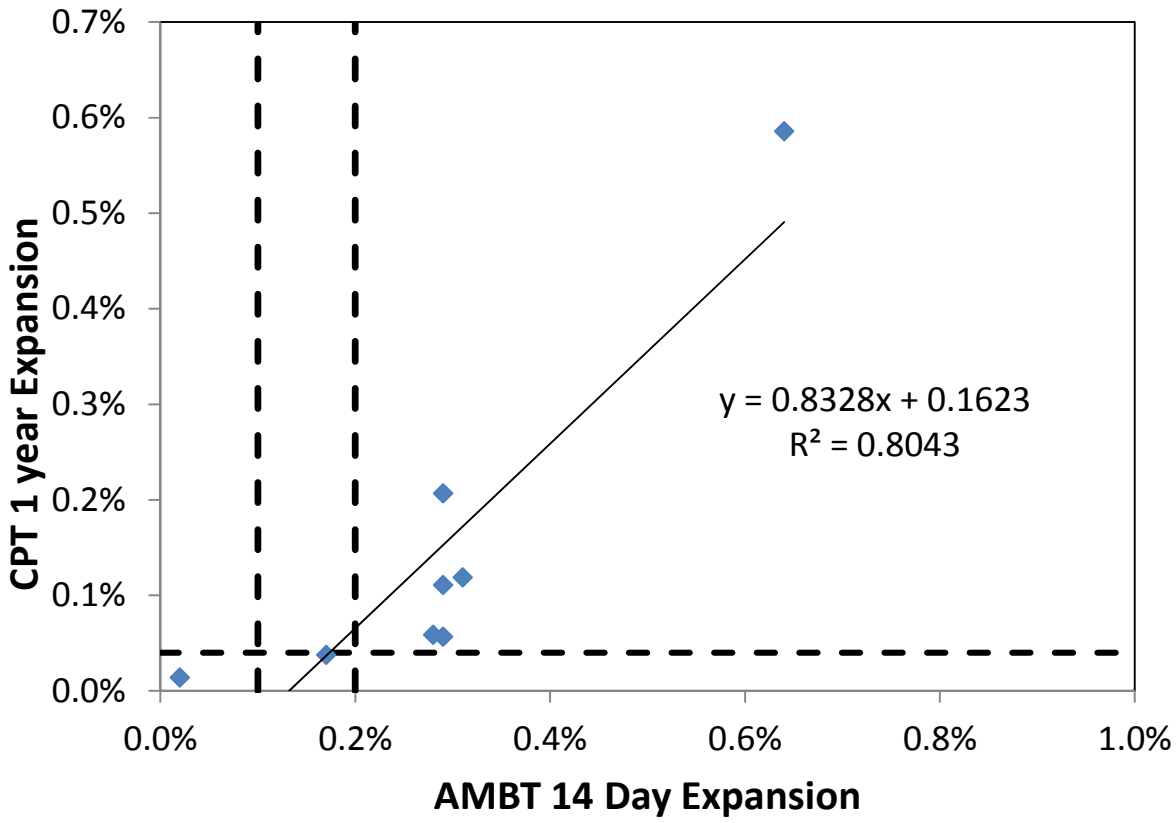

Figure 16: AMBT vs. CPT: Fine aggregate (Idecker 2012).

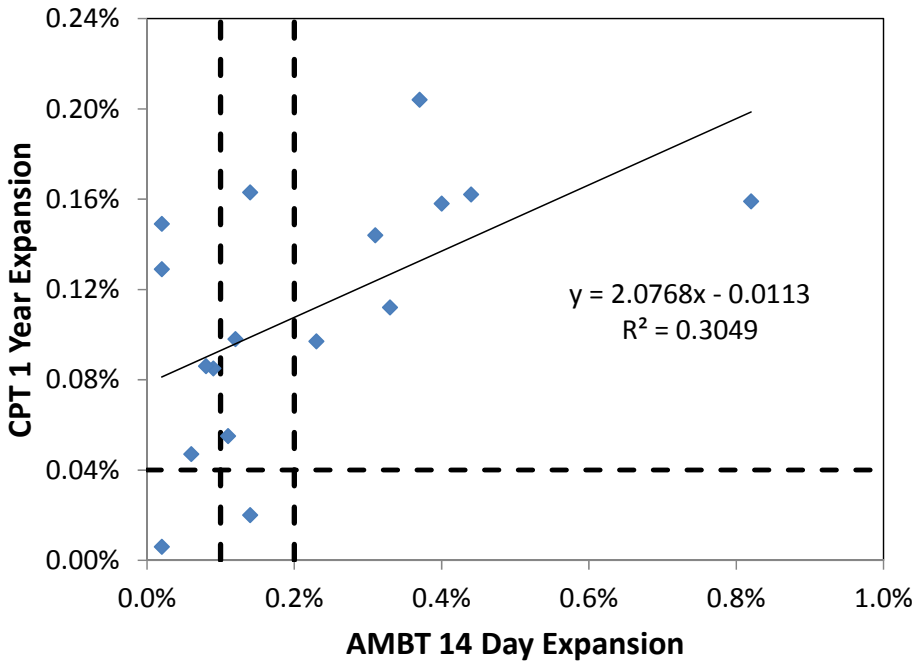

Figure 17: AMBT vs. CPT: Coarse aggregate (Idecker 2012).

The fine aggregates showed good agreement in classification and correlation (R^2=0.80). A linear regression analysis of this data showed a p-value of 0.003 for the linear coefficient (α=0.05). The coarse aggregate was more variable with 5 of the 17 aggregates passing the AMBT and failing the CPT. The correlation between the AMBT and the CPT was less strong than the fine aggregate with a R^2=0.30. The regression analysis of the coarse data resulted in a p-value of 0.022 for the linear coefficient (α=0.05). The small p-value indicates a correlation between the CPT and AMBT even though a low value for R^2 was observed for the fine and coarse specimens. The observed variance in the Lu and Idecker data could be attributed to expected experimental variance in materials used, concrete mixture, or machine error. In all cases, it has been shown that there is a definite correlation between the ASTM C1293 and ASTM C1260 tests even though the variance is slightly larger than would be desired.

When the expansion limits are applied to the AMBT versus CPT correlation graphs, four general areas are created. The lower left and upper right areas indicate areas where the AMBT and CPT classifications agree. The lower right area indicates an area where the AMBT classified an aggregate as reactive, but the CPT reclassifies it as non-reactive. This contradiction is resolved through the requirement that the AMBT be verified by the CPT. The area of greatest concern is the upper left area. Here, the AMBT classifies an aggregate as non-reactive but the CPT classifies it as reactive. To date, neither standard addresses this type of disagreement between results. In general, it was shown that when the reactivity of an aggregate was classified with the AMBT, it was classified similarly by the CPT. Compared to the CPT, the AMBT could both over and underestimate the reactivity of the aggregate.

From these cases, it can be assumed that a positive linear correlation would be expected between the AMBT and CPT. However, previous research on eight aggregates in Wyoming has shown the scattered results of Figure 18. These results make it impossible to apply the same correlation observed in the Lu and Idecker results. The most likely cause of this is the harshness of the AMBT.

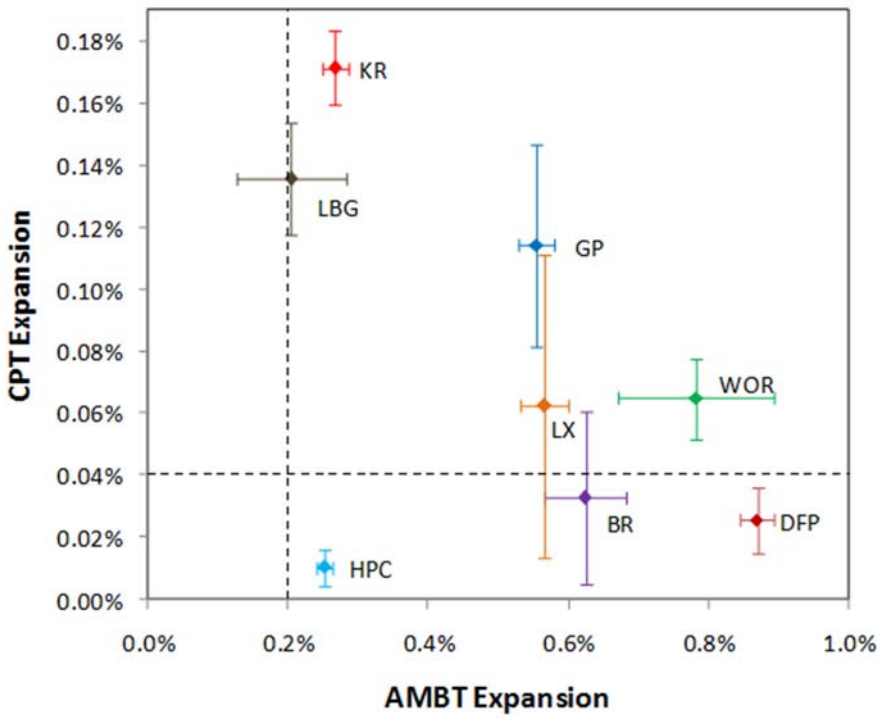

Figure 18: AMBT vs. CPT Wyoming aggregates.

3.5 Petrography

Often, it is difficult to confirm that an ASR reaction is taking place within a concrete specimen. By the time map cracking is visible in concrete, the reaction has produced sufficient gel and imbibed enough water to produce significant expansive pressure within the concrete. In laboratory experimentation, it is important to confirm that the observed expansion can be attributed to ASR. Petrographic analysis of hardened concrete is described in ASTM C856 and is indicated for the presence of ASR and its effect on the overall concrete.

It has been established that opal, granitic gneiss, and basalts show potential for reactivity. This test can be used for both experimental and in-service concrete as a determining factor for exactly how much ASR has taken place and the subsequent classification process. In general, it is

assumed that petrographic results from accelerated test methods exhibit more ASR damage and would obtain a more conservative classification than their in-service counterparts. The standard outlined in C856 can be supplemented by electron microscopy as outlined in ASTM C1723.

In 2010, an examination of the CPT and AMBT of the Wyoming aggregates was performed using petrographic analysis. This study consisted of five reactive field specimens based on expansion to date and the eight aggregates for the CPT and AMBT test specimens. At the time of the petrographic analysis, the field blocks ranged from two to three years in age. For the petrographic analysis, the scale used to classify the presence of ASR is shown in Table 9.

Table 9: Scale used to determine the severity of ASR.

ASR Presence Ranking	Description
None	No evidence of ASR.
Negligible	Reaction rims abundant; no micro cracking linked to ASR observed.
Minor	Reaction rims observed, rare microcracks associated with ASR; gel deposits occasionally present.
Moderate	Microcracks filled with ASR commonly cut paste; deposits of gel commonly observed in voids.
Severe	Macroscopic cracks and microcracks filled with ASR gel commonly observed; abundant reaction rims and gel deposits in voids commonly observed.

The petrographic classifications for the AMBT and CPT can be seen in Figure 18. The results for the accelerated test method and the corresponding petrographic classification as well as the field blocks are shown in Table 10 through 12 (Jones 2012).

Table 10: AMBT laboratory reactivity classifications versus petrographic classification.

Aggregate Source	Laboratory Classification	Petrographic Classification
Black Rock (BR)	reactive	severe
Devries Farm Pit (DFP)	reactive	severe
Goton Pit (GP)	reactive	moderate
Harris Pit (HPC)	reactive	moderate
Knife River Pit (KR)	reactive	moderate
Labarge Pit (LBG)	reactive	severe
Lamax Pit (LX)	reactive	severe
Worland (WOR)	reactive	moderate

Table 11: CPT laboratory reactivity classifications versus petrographic classification.

Aggregate Source	Laboratory Classification	Petrographic Classification
Black Rock (BR)	reactive	moderate
Devries Farm Pit (DFP)	nonreactive	minor
Goton Pit (GP)	reactive	minor
Harris Pit (HPC)	nonreactive	negligible
Knife River Pit (KR)	reactive	negligible
Labarge Pit (LBG)	reactive	minor to moderate
Lamax Pit (LX)	reactive	minor to moderate
Worland (WOR)	reactive	minor

Table 12: Large scale field block condition versus petrographic classification.

Large Scale Block	Field Observations	Petrographic Classification
Black Rock (BHC-1)	hairline cracking (2%)	none
Devries Farm Pit (DFP-1)	hairline cracking (1%)	none
Goton Pit (GP-2)	hairline cracking (1%)	none
Harris Pit (HPC-1)	hairline cracking (2%)	none
Knife River Pit (KR-2)	0.2mm cracking (75%)	none
Labarge Pit (LBG-2)	hairline cracking (5%)	none
Lamax Pit (LX-1)	0.5mm cracking (15%)	none
Worland (WBP-2)	0.2mm cracking (20%)	none

This study clearly illustrates the confusing nature of the ASR problem. The AMBT indicated that all eight aggregates were reactive, while the CPT classified six of the eight as reactive. Jones (2012) indicated that the lack of ASR in the petrographic analysis of the field blocks was most likely due to the relatively young age of the specimens and further observation was needed as the blocks age. It is clear that, while a petrographic analysis plays an important part in the classification of potential deleterious materials, there are issues with the results shown above. The most concerning is the Knife River aggregate. It was shown to be reactive in all three tests; however, it was classified as non-reactive by the petrographic analysis for both the CPT and the field block tests. Furthermore, the aggregate is considered to be a classic expansive aggregate based on previous field experience and observation. Due to these results, the investigation of this aggregate is ongoing.

3.6 Autoclave Concrete Prism Test (ACPT)

The ACPT used here was developed by researchers at the University of Alabama (UA) to satisfy the criteria set forth by Grattan-Bellew (1997) for ultra-accelerated tests of aggregate reactivity. These criteria include:

1. Duration should be no more than a few weeks, preferably a few days.
2. Test should be simple and not require an “excessively expensive” apparatus.
3. Test results and field experience should be in agreement.
4. Test should correctly identify the reactivity of more than 90 percent of aggregates.
5. Reaction products should be similar to those found in field concrete and the CPT.

6. The expansion limit should be greater than 0.05 percent.

7. The coefficient of variation (COV) should be less than 10 percent for a single operator and 12 percent for inter-laboratory tests.

The testing program uses ASTM C1293 specimens boosted to three percent Na_2O equivalent through the addition of NaOH. These specimens are cured for 24 hours in a moist curing room. Specimens are then demolded, wrapped in saturated felt and returned to the curing room for 24 hours. This procedure is detailed in the report *A Rapid Test to Determine Alkali-Silica Reactivity of Aggregates using Autoclaved Concrete Prisms* (Giannini and Folliard 2013). Applied pressure is believed to assist in decreasing the effect of alkali leaching and decrease the necessary length of exposure.

ASTM C1293 specimens are used in autoclave testing. These specimens are prepared in the same manner as the CPT specimens with the exceptions of the aggregate used and the boosting levels. ACPT isolates the coarse or fine aggregate fraction being tested. The aggregate fraction not being tested is then replaced by a nonreactive aggregate source. Autoclaved specimens are boosted to three percent Na_2O equivalent in order to accelerate the alkali-silica reaction and reduce any effects due to leach of alkalis during the autoclaving process.

3.6.1 Casting

Prisms were proportioned according to ASTM C1293 using a water-to-cement ratio of 0.45. NaOH pellets brought the alkalinity of the concrete mixture to three percent Na_2O equivalent by mass of the cement. The mass addition was determined using the equation in Figure 9. The

resulting NaOH addition was 0.21 kg (0.47 lb). Table 49 through Table 51 in Appendix A provide material quantities and compressive strengths.

An electric concrete mixer was used to mix the materials. The mixing procedure was the same as that used for CPT described in 3.2.1. Slump was measured in accordance with ASTM C143.

Next, the concrete was placed in the prism molds (Figure 10) and 100 mm (4 inch) cylinder molds for 28 day compressive strength testing. A debonding agent was applied before the measurement gauge studs were screwed in place to avoid weakening the bond between the studs and the concrete. Concrete was placed in the molds in two equal layers and each layer was rodded 33 times. After the concrete was placed, the ends and corners of the molds were tapped with a rubber mallet to aid in the consolidation process. The surface of the mold was struck off flush and finished.

Immediately after the concrete was placed in the molds and cylinders, they were taken to a moist curing room for 24 hours. Prism molds were covered with wet felt and cylinders were covered with plastic wrap to limit moisture loss.

3.6.2 Measurement and Storage

Once the concrete had cured for 24 hours, the ACPT specimens were demolded, wrapped in new saturated felt and returned to the moist cure room for another 24 hours.

Initial length and mass measurements were taken before autoclave testing. The specimen was placed in the comparator and then spun gently, and when the measurement settled on a number,

it was recorded. Mass was taken to provide information for future correlations between absorption and expansion.

All specimens were placed into a specimen storage basket in a commercially available autoclave (Figure 19). Each specimen was stored in a vertical position such that the weight did not rest on the pin. Final test measurements occurred after 24 hours of exposure at 133 °C (271 °F) or 130 °C (266 °F). Specimens were allowed to cool for 1 hour under laboratory conditions and subsequently cooled in a running cool water bath for 15 minutes or until the surface temperature of the specimens had stabilized.

Figure 19. ACPT specimens in autoclave.

At the completion of autoclave testing, expansion values that exceed 0.08 percent indicate a potentially reactive aggregate, while expansions less than 0.08 percent indicate a nonreactive aggregate. This expansion limit is preliminary and may change with further testing. Work conducted using the ACPT is largely exploratory in nature and is excluded from the final aggregate reactivity classifications.

4 Mitigation Test Methods and Procedures

Once aggregate sources have been classified as reactive, the effectiveness of any proposed mitigation method needs to be evaluated. The effectiveness of a mitigation technique is commonly tested using the Mitigated Concrete Prism Test (MCPT) or the Mitigated Accelerated Mortar Bar Test (MAMBT). These tests were conducted on the potentially reactive and reactive Wyoming aggregates including Black Rock, Goton Pit, Knife River, Labarge, Lamax and Worland. Two nonreactive aggregates (Devries Farm and Harris Pit) were also tested using the MAMBT. Fly ash was used as the mitigating agent in both tests. Mitigation testing methods are outlined in Table 13. This section discusses the procedures for each method.

Table 13. Mitigation testing methods.

Test	Specimen Alkali-Boosting	Specimen Size	Storage Environment	Testing Duration
MCPT	1.25%	75 x 75 x 285 mm (3 x 3 x 11.25 inch)	100 percent relative humidity 38 °C (100 °F)	Two years
MAMBT	Unboosted	25 x 25 x 285 mm (1 x 1 x 11.25 inch)	1 N NaOH solution 80 °C (176 °F)	14 days

4.1 Mitigated Concrete Prism Test (MCPT) – ASTM C1293

MCPT is a variation of the CPT that allows the addition of mitigating agents such as supplementary cementitious materials (SCMs). The test uses 75 x 75 x 285 mm (3 x 3 x 11.25 inch) prisms with a water-to-cement ratio between 0.42 and 0.45, a specific proportion of coarse and fine aggregate, and a cementitious content of 420 kg/m^3 (26.2 lb/ft^3). Cement is required to have a total base alkali content of 0.9 ± 0.1 percent Na_2O equivalent which is boosted to 1.25

percent by mass of cement through the addition of NaOH. Testing conditions remain the same as those for the CPT with the exception of exposure time. Measurement beyond the two-year point has been suggested to be impertinent as expansion plateaus due to alkali-leaching at approximately two years (Duchesne and Berube 2001).

Shehata determined that increasing the level of replacement of a particular fly ash further reduced expansion (2000). Twenty-five percent Class F fly ash replacement typically mitigates ASR in reactive aggregates. A particular aggregate is classified as unmitigated if the expansion at two years is equal to or greater than 0.04 percent. The same FHWA classification limits used for CPT test specimens will be applied to the MCPT expansions.

4.1.1 Casting

The concrete was proportioned and mixed according to ASTM C1293 and as outlined in 3.2.1. Table 52 and

Table 53 of Appendix B summarize the materials used in each concrete mixture and give the compressive strengths of the cylinders from each batch. Slump was measured in accordance with ASTM C143. Casting and curing procedures were also the same as the CPT test.

4.1.2 Measurement and Storage

When the concrete had cured for 24 hours, MCPT specimens were removed from their molds and measured using the comparator shown in Figure 22. Next, specimens were placed in the comparator and spun gently; when the displacement transducer settled on a number, it was recorded. Each specimen was labeled with a name and arrow to ensure that it was measured with

the same end up each time. MCPT specimens were removed from the storage environment for 16 ± 4 hours to allow them to cool to room temperature before measurements were taken. All specimens were measured periodically for two years. After each measurement, the specimens were stored with a different end facing up to limit alkali migration. The storage environment, specified by ASTM C1293, is the same as used for CPT testing.

At the end of two years, expansion values that exceed 0.04 percent indicate an unmitigated aggregate, while expansions less than 0.04 percent indicate a mitigated or nonreactive aggregate.

4.2 Mitigated Accelerated Mortar Bar Test (MAMBT) – ASTM C1567

MAMBT is a variation of the ASTM C1260 test modified to allow the testing of mitigated concrete mixes. Despite the authors' concerns about the harsh environmental conditions, the modified ASTM C1260 "can reasonably well reproduce the field performance of SCM in controlling expansion due to ASR" (Fournier et al. 2004).

While the ASTM C1260 test is often described as being controlled by the solution chemistry, the presence of SCMs affects the pore solution chemistry limiting the migration of alkalis during the initial period of testing. SCMs reduce the permeability of the concrete causing an increased period of time for the pore solution to reach equilibrium with the immersion solution. After approximately 14 days, the beneficial effects of the SCMs are negated by the alkali solution. (Berube et al. 1995). The negation of the beneficial effects does not necessarily inply a plateau in the reaction but rather a change in the rate of reaction as alkalis become available to the concrete.

MAMBT aggregate gradation is the same as that outlined in 3.3.1. ASTM C1567 dictates that fine aggregate be used in testing unless there were specific concerns regarding the coarse portion of the aggregate. Fine aggregates were used in all 1567 testing.

4.2.1 Casting

ASTM C1567 requires a cement-to-aggregate ratio of 1:2.25 and a water-to-cement ratio of 0.47 by mass. Twenty-five percent of the cement by mass was replaced with fly ash for mitigation testing. ASTM C1260 mixing and casting procedures were followed, Section 3.3.1.

4.2.2 Measurement and Storage

Measurement and storage procedures follow the ASTM C1567 standard. After casting, the specimens were placed in a fog room conforming to ASTM C511 for 24 hours. Bars were then demolded, and initial length measurements were taken. The bars were placed in a tap water solution at 80 °C (176 °F) for 24 hours and measured again before they were placed in a 1 normal (N) NaOH solution at 80 °C (176 °F). The bars were measured periodically, in accordance with the standard, for 14 days after immersion in the NaOH solution. Expansion measurements were continued for an additional 42 days to study long-term behavior of mitigated specimens.

Specimen lengths are measured by a comparator reading. A single bar was removed from the soak solution container and toweled dry. It is then placed in the length comparator and gently spun. The smallest reading displayed on the indicator during the spinning process indicates that the bar was plumb. The bar was then set aside, out of the container, while the other specimens

were measured. Percent expansion was calculated using a 254 mm (10 inch) gauge length. The mix is considered innocuous if the 14 day expansion is less than 0.10 percent.

5 Materials and Equipment

Aggregates, cements, and admixtures used in the testing process are described in the following materials section. Equipment, including mixers and storage ovens, is discussed in Section 5.2.

5.1 Materials

Eight different aggregate sources were evaluated in this research. Names, locations, and abbreviations used in this document are identified in Table 1 and Figure 1. Additional aggregate was procured for several pits in 2013 and is denoted by the addition of UW to the original abbreviation. For example, additional Knife River aggregate is denoted as KRUW. Table 14 contains aggregate properties based on aggregate as it was received from the source.

Table 14. Aggregate properties.

	Coarse Aggregate			Fine Aggregate	
Aggregate Name	**Specific Gravity (SSD)**	**Absorption**	**Unit Weight (pcf)**	**Specific Gravity (SSD)**	**Absorption**
Black Rock	2.59	1.80%	97.7	2.60	2.15%
Devries Farm	2.52	2.19%	96.6	2.61	1.56%
Goton Pit	2.58	1.07%	99.0	2.63	1.01%
Harris Pit	2.60	1.83%	97.2	2.62	2.25%
Knife River	2.66	0.67%	98.8	2.63	0.91%
Knife River UW	2.64	0.75%	98.8	2.93	2.86%
Labarge	2.60	0.67%	98.8	2.62	1.05%
Lamax	2.54	2.02%	97.7	2.60	1.81%
Worland	2.55	1.45%	99.0	2.61	1.56%
Worland UW	2.58	1.77%	99.0	2.27	2.63%

Holcim Type I/II cement was used for all concrete mixtures in this research. Two individual batches of cement were used. Both batches were analyzed in accordance with ASTM C114. Results of these analyses are included in Figure 78 and Figure 79 in Appendix C. Total

alkalinity, measured as Na_2O equivalent, of the two batches was measured to be 0.706 percent and 0.710 percent, respectively.

Technical grade NaOH pellets were purchased from the chemical stockroom and used to make a solution for mitigated and unmitigated AMBT and to boost the alkalinity of field specimens, CPT, and ACPT prisms. A polycarboxylate-based superplasticizer was also added to improve workability for field and CPT specimens. Air entrainment composed of a blend of high-grade saponified rosin and organic acid salts was added to the field specimen mixtures.

Fly ash from Craig, CO was used for mitigation of ASR. Fly ash was analyzed in accordance with ASTM C311. The fly ash was tested to have a 0.70 percent Na_2O content and a 9.67 percent CaO content. This fly ash is classified as Class F according to ASTM C618. Full analysis results are included in Figure 80 of Appendix C.

Martin Marietta Beckmann aggregate is nonreactive and was used to isolate reactivity of coarse and fine aggregates for ACPT testing. Nonreactivity was confirmed according to ASTM C1260, as shown in Figure 20 and Figure 21. The horizontal dashed lines represent the reactivity limits. The vertical dashed lines indicate the classification time of 14 days.

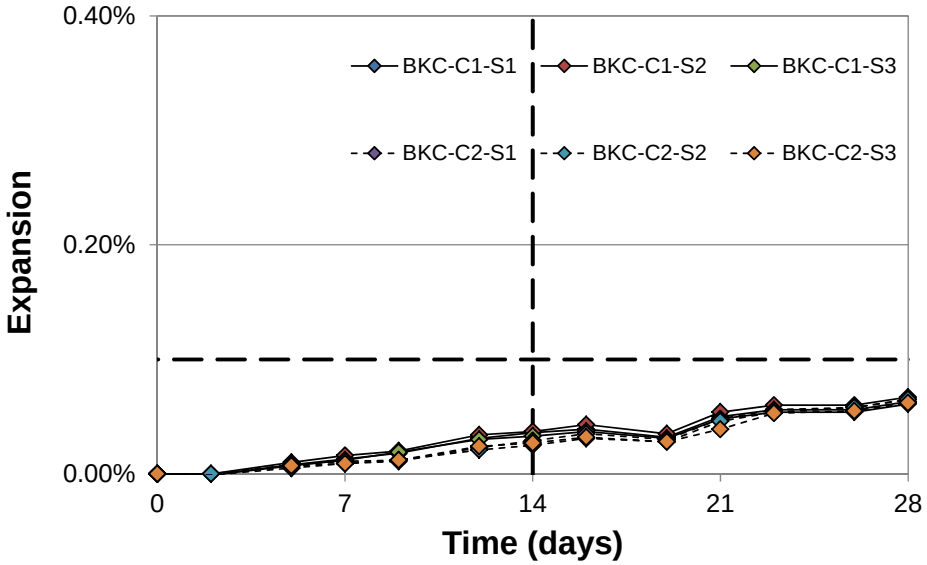

Figure 20. ASTM C1260 Beckmann coarse aggregate results.

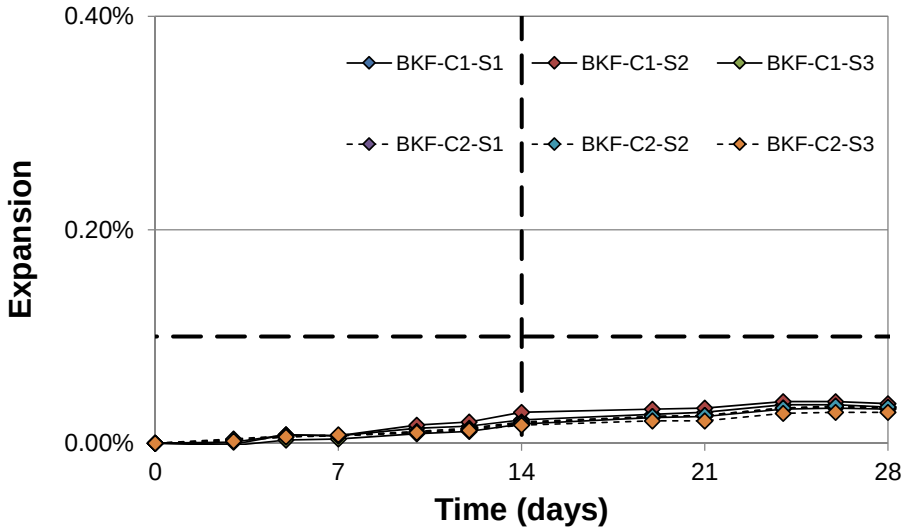

Figure 21. ASTM C1260 Beckmann fine aggregate results.

5.2 Equipment

A length comparator was used to measure the length change of the accelerated test specimens. A fixed height and an adjustable height comparator, shown in Figure 22, were used in the

measurement of these specimens. An experimental error study was conducted by measuring the reference bar, for each comparator, twenty times. The measurement error was smaller than the displacement gage resolution.

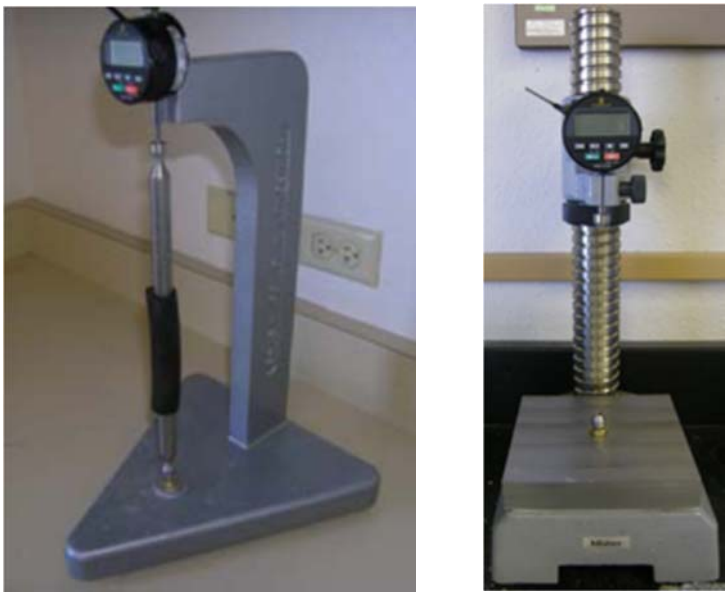

a) b)

Figure 22. Length comparators: a) fixed height and b) adjustable height.

A mechanical strain gauge with a digital indicator was used to measure field specimen expansion in this research. The instrument is shown in Figure 23.

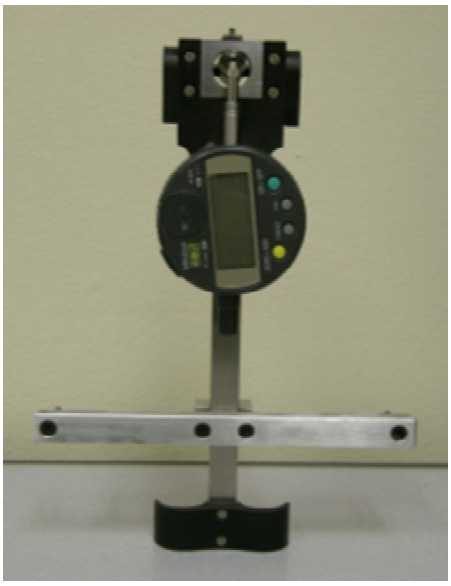

Figure 23. Demec mechanical strain gauge instrument.

An analysis of measurement error using the strain gauge was conducted by measuring the supplied reference bar twenty times. Error was determined to be 1.2 micrometers (0.47×10^{-6} inch). A separate analysis was conducted to determine the effects of rotation on the readings. Reference bar readings were taken perpendicular to the surface and at five and 10 degrees toward and away from the researcher. A total of 15 sets of measurements were taken. T-tests were conducted to determine variations in measurements based on rotation toward and away from the researcher as well as comparing the perpendicular readings to the tilted measurements. Measurements at five degrees of rotation did not show significant variation based on forward and back tilt (p-value = 0.668), while significant difference was determined for the same measurements conducted at 10 degrees of rotation (p-value = 0.049). At larger angles, the direction of tilt from perpendicular becomes significant. All rotated measurements greater than five degrees were determined to be significantly different than their paired perpendicular measurements with p-values ranging from 0.000 to 0.013. The largest error observed in this

investigation was 0.138 and 0.184 percent of the reference length for five and ten degrees of rotation, respectively. This error corresponds to three micrometers (0.118×10^{-3} inch) and 4 micrometers (0.157×10^{-3} inch), respectively.

Various scientific ovens were used for accurate temperature control during the storage of AMBT, MAMBT, CPT, and MCPT specimens. One such oven is shown in Figure 24. Each oven was checked for spatial temperature consistency before use and during testing.

Figure 24. Storage oven.

A commercially-available sanitizer, or autoclave, was used to conduct the ACPT. The machine was required to maintain 0.2 MPa (29 psi) of pressure for 24 hours. The model selected is shown in Figure 25.

Figure 25. Autoclave.

6 Classification Test Results

This chapter outlines the classification test results for the eight Wyoming aggregate sources. The aggregate sources are classified based on field exposure, Concrete Prism Test (CPT), and Accelerated Mortar Bar Test (AMBT) programs. Results are presented by test. The chapter concludes with an evaluation of the exploratory Autoclaved Concrete Prism Test (ACPT).

6.1 Field Exposure Test Results

Field exposure testing was conducted on 28 field exposure blocks. These specimens include both boosted and unboosted specimens for a variety of aggregates. Boosting increases alkali content in an effort to speed reaction, while unboosted specimens contain naturally occurring alkalis from the cement. Representative expansions for highly reactive, moderately reactive, and nonreactive aggregates are included in Figure 26.

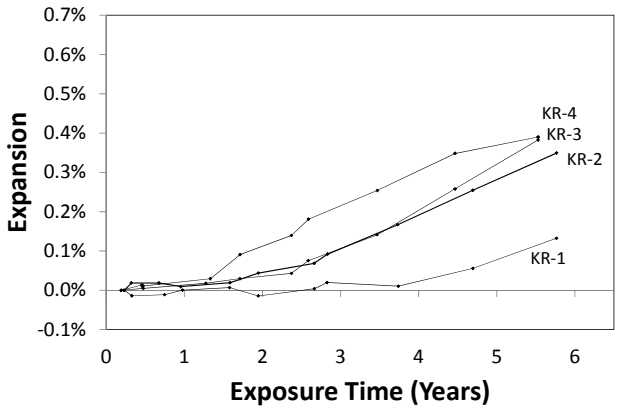

a)

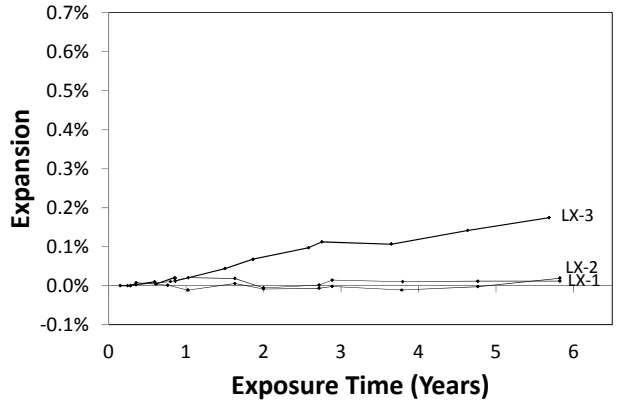

b)

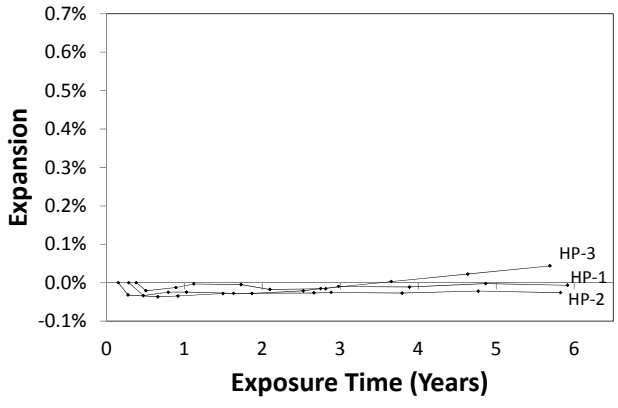

c)

Figure 26. Representative field exposure expansion. a) highly reactive aggregate, b) moderately reactive aggregate and c) nonreactive aggregate.

At the start of this project there were only a few field exposure sites. That number had grown to 23 by 2012 (Ideker et al. 2012). Because limited testing has been conducted, little work has been done and published to date on the establishment of expansion limits for reactivity classification. The Wyoming ASR research group has developed preliminary limits in the hope of providing future guidelines for field classifications, in addition, to using these findings as a basis of classifying a particular aggregate source.

The measured field expansion curves are generally linear with a plateau that represents the completion of the reaction. The research group decided to base the evaluation of the aggregate at the point of greatest expansion after five years. Limits were proposed using a linear relationship relating the exposure time and the expansion. Limits were developed based on the results for the boosted specimens for the eight Wyoming aggregate sources which had fallen naturally into three groups. In this manner, proposed expansion limits are a 0.02 percent increase in expansion per year separating nonreactive from moderately reactive specimens and a 0.06 percent increase in expansion per year separating moderately reactive and highly reactive aggregates. Half of these limits are applied to unboosted specimens; 0.01 percent for nonreactive to moderately reactive and 0.03 percent for moderately reactive to highly reactive. Both boosted and unboosted data and limits are plotted in Figure 27. For example, unboosted Knife River block expansion met the classification limit line at three and a half years. Unboosted Goton Pit and Worland reached the moderately reactive classification line at approximately four and a half years. Individual specimen expansion graphs are included in Appendix D.

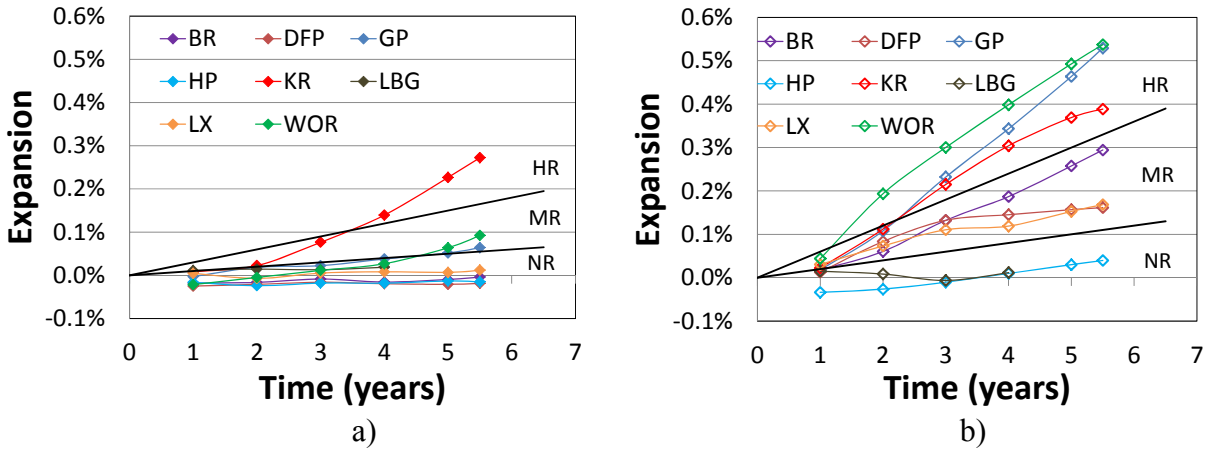

Figure 27. Expansion limits for a) unboosted and b) boosted field exposure specimens.

If classification limits continue to increase with time and measured aggregate expansion plateaus, the reactivity classification could appear to be reduced. In such a case, the harshest classification at any given time would still apply to this aggregate.

Average expansion values and failure ratios for each aggregate are included in Table 15. Expansion measurements are taken at five years unless otherwise noted. Failure ratios are defined as the measured expansion divided by a particular expansion limit. Values greater than one indicate the measured expansion exceeds the limit.

Table 15. Field exposure test results at five years.

	Average Expansion		Failure Ratio		Classification	
Pit	**Field Specimen Unboosted**	**Field Specimen Boosted**	**Field Specimen Unboosted**	**Field Specimen Boosted**	**Field Specimen Unboosted**	**Field Specimen Boosted**
BR	Negligible	0.258%	-	MR: 2.58 HR: 0.86	Nonreactive	Moderately Reactive
DFP	Negligible	0.157%	-	MR: 1.57 HR: 0.52	Nonreactive	Moderately Reactive
GP	0.052%	0.464%	MR: 1.03 HR: 0.34	MR: 4.64 HR: 1.55	Moderately Reactive	Highly Reactive
HP	Negligible	0.030%	-	MR: 0.30 HR: 0.10	Nonreactive	Nonreactive
KR	0.159%	0.369%	MR: 3.17 HR: 1.06	MR: 3.96 HR: 1.23	Highly Reactive	Highly Reactive
LBG *	0.011%	0.022%	MR: 0.25 HR: 0.08	MR: 0.22 HR: 0.07	Nonreactive	Nonreactive
LX	0.007%	0.153%	MR: 0.14 HR: 0.05	MR: 1.54 HR: 0.51	Nonreactive	Moderately Reactive
WOR	0.064%	0.493%	MR: 1.28 HR: 0.43	MR: 4.93 HR: 1.64	Moderately Reactive	Highly Reactive

* Expansion measurements taken at 4.5 years

Most field specimens for the same aggregate and boosting condition exhibited similar expansion for all specimens; two exclusions to this were the Black Rock boosted and the Knife River unboosted specimens. The Black Rock BHC-3 specimen has approximately three times the expansion of the BHP-3 specimen shown in Figure 28. BHC and BHP represent two separate shipments of aggregate from the Black Rock pit. Similar behavior is observed in the unboosted Knife River specimens in which specimens KR-2 and KR-3 expansion is approximately three times more than the KR-1 specimen. There is currently no explanation for these variations within the aggregate sources but it is believed to relate to variation in the aggregate reactivity.

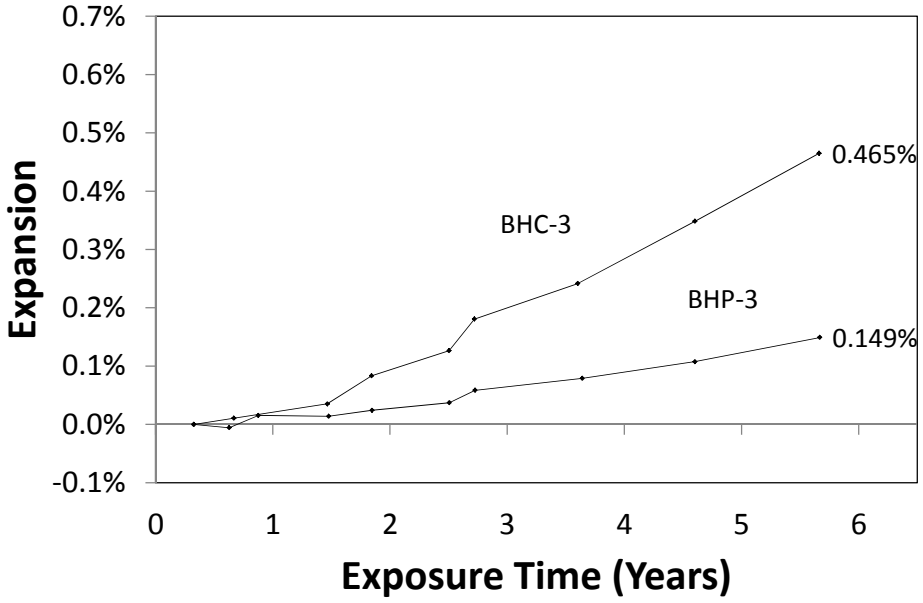

Figure 28. Field exposure results for Black Rock boosted specimens.

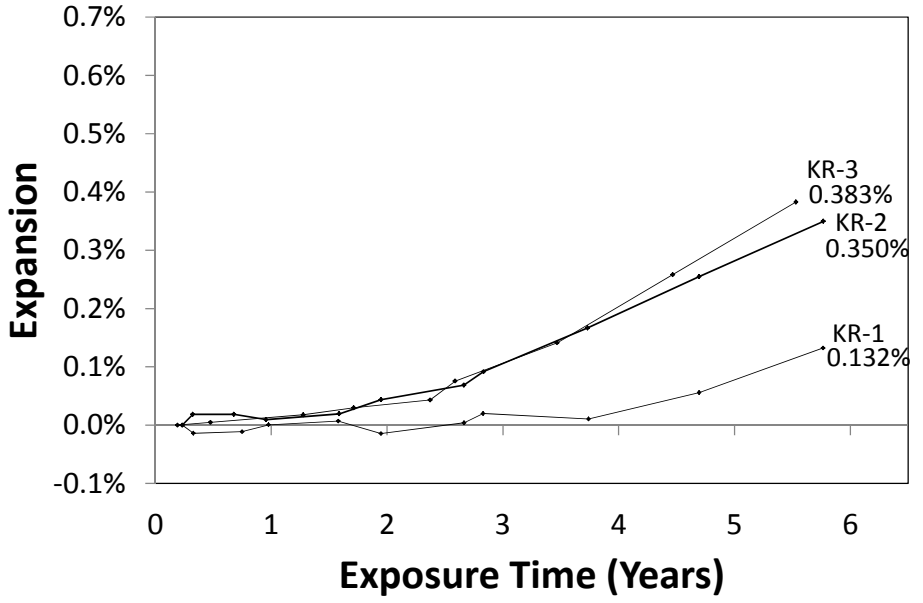

Figure 29. Field exposure results for Knife River unboosted specimens.

Additional field exposure testing is being conducted for the Knife River aggregate source by The University of Texas at Austin (UT) ASR research group. Results for both research groups are shown in Figure 30. All specimens are air-entrained. Although UW field blocks are slower to start expanding, it is interesting to note that the cold climate exposure blocks reached the same expansion levels as the warm climate expansions at approximately five years. Testing by both research groups indicate highly reactive average expansive for the unboosted specimens at five years.

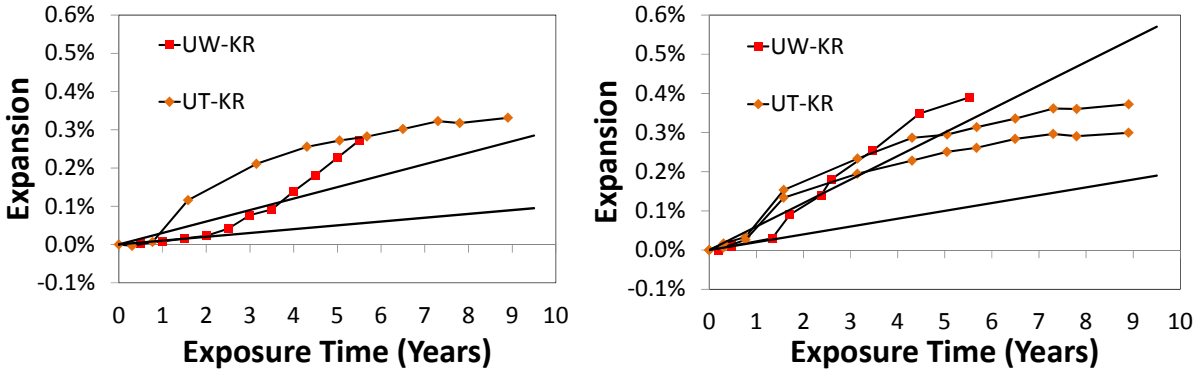

Figure 30. Comparison of average UW to UT field exposure expansion for Knife River - a) unboosted and b) boosted.

It has been noted that field specimens will exhibit different expansions based on the face that is being measured. This was true for Wyoming field specimens as well. Representative expansion graphs for unboosted KR-3 and boosted KR-4, Figure 31, are included to illustrate this variation. The average top expansion for the KR-3 specimen was 3 times the side expansion compared to 2.2 times for the KR-4 specimen. In general, top expansions ranged from two to four times the side expansions. This difference is attributed to increased water penetration on the top of the blocks. Separate measurements of these faces lends better understanding of the expansion that is

experienced in concrete configurations such as slabs and pavements versus walls. Wyoming field specimen measurements are evenly divided between top and side measurements. A total of six vertical and six horizontal expansions are recorded and averaged.

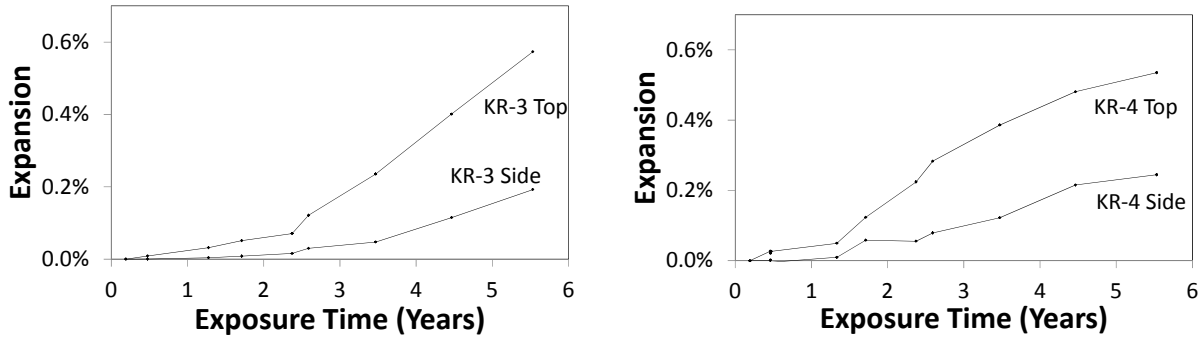

a) b)

Figure 31. Comparison of top and side field specimen expansion for a) unboosted and b) boosted specimens.

6.2 Petrography

Cores were taken from the side of each of the field blocks and measured 95 mm (3 ¾ in) in diameter and approximately 102 mm (4 in) in length. The outer surface was formed and the inner surface was fractured, such that the core was only a portion of the through thickness of the block and can be seen in Figure 32.

Figure 32. Core Specimen.

Table 16 summarizes the geological composition of the aggregates in order of decreasing abundance.

Table 16. Geological composition of the aggregates.

Aggregate	Major	Other
Black Rock	Rhyolite	Andesite, Quartzite, and Limestone
Goton	Rhyolite	Granite, Quartzite, Andesite, and Chert
Knife River	Granitic	Rhyolite
Labarge	Granitic	Quartzite
Lamax	Rhyolite	Andesite, Quartzite, Limestone, and Dioritic
Worland	Rhyolite	Quartzite, Andesite, Granite, and Limestone

Note: Non-reactive aggregates are not included in this table.

This petrographic analysis used the same classification scale established for the 2010 study and is outlined in Table 17.

Table 17. Petrographic classification scale.

ASR Presence Ranking	Description
None	No evidence of ASR.
Negligible	Reaction rims abundant; no micro cracking linked to ASR observed.
Minor	Reaction rims observed, rare microcracks associated with ASR; gel deposits occasionally present.
Moderate	Microcracks filled with ASR commonly cut paste; deposits of gel commonly observed in voids.
Severe	Macroscopic cracks and microcracks filled with ASR gel commonly observed; abundant reaction rims and gel deposits in voids commonly observed.

Initially, the cores were analyzed using standard optical petrographic examination. The samples were then subjected to an elevated temperature/relative humidity exposure test. This involved partially submerging the polished slab in water in an air-tight container in an oven for 72 hours. This provided an environment with 100 percent relative humidity and an elevated temperature of 40.5˚C (105˚F). The exudations produced through this process were subjected to scanning electron microscopy (SEM) with energy-dispersive x-ray spectrometry (EDS) to document the chemical composition of the gel.

Upon initial examination, the only evidence of ASR observed from the standard petrographic examination was the presence of reaction rims on various aggregate particles. There were no observations of deposits of gel, microcracks associated with reactive aggregates, or other evidence of ASR in any core. After increasing the RH and temperature of the specimens, the secondary examination revealed that there were exudation sites present in all six cores. A SEM/EDS analysis of the exudations confirmed the gel composition was consistent with ASR gel. The petrographer concluded that this was indicative of the presence of ASR in the cores that

has not progressed to the point where microcracking and gel deposits have formed in microcracks or voids.

Table 18. Petrographic classification.

Aggregate	Rating	Exudation Sites
BR	None	8
GP	Negligible	36
KR	Negligible	16
LBG	Negligible	33
LAX	Negligible	35
WOR	Negligible	19

The petrographer classified five of the six specimens as negligible based on the presence of reaction rims. However, petrographic examination validated that ASR gel is present in each of the six cores. One aggregate classified as “None”, Black Rock, did show the presence of ASR gel in exudation sites, only on a lower scale than its counterparts. Using this data, it is impossible to complete a final classification of the potential deleterious reactivity of the aggregates. It does confirm that ASR gel exists in the blocks and helps in proving that ASR is responsible for at least a portion of the expansion in the field blocks. Observations of ASR activity for the individual aggregate sources are included in Appendix D.

After approximately 6 years, the ASR reaction is still progressing with no way of knowing the length of time it will take until the reaction reaches completion. This emphasizes the need for long term studies using field blocks. Long term studies provide the best tactic to approximating the in-service conditions of the concrete and can accommodate the length of time required for the ASR to be competed. Long term data can be a basis for potential expansion predictions of in-service concrete. It also helps to establish expansion curves for specific aggregates. Therefore,

there is merit in trying to mimic field concrete by more closely approximating field conditions using the block specimens.

6.3 CPT Results

Concrete prism testing was conducted by Fertig on the eight Wyoming aggregate sources. Figure 33 shows the expansions with respect to time for each pit. Each figure indicates the 0.04 percent limit separating nonreactive and moderately reactive aggregates and the 0.12 percent expansion limits separating moderately reactive and highly reactive aggregates as horizontal dashed lines (FHWA 2012). Most specimens exhibited minor contraction followed by expansions that plateaued during the test.

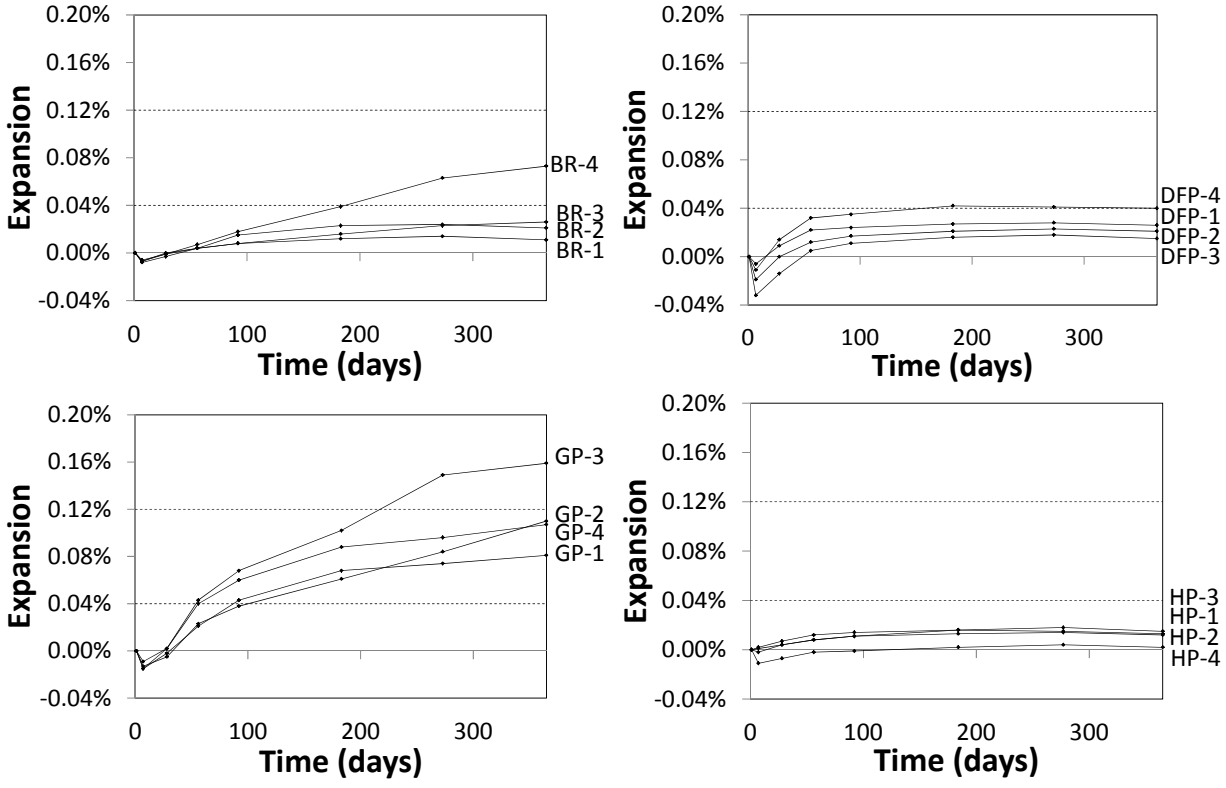

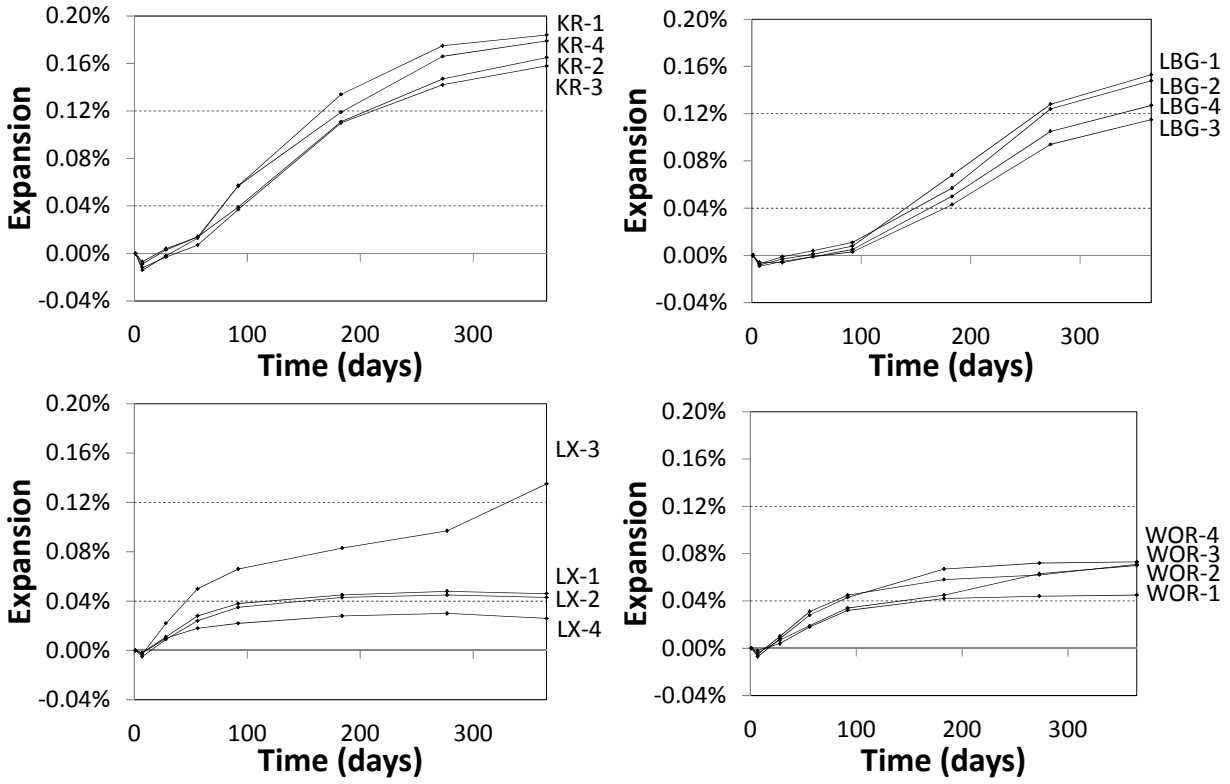

Figure 33. Individual ASTM C1293 results. (Fertig 2010).

While most aggregates exhibit similar behavior throughout the testing period, Black Rock, Goton Pit, and Lamax each have a single specimen that exceeds the average expansion by at least 40 percent. For example, LX-3 experienced over three times the average expansion of the remaining three, while the BR-4 experienced approximately two times the expansion of the other specimens. The effects of the more reactive Lamax specimen were not significant enough to change the aggregate classification and therefore the source was not retested. In other words, the average Lamax expansion, 0.063 percent, exceeded the 0.04 percent limit. Although the average Black Rock expansion was 0.033 percent, the most expansive Black Rock specimen warranted further testing.

An additional eight Black Rock specimens were cast to further investigate. Results are shown in Figure 34. These specimens were cast as a single batch and stored in two separate airtight containers represented and are differentiated on the graph by the use of solid and dashed line styles. Each bucket had a single specimen exhibiting more expansion than the remaining three. The one-year average expansion value for the prisms is 0.064 percent. Although recasting the specimens did not confirm that Fertig BR-4 specimen was an outlier, the increased data set shows the variability that may occur within a batch.

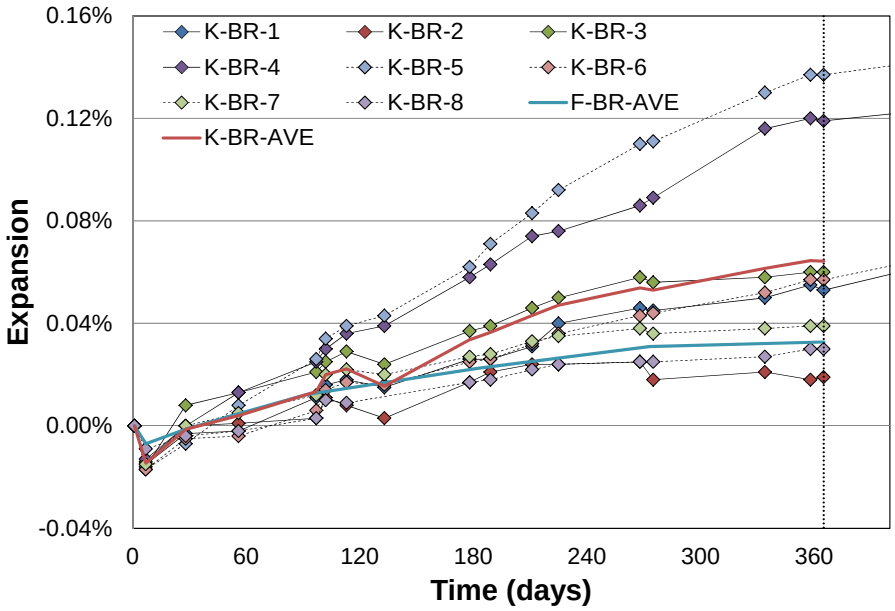

Figure 34. ASTM C1293 results for Black Rock aggregate.

Average expansion for all four Fertig specimens and all eight Kimble specimens are 0.033 percent and 0.064 percent, respectively. Because the expansion of the complete data set exceeds the 0.04 percent expansion limit at one year, the aggregate is classified as moderately reactive based on the CPT.

Average expansion values, failure ratios, and classifications at one year for all aggregates are presented in Table 19. Failure ratios are the proportion of measured expansion to the expansion limit, 0.04 percent for nonreactive to moderately reactive and 0.12 percent for moderately reactive to highly reactive. Values greater than one indicate reactive expansion while values less than one indicate nonreactive aggregates. The test results are presented graphically in Figure 35. Failure ratios presented in the graph are for the highest expansion limit exceeded.

Table 19. ASTM C1293 test results.

Pit	Average Expansion (%)	Failure Ratio	Classification
BR	0.054	MR: 1.34 HR: 0.45	Moderately Reactive
DFP	0.026	MR: 0.64 HR: 0.21	Nonreactive
GP	0.114	MR: 2.86 HR: 0.95	Moderately Reactive
HP	0.011	MR: 0.26 HR: 0.09	Nonreactive
KR	0.172	MR: 4.30 HR: 1.43	Highly Reactive
LBG	0.136	MR: 3.40 HR: 1.13	Highly Reactive
LX	0.063	MR: 1.56 HR: 0.52	Moderately Reactive
WOR	0.065	MR: 1.62 HR: 0.54	Moderately Reactive

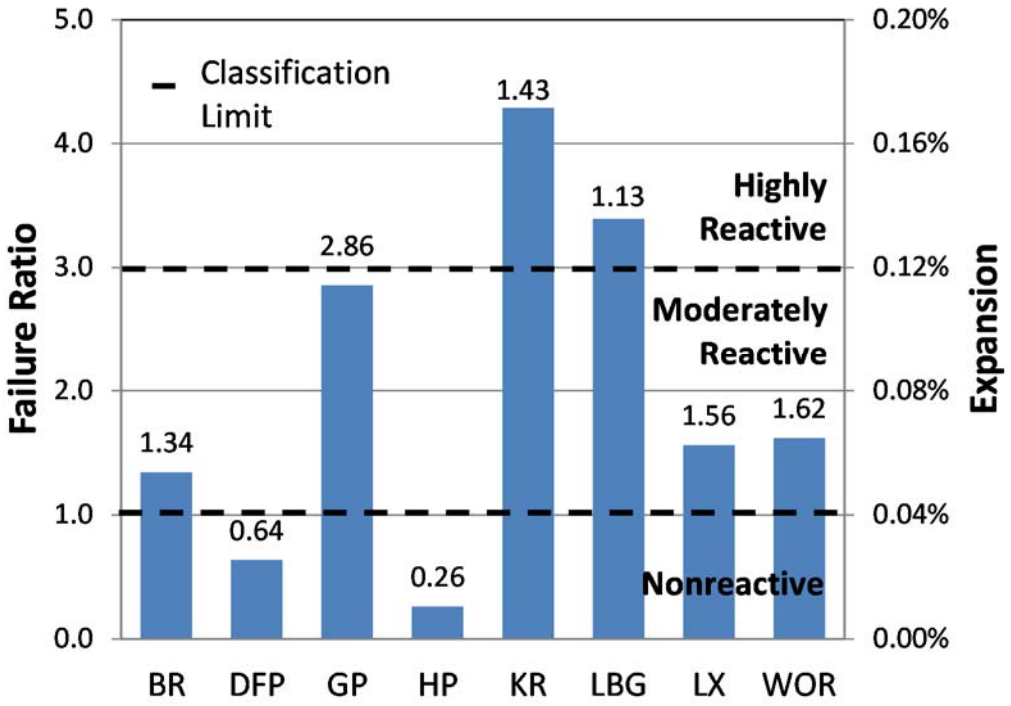

Figure 35. ASTM C1293 test results.

6.4 AMBT Results

The AMBT has been run by researchers Fertig (2010) and Hacker (2014) of the Wyoming ASR research group for classification purposes. Both Fertig and Hacker tested a 60 to 40 percent crushed coarse to fine aggregate blend. Additionally, Hacker tested the fine and crushed coarse components separately to compare expansion results for the different size fractions. The compilation of this testing is used here to evaluate variations in expansion results and provide a better picture of the reactivity of each given aggregate. Expansion with respect to time for each aggregate is presented alphabetically by pit in Figures 36 to 43. Dashed horizontal lines represent the 0.10 percent expansion limit separating nonreactive and moderately reactive aggregates, the 0.30 percent limit distinguishing moderately reactive and highly reactive aggregates, and the 0.45 percent expansion limits characterizing the boundary between highly reactive and very

highly reactive aggregates (FHWA 2012). The vertical dashed lines shows the classification time.

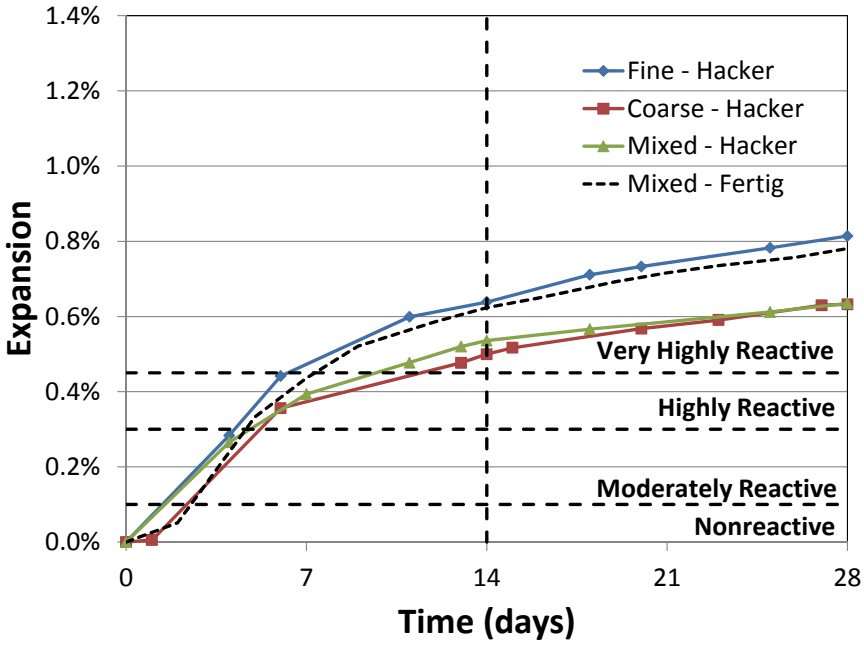

Figure 36. ASTM C1260 test results for Black Rock.

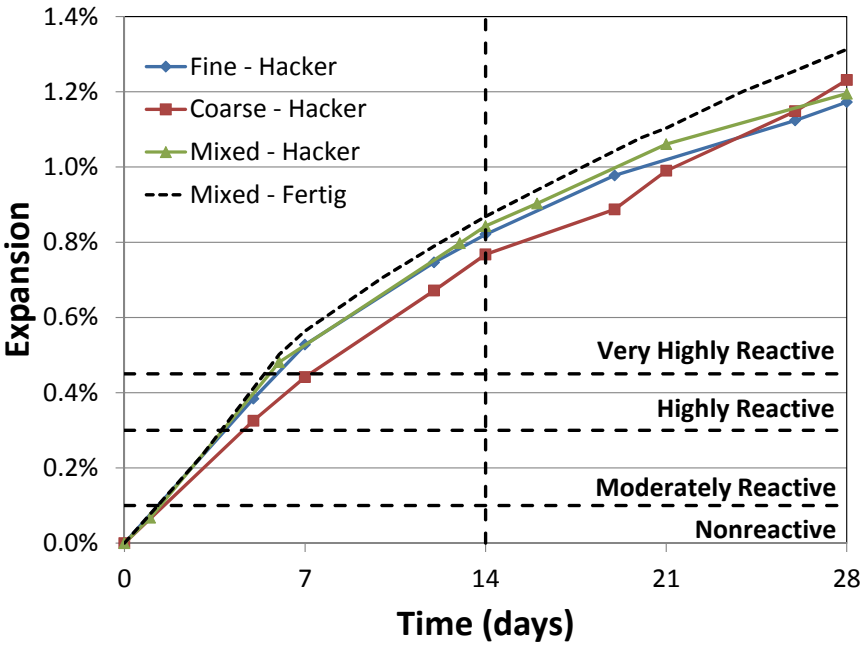

Figure 37. ASTM C1260 test results for Devries Farm.

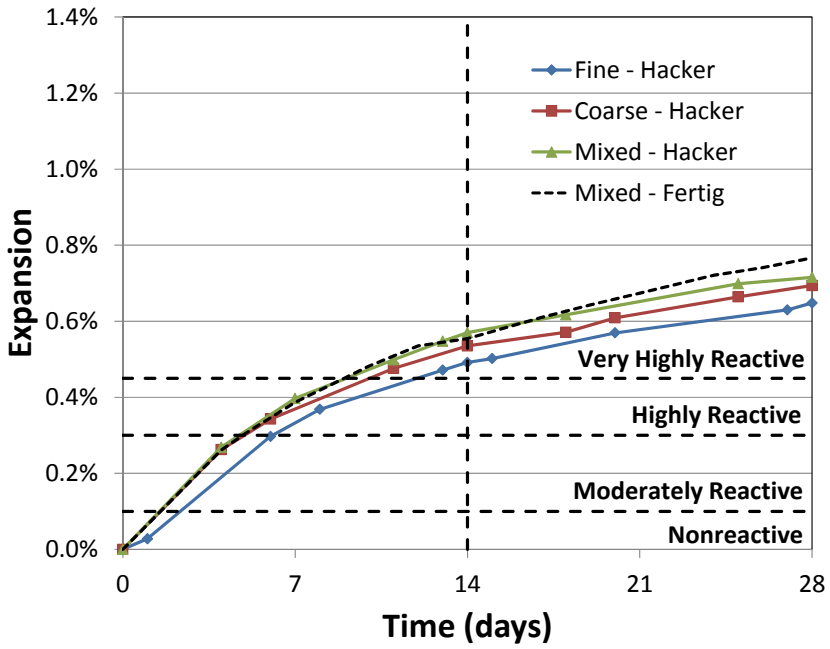

Figure 38. ASTM C1260 test results for Goton Pit.

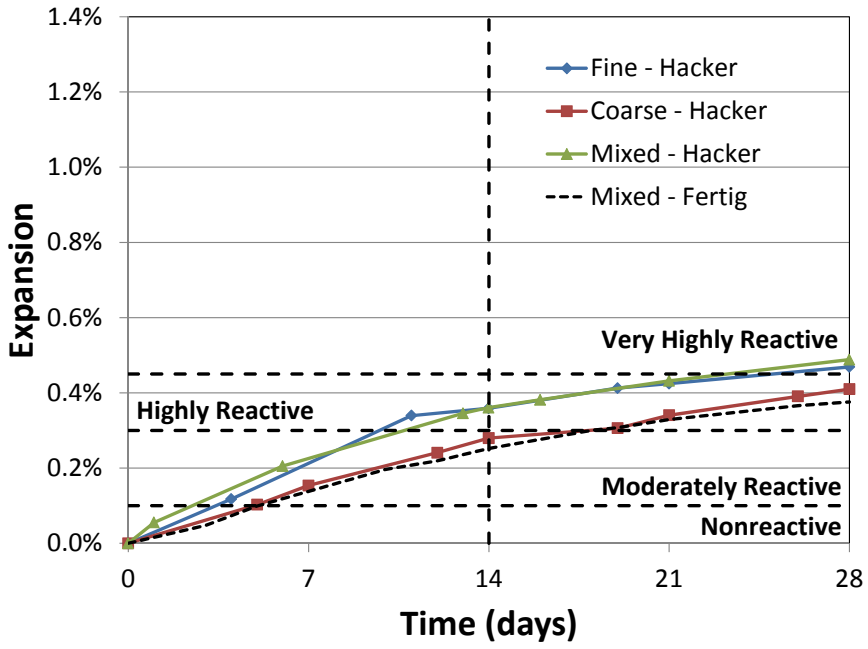

Figure 39. ASTM C1260 test results for Harris Pit.

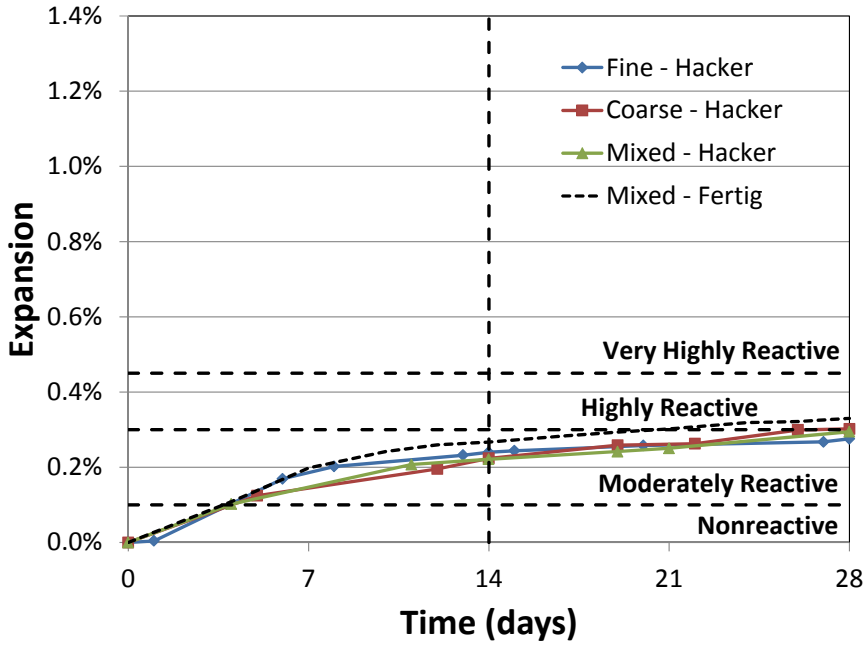

Figure 40. ASTM C1260 test results for Knife River.

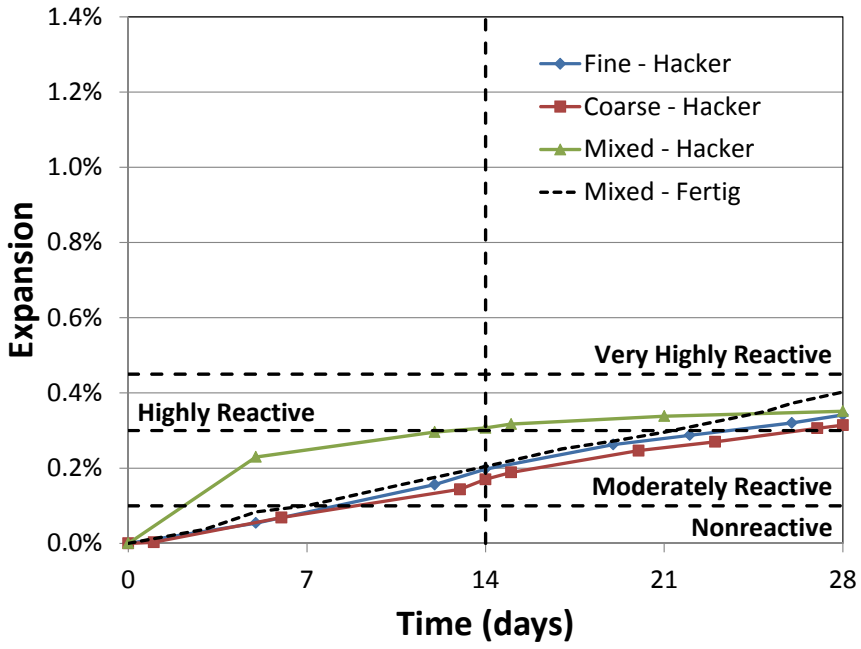

Figure 41. ASTM C1260 test results for Labarge.

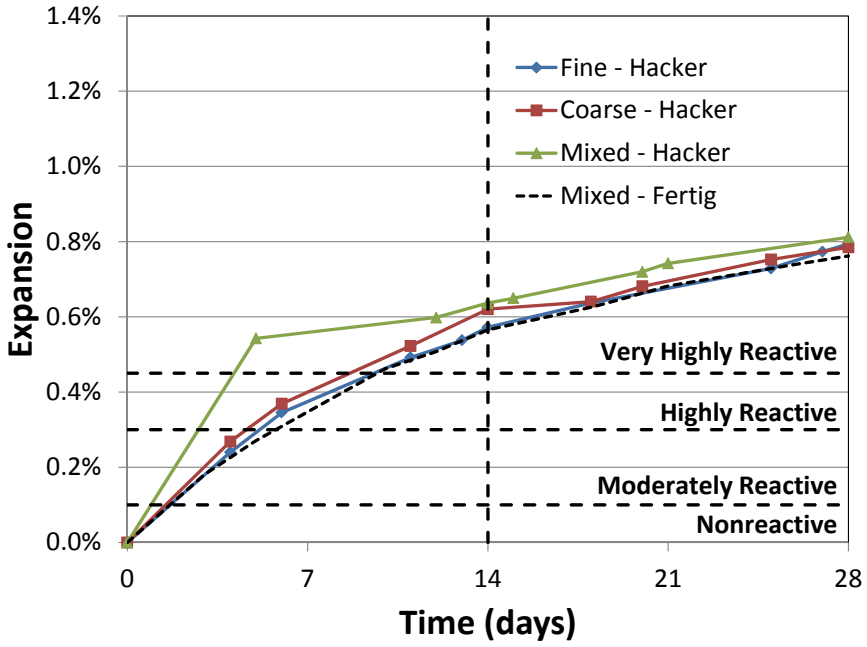

Figure 42. ASTM C1260 test results for Lamax.

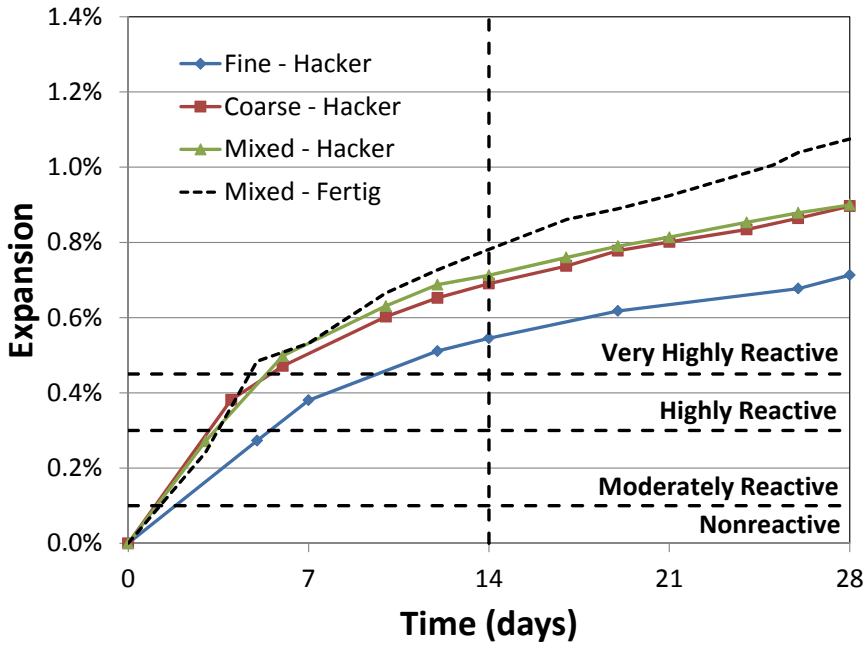

Figure 43. ASTM C1260 test results for Worland.

Average expansion values, failure ratios and classifications for each pit are shown below in Table 20. Expansions for coarse, fine and mixed AMBT are included in Table 54 in Appendix D. With the exclusion of Harris Pit aggregate, all aggregates were classified the same regardless of component being tested. The Harris Pit fine aggregate was classified highly reactive compared to the moderately reactive coarse and mixed test results. Failure ratios are the proportion of measured expansion to the expansion limit, 0.10 percent separating nonreactive and moderately reactive aggregates, 0.30 percent differentiating moderately reactive and highly reactive aggregates, and 0.45 percent splitting highly reactive and very highly reactive aggregates. Values greater than one indicate the higher reactivity level. The test results are presented graphically in Figure 44. Failure ratios presented in the graph are for the highest expansion limit exceeded.

Table 20. ASTM C1260 test results.

Pit	Average Expansion (%)	Failure Ratio	Classification
BR	0.598	MR: 5.98 HR: 1.99 VHR: 1.33	Very Highly Reactive
DFP	0.844	MR: 8.44 HR: 2.81 VHR: 1.88	Very Highly Reactive
GP	0.543	MR: 5.43 HR: 1.81 VHR: 1.21	Very Highly Reactive
HP	0.299	MR: 2.99 HR: 0.998 VHR: 0.67	Moderately Reactive
KR	0.248	MR: 2.48 HR: 0.83 VHR: 0.55	Moderately Reactive
LBG	0.215	MR: 2.15 HR: 0.72 VHR: 0.48	Moderately Reactive
LX	0.588	MR: 5.88 HR: 1.96 VHR: 1.31	Very Highly Reactive
WOR	0.716	MR: 7.16 HR: 2.39 VHR: 1.59	Very Highly Reactive

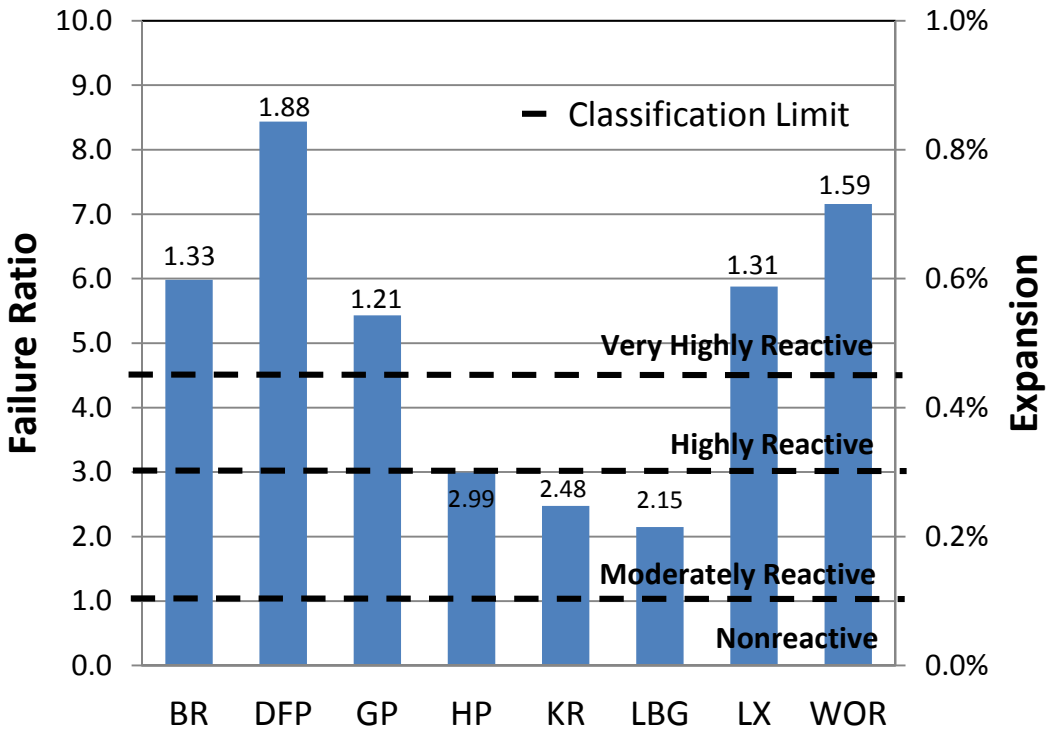

Figure 44. ASTM C1260 test results.

6.5 Discussion of Results

The results from the UW ASR research group classification testing are presented in Table 21. All results are presented as failure ratios comparing measured expansion to the classification limits presented in Sections 6.1, 6.3 and 6.4. Values greater than one indicate reactive expansion while expansions less than one result in lower classification or non-reactivity.

Petrography results for the recent study concluded that a portion of the expansion experienced in the field specimens is attributed to ASR. At that time, the study was unable to classify the reactivity of the aggregates and is therefore excluded from the determination of aggregate reactivity.

Table 21. Classification failure ratios.

Pit	Field Specimen Unboosted	Field Specimen Boosted	CPT	AMBT
BR	Negligible	MR: 2.58 R: 0.86	MR: 1.34 HR: 0.45	MR: 5.98 HR: 1.99 VHR: 1.33
DFP	Negligible	MR: 1.57 R: 0.52	MR: 0.64 HR: 0.21	MR: 8.44 HR: 2.81 VHR: 1.88
GP	MR: 1.03 R: 0.34	MR: 4.64 R: 1.55	MR: 2.86 HR: 0.95	MR: 5.43 HR: 1.81 VHR: 1.21
HP	Negligible	MR: 0.30 R: 0.10	MR: 0.26 HR: 0.09	MR: 2.99 HR: 0.998 VHR: 0.67
KR	MR: 3.17 R: 1.06	MR: 3.96 R: 1.23	MR: 4.30 HR: 1.43	MR: 2.48 HR: 0.83 VHR: 0.55
LBG	MR: 0.25 R: 0.08	MR: 0.22 R: 0.07	MR: 3.40 HR: 1.13	MR: 2.15 HR: 0.72 VHR: 0.48
LX	MR: 0.14 R: 0.05	MR: 1.54 R: 0.51	MR: 1.56 HR: 0.52	MR: 5.88 HR: 1.96 VHR: 1.31
WOR	MR: 1.28 R: 0.43	MR: 4.93 R: 1.64	MR: 1.62 HR: 0.54	MR: 7.16 HR: 2.39 VHR: 1.59

It is generally accepted that field exposure testing provides the most accurate evaluation of aggregate reactivity for a given mix design. Using field exposure as a primary classification test is impractical, however, due to the extended testing period.

The CPT is generally considered the most accurate of the accelerated testing methods because the testing conditions most closely mimic normal concrete exposure. CPT is a preferable test because it is able to test both coarse and fine aggregate constituents without crushing. Although

the CPT provides results that closely match field performance, its use is disadvantaged by the one-year testing period.

The AMBT has become the most commonly used test due to the short testing duration. Harsh conditions of this test are attributed to problems with false negative and positive results, however. Some of these problems may be seen in testing conducted at the University of Wyoming when AMBT results are compared to the results of the other methods. Although many of the aggregates in the testing set are reactive, Devries Farm and Harris Pit are nonreactive aggregates. The fact that all aggregates are classified as reactive confirms the harshness of this test. For example, Devries Farm which is normally a nonreactive aggregate shows the highest average expansion in this testing set. Devries Farm expansions are small when exposed to low alkali environments. Measurements show that Devries Farm expansions increase dramatically with increased alkali content. All of these observations indicate that Devries Farm aggregates are sensitive to alkali loading. The AMBT classification for Devries Farm is likely, based on field exposure and historic behavior, a false positive. Knife River results, alternatively, show the second lowest expansion in the testing set and have a history of poor field performance. These two examples show that the AMBT should be used with caution due to problems of false positives and negatives.

Evaluating all of the advantages and disadvantages of the testing methods and conditions, the research team based classification primarily on field exposure and CPT results. Unboosted field results are used because the lower alkali levels approximate field conditions; on the other hand, boosted field specimens expansions provide expansion data more quickly. Initial classifications are primarily based on result of unboosted field and CPT expansions. These classifications are

then adjusted, using engineering judgment, to account for additional reactivity potential seen in boosted field specimens. Results and discussion of each aggregate source and individual tests are now presented in alphabetical order.

6.5.1 Black Rock Pit

Individual test results and classifications for Black Rock aggregate are presented in Table 22. Based on moderately reactive CPT results, Black Rock aggregate is classified moderately reactive. Black Rock has shown negligible early reactivity in unboosted field exposure but has exhibited a constant rate of reaction in the boosted field specimens. This is an aggregate that may be slower to show reactivity but exhibits moderate reactivity in both boosted field exposure and CPT thereby maintaining the initial classification.

Table 22. Classification results for Black Rock.

	Classification by Test				
Pit	**Field Specimen Unboosted**	**Field Specimen Boosted**	**CPT**	**AMBT**	**Final Classification**
Failure Ratios	Negligible	MR: 2.58 HR: 0.86	MR:1.34 HR: 0.45	MR: 5.98 HR: 1.99 VHR: 1.33	Moderately Reactive
Classification	NR	MR	MR	VHR	

6.5.2 Devries Farm Pit

Classification test results for Devries Farm aggregate are presented in Table 23. Both unboosted field specimen and CPT expansion classify this aggregate nonreactive. While moderately

reactive boosted field specimen expansions can be used to predict reactivity in the future, that the aggregate expands much more under increased alkali conditions makes the increased expansivity a likely characteristic of the alkali-boosting rather than an indication of future expansion. Because two of the three classification test results indicate a nonreactive aggregate, Devries Farm aggregate is nonreactive. This aggregate should be used with caution in high alkali situations because of the tendency towards increased expansion at higher alkali contents.

Table 23. Classification results for Devries Farm.

	Classification by Test				
Pit	**Field Specimen Unboosted**	**Field Specimen Boosted**	**CPT**	**AMBT**	**Final Classification**
Failure Ratios	Negligible	MR: 1.57 HR: 0.52	MR: 0.64 HR: 0.21	MR: 8.44 HR: 2.81 VHR: 1.88	Nonreactive
Classification	NR	MR	NR	VHR	

6.5.3 Goton Pit

Individual test results and classifications for Goton Pit aggregate are presented in Table 24. Classification based on unboosted field exposure and average CPT expansion results in a moderately reactive classification.

While Goton Pit aggregate is numerically classified as moderately reactive, the research team sees merit in cautiously classifying this aggregate as highly reactive based on the expansion behavior of the boosted field specimens and the single CPT expansion that falls within the HR category. As seen in Figure 27, boosted field specimens experienced 36 percent greater

expansion than the highly reactive Knife River specimens at 5.5 years. Such expansions warrant a highly reactive classification. On the other hand, the moderately reactive CPT rating is based on the average specimen expansion for the four specimens. One of the four CPT specimens is classified as highly reactive indicating a potential for higher reactivity. While current expansions classify Goton Pit aggregate as moderately reactive, the behavior of the boosted field specimens and the variation in one individual CPT expansion caused the researchers to use a dual classification of moderate/highly reactive.

Table 24. Classification results for Goton Pit.

	Classification by Test				
Pit	**Field Specimen Unboosted**	**Field Specimen Boosted**	**CPT**	**AMBT**	**Final Classification**
Failure Ratios	MR: 1.03 HR: 0.34	MR: 4.64 HR: 1.55	MR: 2.86 HR: 0.95	MR: 5.43 HR: 1.81 VHR: 1.21	Moderately/Highly Reactive
Classification	MR	HR	MR	VHR	

6.5.4 Harris Pit

Classification test results and classifications for Harris Pit aggregate are presented in Table 25. All three test results used for classification are nonreactive resulting in a nonreactive classification.

Table 25. Classification results for Harris Pit.

	Classification by Test				
Pit	**Field Specimen Unboosted**	**Field Specimen Boosted**	**CPT**	**AMBT**	**Final Classification**
Failure Ratios	Negligible	MR: 0.30 HR: 0.10	MR: 0.26 HR: 0.09	MR: 2.99 HR: 0.998 VHR: 0.67	Nonreactive
Classification	NR	NR	NR	MR	

6.5.5 Knife River Pit

Individual test results and classifications for Knife River aggregate are presented in Table 26. Reactive boosted and unboosted field blocks, and reactive CPT specimens result in a highly reactive classification.

Although Knife River is classified as highly reactive, the AMBT and other test methods disagree. Knife River unboosted field blocks are by far the most expansive unboosted field specimens to date and yet the boosted specimens are not the most reactive. It is interesting to note that one of the three unboosted field blocks shows less expansion than the remaining two. This highlights the need to conduct replicate specimens when creating a field site. Knife River concrete prisms also have the highest expansion results for this testing method. Mortar Bar test specimens are classified as moderately reactive for a test that has produced high expansions in most aggregates. These results all indicate a trend of lower expansions for highly boosted testing conditions. This is likely due to the pessimum effect explaining decreased expansion at higher alkali levels. A strict interpretation of Thomas et al. 2012 classifies this aggregate as highly reactive. To reduce

the level of risk in certain structures, the aggregate may be treated as VHR and mitigated accordingly.

Table 26. Classification results for Knife River.

	Classification by Test				
Pit	**Field Specimen Unboosted**	**Field Specimen Boosted**	**CPT**	**AMBT**	**Final Classification**
Failure Ratios	MR: 3.17 HR: 1.06	MR: 3.96 HR: 1.23	MR: 4.30 HR: 1.43	MR: 2.48 HR: 0.83 VHR: 0.55	Highly Reactive
Classification	HR	HR	HR	MR	

6.5.6 Labarge Pit

Classification test results for Labarge aggregate are presented in Table 27. Labarge aggregate is a more challenging aggregate to classify due to the split in classification results. Field exposure results are nonreactive, while CPT specimens are quite expansive. Measured expansions will be re-evaluated as the field blocks reach a five years.

Table 27. Classification results for Labarge.

	Classification by Test				
Pit	**Field Specimen Unboosted**	**Field Specimen Boosted**	**CPT**	**AMBT**	**Final Classification**
Failure Ratios	MR: 0.25 HR: 0.08	MR: 0.22 HR: 0.07	MR: 3.40 HR: 1.13	MR: 2.15 HR: 0.72 VHR: 0.48	Potentially Reactive
Classification	NR	NR	HR	MR	

6.5.7 Lamax Pit

Individual test results and classifications for Lamax aggregate are presented in Table 28. Lamax aggregate shows a moderate level of reactivity for both field exposure and CPT testing compared to the nonreactive and reactive aggregates tested. Moderately reactive boosted field block and CPT specimen results indicate a moderate reactivity.

Table 28. Classification results for Lamax.

	Classification by Test				
Pit	**Field Specimen Unboosted**	**Field Specimen Boosted**	**CPT**	**AMBT**	**Final Classification**
Failure Ratios	MR: 0.14 HR: 0.05	MR: 1.54 HR: 0.51	MR: 1.56 HR: 0.52	MR: 5.88 HR: 1.96 VHR: 1.31	Moderately Reactive
Classification	NR	MR	MR	VHR	

6.5.8 Worland Pit

Classification test results for Worland aggregate are presented in Table 29. Worland aggregate is classified as moderately reactive based on unboosted field exposure and CPT results.

Although Worland aggregate is classified as moderately reactive, the investigators recommend that design engineers use caution when considering potential mitigation measures because the boosted Worland field specimens (Figure 27) experienced the most expansion of any of the field specimens to date. While the single specimen expansion could be attributed to a sensitivity to high-alkali exposure, the authors deferred to the behavior of unboosted field specimens when determining the final classification.

Table 29. Classification results for Worland.

	Classification by Test				
Pit	**Field Specimen Unboosted**	**Field Specimen Boosted**	**CPT**	**AMBT**	**Final Classification**
Failure Ratios	MR: 1.28 HR: 0.43	MR: 4.93 HR: 1.64	MR: 1.62 HR: 0.54	MR: 7.16 HR: 2.39 VHR: 1.59	Moderately Reactive
Classification	MR	HR	MR	VHR	

6.6 Classification Summary

Final reactivity classifications for the eight Wyoming aggregates are included in Table 30. This table also shows the classifications from each reactivity test.

Table 30. Aggregate classification summary.

Pit	Classification by Test				Final Classification
	Field Exposure Unboosted	Field Exposure Boosted	CPT	AMBT	
BR	NR	MR	MR	VHR	Moderately Reactive
DFP	NR	MR	NR	VHR	Nonreactive
GP	MR	HR	MR	VHR	Moderately/Highly Reactive
HP	NR	NR	NR	MR	Nonreactive
KR	HR	HR	HR	MR	Highly Reactive
LBG	NR	NR	HR	MR	Potentially Reactive
LX	NR	MR	MR	VHR	Moderately Reactive
WOR	MR	HR	MR	VHR	Moderately Reactive

6.7 Autoclave Testing Results – Exploratory

The ACPT was investigated for four of the eight Wyoming aggregate sources. Testing was conducted for both coarse and fine fractions. A preliminary expansion limit of 0.08 percent was applied. These testing outcomes were then compared to research conducted by the University of Alabama (UA) and The University of Texas at Austin (UT). Table 51 of Appendix D presents the complete testing matrix and data for each source.

6.7.1 Black Rock

Expansion results for coarse aggregate, shown in Table 31, are less than the proposed limit and the coarse fraction is classified as nonreactive. Fine aggregate expansions are greater than 0.08 percent resulting in a reactive classification.

Table 31. UW ACPT results for Black Rock.

Aggregate C:F	Autoclave Temp °C (°F)	Average Expansion	Std. Dev.	COV	Failure Ratio
BR:BK	133 (271)	0.073%	0.0046%	6.2%	0.92
BR:BK	130 (266)	0.062%	0.0034%	5.4%	0.78
BK:BR	133 (271)	0.270%	0.0109%	4.1%	3.37
BK:BR	130 (266)	0.305%	0.0140%	4.6%	3.81

Black Rock aggregate was also investigated by the UA research group using nonreactive aggregate from the same source and the same cement, Table 32. UA had higher expansion in both tests conducted at 133 °C (271.4 °F). Although the coarse aggregate fraction received different classifications between the two research groups, values were close to one. Inter-laboratory coefficients of variation were 22.1 and 12.2 percent for coarse and fine aggregate testing, respectively.

Table 32. UA ACPT results for Black Rock.

Aggregate C:F	Autoclave Temp °C (°F)	Average Expansion	Std. Dev.	COV	Failure Ratio
BR:BK	133 (271)	0.109%	0.0031%	2.8%	1.37
BK:BR	133 (271)	0.362%	0.0071%	2.0%	4.52

6.7.2 Goton Pit

Expansion results for both coarse and fine aggregate exceed the proposed 0.08 percent limit, as shown in Table 33, resulting in a reactive classification.

Table 33. UW ACPT results for Goton Pit.

Aggregate C:F	Autoclave Temp °C (°F)	Average Expansion	Std. Dev.	COV	Failure Ratio
GP:BK	133 (271)	0.087%	0.0042%	4.9%	1.08
GP:BK	130 (266)	0.090%	0.0036%	4.0%	1.13
GP:BK	130 (266)	0.101%	0.0045%	4.5%	1.26
BK:GP	133 (271)	0.280%	0.0120%	4.3%	3.50
BK:GP	130 (266)	0.173%	0.0282%	16.4%	2.16
BK:GP	130 (266)	0.273%	0.0089%	3.3%	3.41

Goton Pit aggregate was also investigated by the UA research group using nonreactive aggregate from the same source and the same cement, Table 34. UA had higher expansion in both tests conducted at 133 °C (271.4 °F). Inter-laboratory coefficients of variation were 19.4 and 13.9 percent for coarse and fine aggregate testing, respectively.

Table 34.UA ACPT results for Goton Pit.

Aggregate C:F	Autoclave Temp °C (°F)	Average Expansion	Std. Dev.	COV	Failure Ratio
GP:BK	133 (271)	0.127%	0.0060%	4.8%	1.58
GP:BK	133 (271)	0.124%	0.0135%	10.9%	1.55
BK:GP	133 (271)	0.366%	0.0118%	3.2%	4.58

6.7.3 Harris Pit

Expansion results for the coarse aggregate are less than the proposed limit shown in Table 35, and the coarse fraction is classified as nonreactive. Fine aggregate expansions exceed 0.08 percent resulting in a reactive classification.

Table 35. UW ACPT results for Harris Pit.

Aggregate C:F	Autoclave Temp °C (°F)	Average Expansion	Std. Dev.	COV	Failure Ratio
HP:BK	133 (271)	0.051%	-	-	0.64
HP:BK	130 (266)	0.067%	0.0006%	0.9%	0.83
BK:HP	133 (271)	0.192%	0.0089%	4.6%	2.39
BK:HP	130 (266)	0.186%	0.0107%	5.7%	2.33

Harris Pit aggregate was also investigated by the UA research group using nonreactive aggregate from the same source and the same cement, Table 36. UA had higher expansion in both tests conducted at 133 °C (271.4 °F). Inter-laboratory coefficients of variation were 11.3 and 20.3 percent for coarse and fine aggregate testing, respectively.

Table 36. UA ACPT results for Harris Pit.

Aggregate C:F	Autoclave Temp °C (°F)	Average Expansion	Std. Dev.	COV	Failure Ratio
HP:BK	133 (271)	0.065%	0.0015%	2.4%	0.81
BK:HP	133 (271)	0.277%	0.0078%	2.8%	3.46

6.7.4 Knife River

Coarse aggregate is nonreactive with expansion results less than the proposed limit, as seen in Table 37. Fine aggregate expansion is greater than 0.08 percent resulting in a reactive classification.

Table 37. UW ACPT results for Knife River.

Aggregate C:F	Autoclave Temp °C (°F)	Average Expansion	Std. Dev.	COV	Failure Ratio
KR:BK	133 (271)	0.060%	0.0057%	9.4%	0.75
KR:BK	133 (271)	0.068%	0.0017%	2.5%	0.85
KR:BK	130 (266)	0.063%	0.0070%	11%	0.79
BK:KR	133 (271)	0.154%	0.0081%	5.3%	1.93

Knife River aggregate was also investigated by the UA research group using nonreactive aggregate from the same source and the same cement, Table 38. UA had higher expansion in both tests conducted at 133 °C (271.4 °F), despite this difference fine aggregates received the same classification. UA test results characterized the coarse aggregate fraction as reactive. Inter-laboratory coefficients of variation were 19.8 and 42.2 percent for coarse and fine aggregate testing, respectively.

Table 38. UA ACPT results for Knife River.

Aggregate C:F	Autoclave Temp °C (°F)	Average Expansion	Std. Dev.	COV	Failure Ratio
KR:BK	133 (271)	0.084%	0.0201%	24%	1.05
BK:KR	133 (271)	0.336%	0.0151%	4.5%	4.20

6.7.5 Summary

The ACPT is harsher than the CPT because testing conditions include an initial boosting to three percent alkalis, increased temperature, and pressure. Accelerating the reaction process requires severe environmental conditions that may not classify all aggregates. Using the proposed limit of 0.08 percent expansion gives the classifications in Table 39.

This test method classifies all of the fine aggregates as reactive including Harris Pit. This contradicts results of the field specimens and CPT nonreactive classifications as shown in Table 25. In addition, Knife River coarse aggregate is classified as nonreactive when the field specimens and CPT testing indicates a highly reactive aggregate, Table 26. Although it is possible to have a nonreactive coarse aggregate and reactive fine aggregate that results in a

combined reactive classification, measured expansions are 0.224 and 0.240 percent for coarse and fine aggregates, respectively. These are illustrated in Figure 40 and quantified in Table 54. As previously mentioned, the classification limit is preliminary.

Table 39. ACPT classification results.

Pit	Component Tested	Classification
BR	Coarse	Nonreactive
	Fine	Reactive
GP	Coarse	Reactive
	Fine	Reactive
HP	Coarse	Nonreactive
	Fine	Reactive
KR	Coarse	Nonreactive
	Fine	Reactive

A comparison of the UW and UA results are shown in Figure 45. This comparison shows a good correlation between coarse aggregate tests with greater variation between expansion results for fine fraction testing. UA expansions are consistently greater than those at UW. While the fine fraction test results appear to show significant variation, part of this difference is explained by a scaling of the differences between the two groups associated with increased expansion values. For coarse aggregate testing, UA expansions exceed those of UW by 1.3 to 1.5 times. The comparison for fine aggregate fraction testing results in a factor of 1.3 to 2.0.

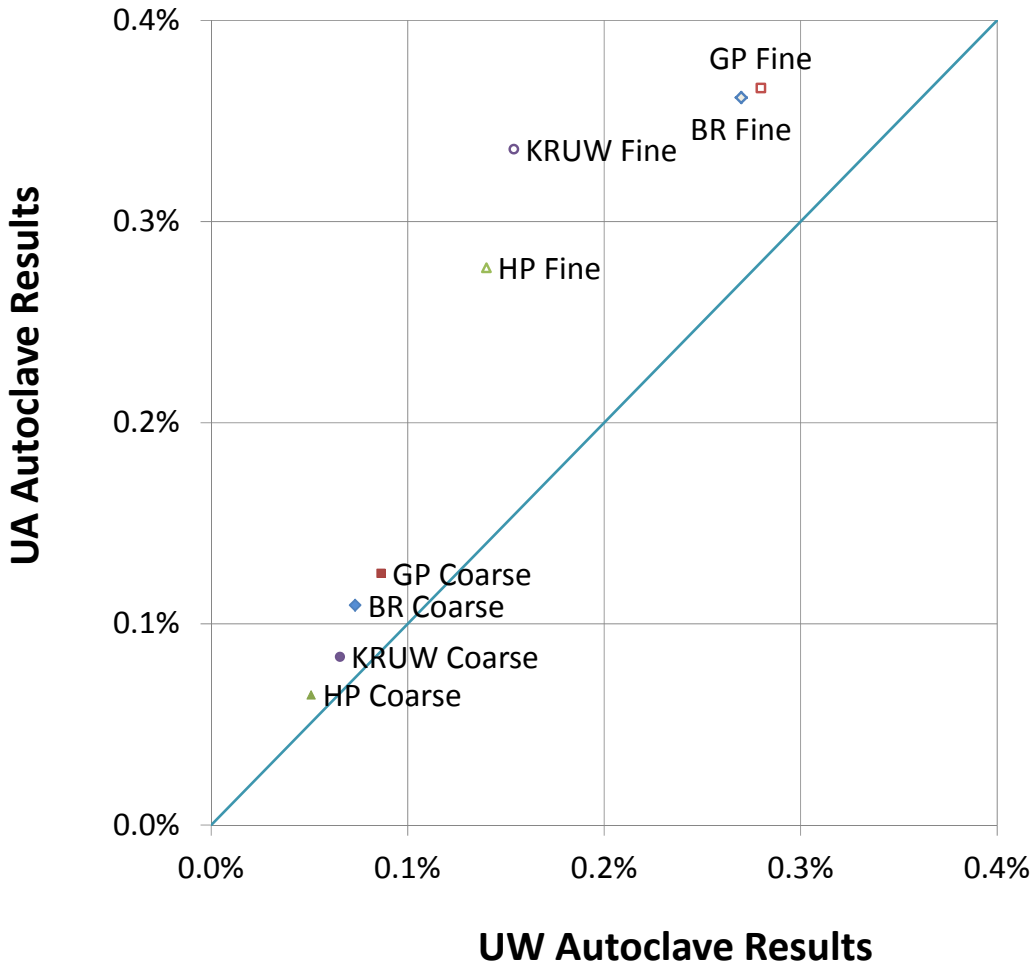

Figure 45. Comparison of UA to UW ACPT expansion results at 133 Celsius.

The remaining variation in the fine aggregate testing is attributed to the quality of the Beckmann aggregate received by UW. Although the Beckmann aggregate passed the friable test, ASTM C142, some aggregates were crushed during compaction of the concrete mixture. This resulted in a weaker concrete as evidenced in the compression test results in Appendix A. Fine aggregate testing would also be more affected by the nonreactive aggregate because the coarse component provides two thirds of the total aggregate mass. This program indirectly tested the effects of the

nonreactive coarse aggregate on expansions. Future comparison studies should use nonreactive materials that come from the same location in a quarry.

Beyond the general repeatability of the test, the ACPT can be evaluated for similarity to other standard ASR test methods. Analysis of these relationships is presented using data from the four Wyoming aggregate sources and work done by Giannini and Folliard (2013). A comparison of results for ACPT and AMBT coarse and fine aggregates is shown in Figure 46 and Figure 47, respectively. ACPT and CPT comparisons for coarse and fine aggregates are shown in Figure 48 and Figure 49, respectively. A linear regression of each data set was conducted, forcing the y-intercept to be zero and is included in Appendix D. All comparisons show a linear relationship and the positive correlation indicates promise for the future use of this test.

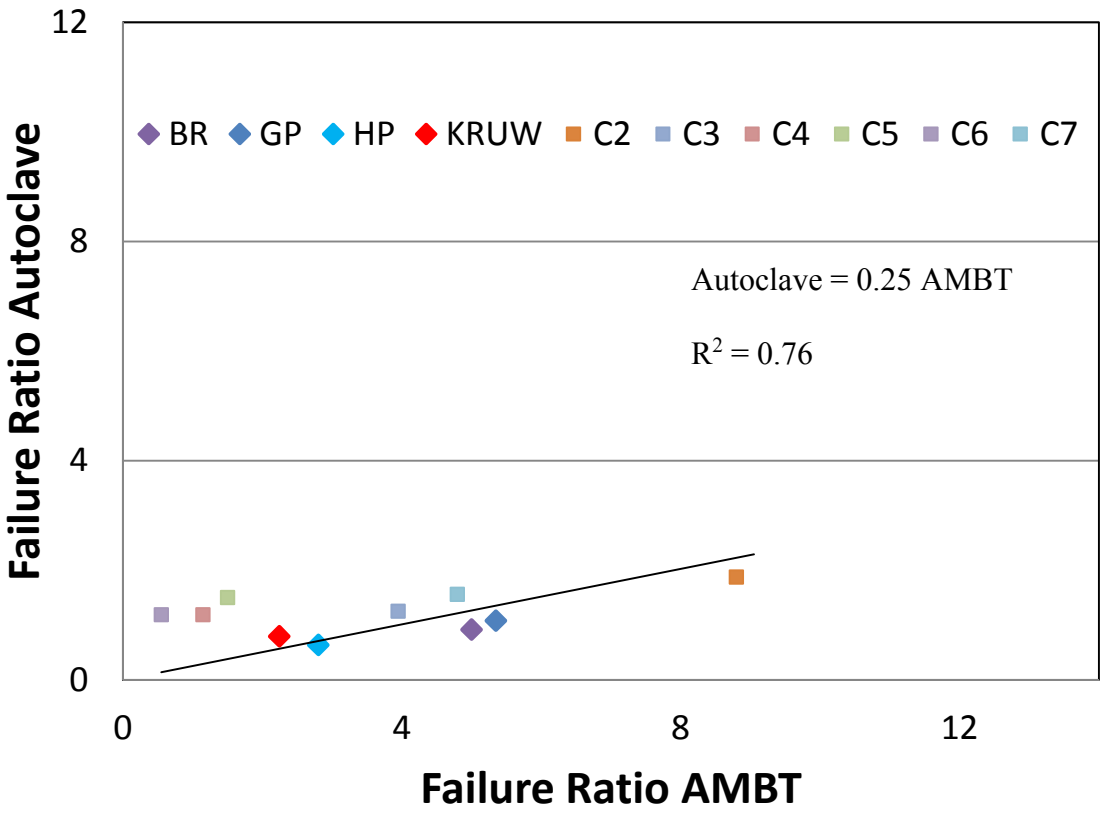

Figure 46. Comparison of Autoclave failure ratios to AMBT failure ratios for coarse aggregate.

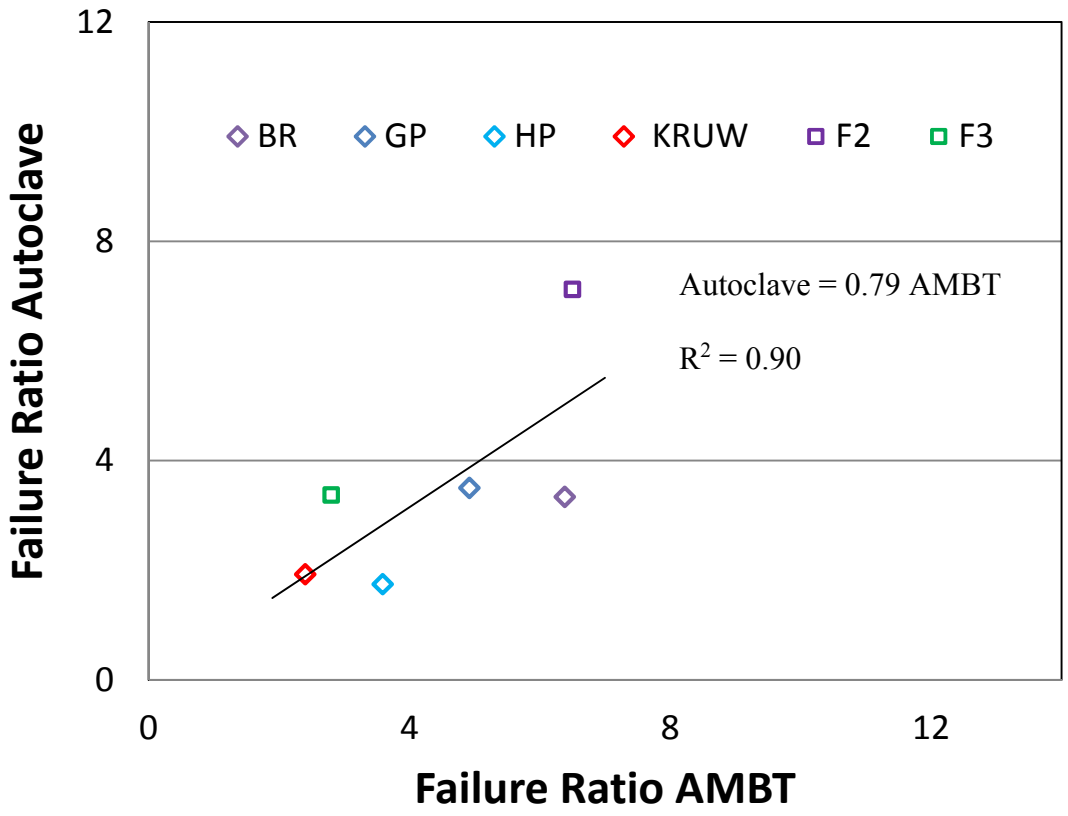

Figure 47. Comparison of Autoclave failure ratios to AMBT failure ratios for fine aggregate.

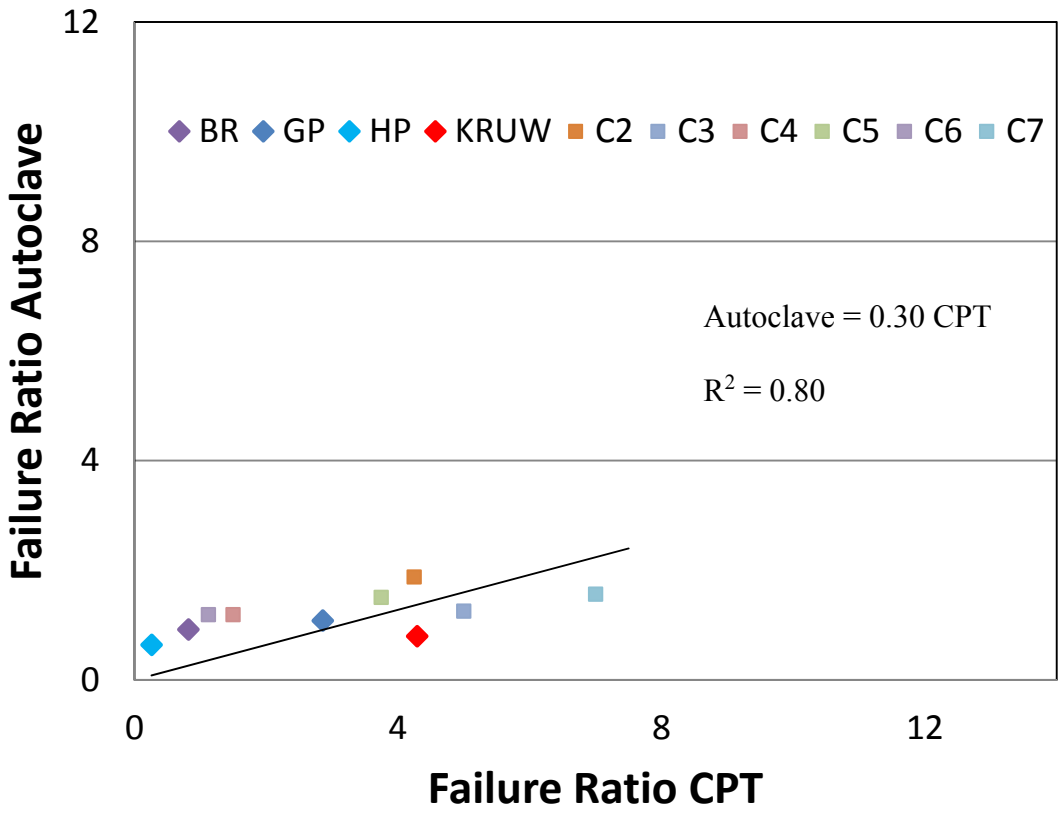

Figure 48. Comparison of Autoclave failure ratios to CPT failure ratios for coarse aggregate.

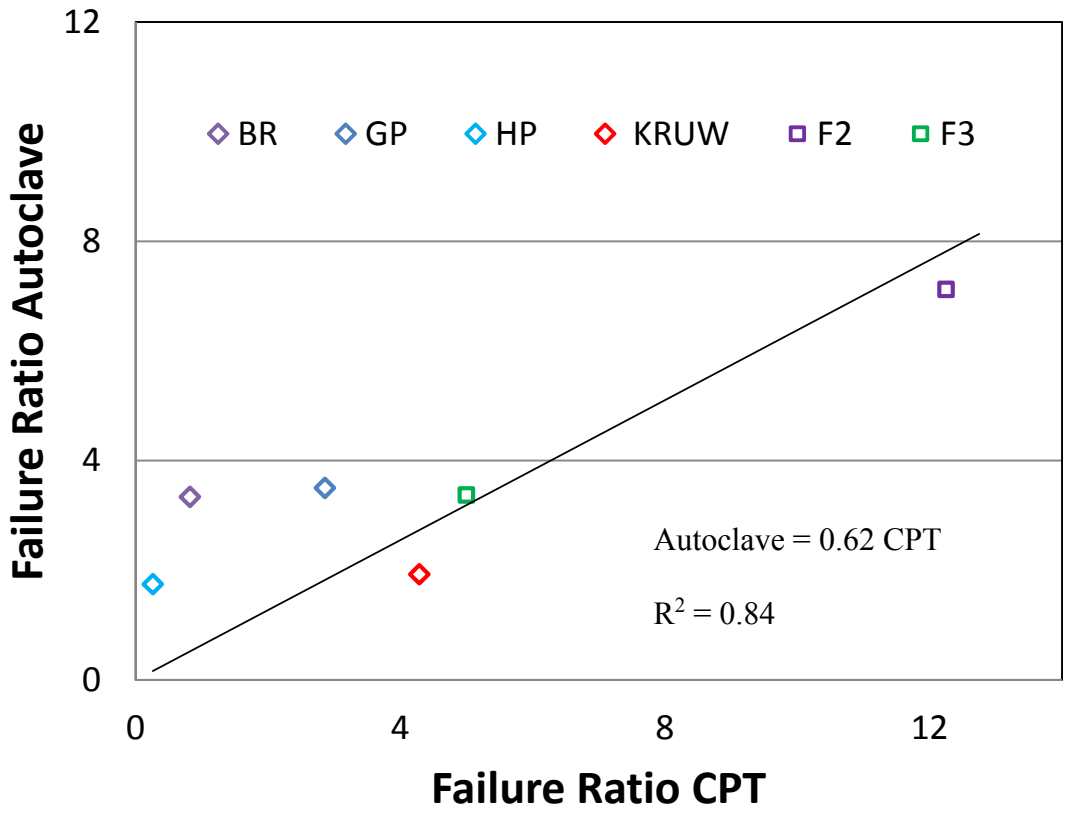

Figure 49. Comparison of Autoclave failure ratios to CPT failure ratios for fine aggregate.

This research provides additional information in the first stages of evaluating the ACPT. The test needs further investigation to confirm the reliability of results and provide a better understanding of the effects of the extreme testing conditions. The possibility of a shorter test for classification merits additional investigation.

7 Mitigation Test Results

This chapter outlines the mitigation test results for the Wyoming aggregate sources. Craig, CO, Class F fly ash with a 0.967 percent calcium oxide (CaO) content was the mitigating agent. The calcium content is significant to the mitigations results as calcium is needed for the development of reaction rims. A 25 percent Class F fly ash replacement was used to evaluate the Mitigated Concrete Prism Test (MCPT) and the Mitigated Accelerated Mortar Bar Test (MAMBT). Results are presented in the following sections and organized by the type of test.

7.1 MCPT Test Results

MCPT is a modified form of the standard CPT using a mitigating agent. Adding mitigating agents extends the test from one year to two years.

MCPT testing was conducted for the six aggregate sources preliminarily classified as reactive: Black Rock, Goton Pit, Knife River, Labarge, Lamax, and Worland. Variation in expansion with respect to fly ash mitigation for Knife River specimens are shown in Figure 50. Unmitigated Knife Rock specimens show significant expansion at one year while the mitigated specimens exhibit expansion close to zero at two years. Both graphs show the 0.04 and 0.12 percent expansion limits used for classification and mitigation testing. The limits are shown on the graphs by horizontal, dashed lines.

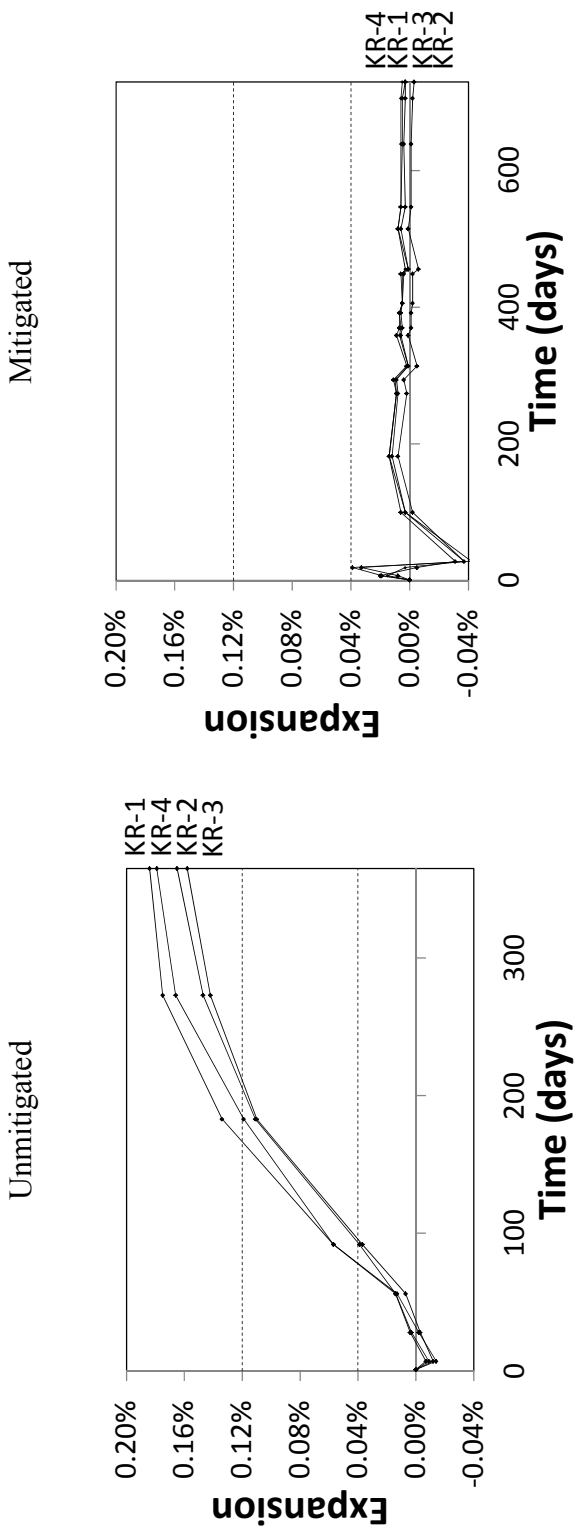

Figure 50. Comparison of unmitigated and mitigated Knife River CPT specimens.

This same decrease in expansion is observed for other five aggregates tested. A direct comparison of expansions for these specimens are shown in Figures 51 through 55. All aggregates have expansion below 0.04 percent at two years indicating successful mitigation with this fly ash at a 25 percent replacement level.

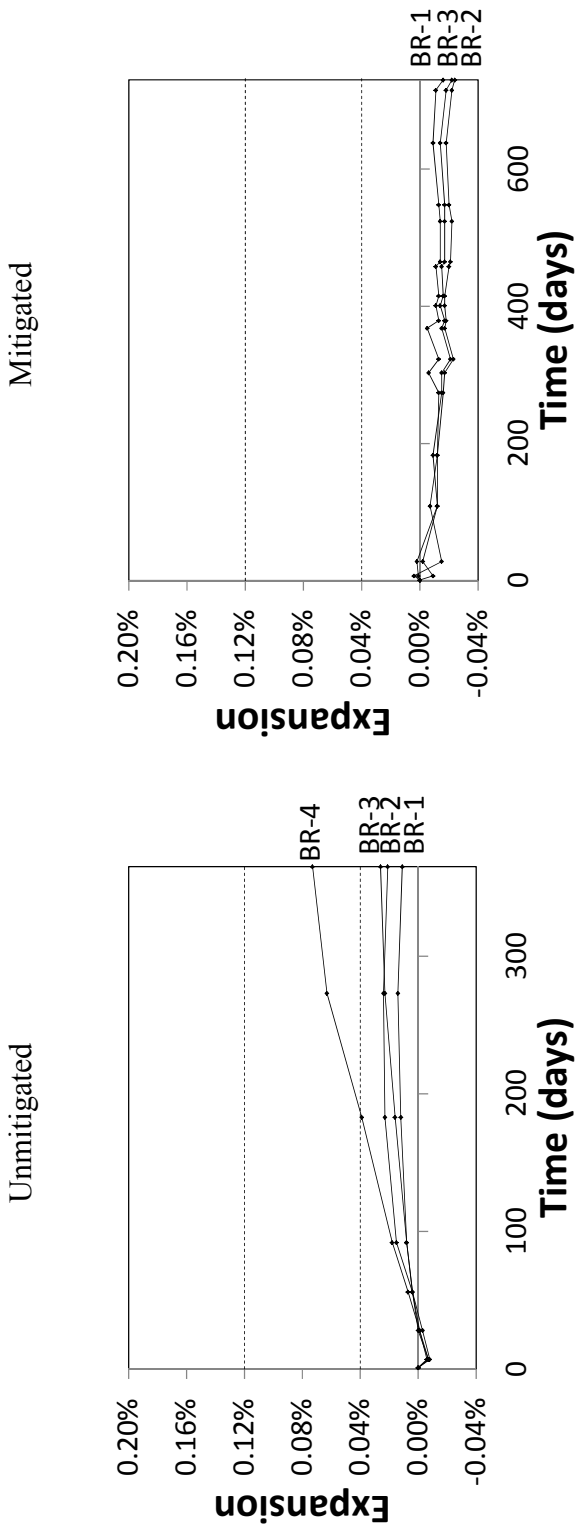

Figure 51. Comparison of unmitigated and mitigated Black Rock CPT specimens.

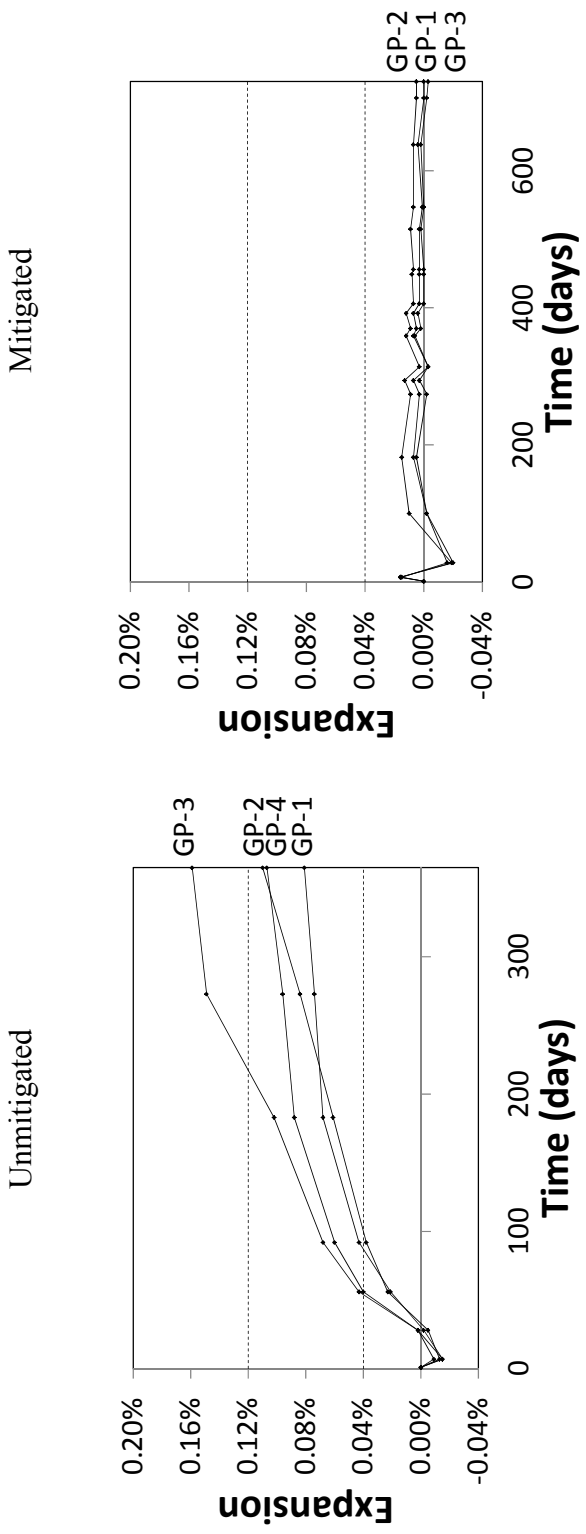

Figure 52. Comparison of unmitigated and mitigated Goton Pit CPT specimens.

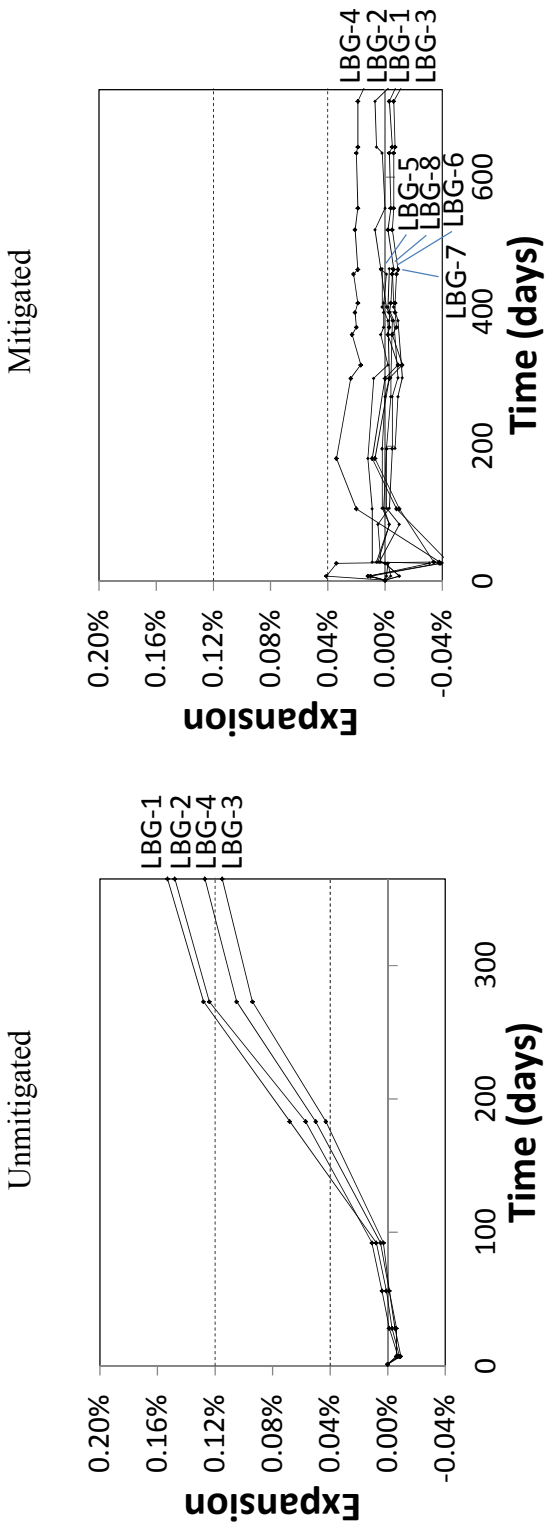

Figure 53. Comparison of unmitigated and mitigated Labarge CPT specimens.

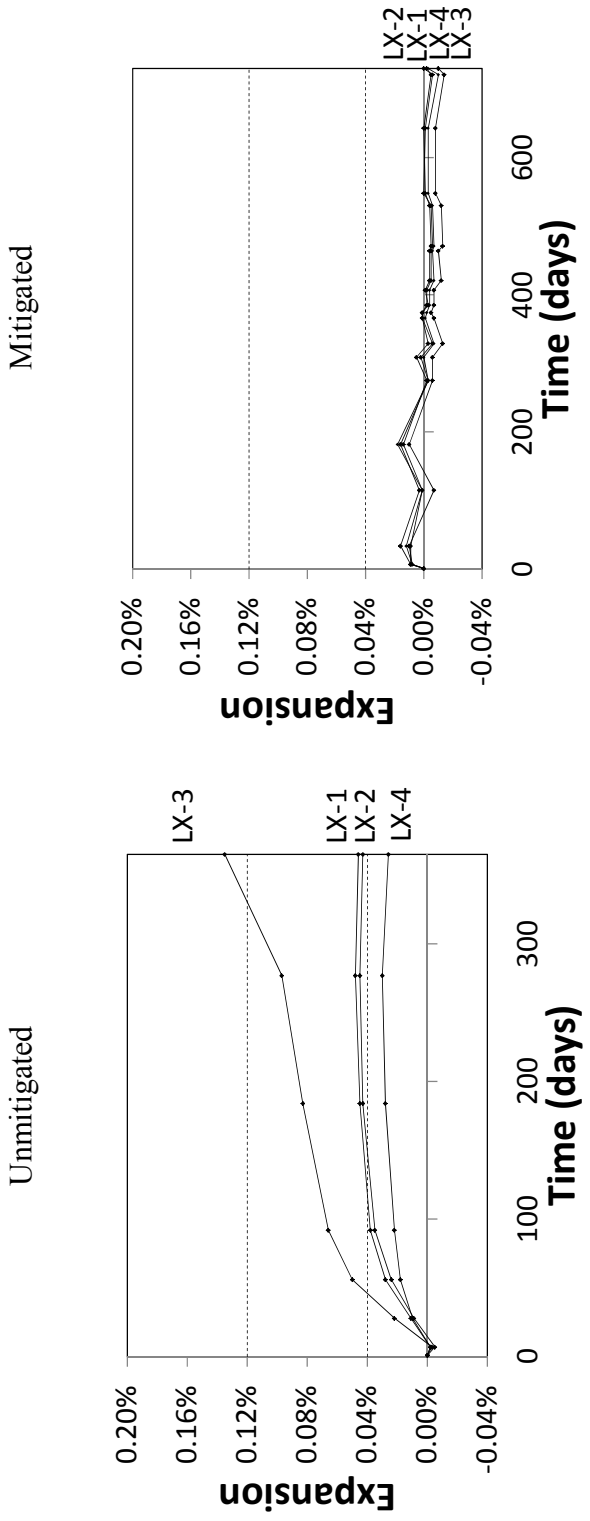

Figure 54. Comparison of unmitigated and mitigated Lamax CPT specimens.

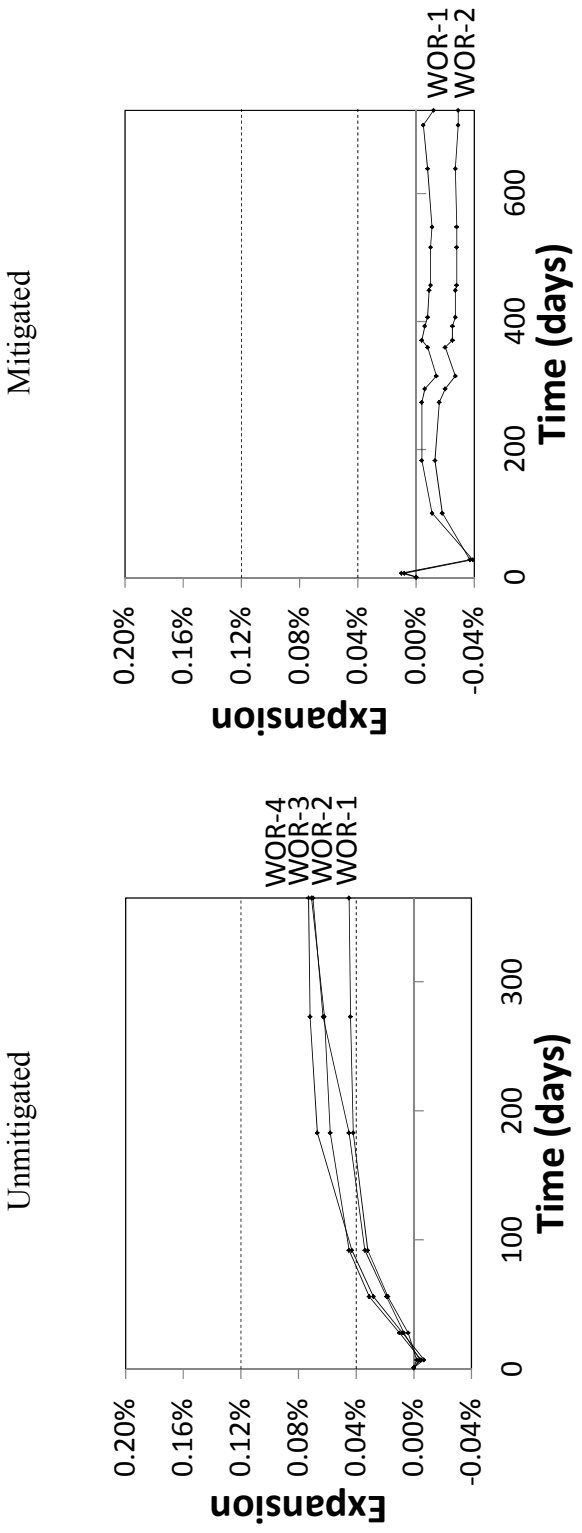

Figure 55. Comparison of unmitigated and mitigated Worland CPT specimens.

Average expansions and failure ratios for this testing are included in Table 40. Failure ratios are the ratio of measured expansion to the expansion limit, 0.04 percent, distinguishing between effective and ineffective mitigation for the MCPT. Values greater than one indicate ineffective treatments while values less than one indicate successful mitigation. The test results are presented graphically in Figure 56. CPT results in this figure use the nonreactive to moderately reactive expansion limit 0.04 percent. All aggregates are mitigated by replacing 25 percent of the cement with Class F fly ash replacement.

Table 40. MCPT test results.

Pit	Average Expansion (%)	Failure Ratio	Classification
BR	Negligible	-	Mitigated
GP	0.001	0.02	Mitigated
KR	0.004	0.09	Mitigated
LBG	Negligible	-	Mitigated
LX	Negligible	-	Mitigated
WOR	Negligible	-	Mitigated

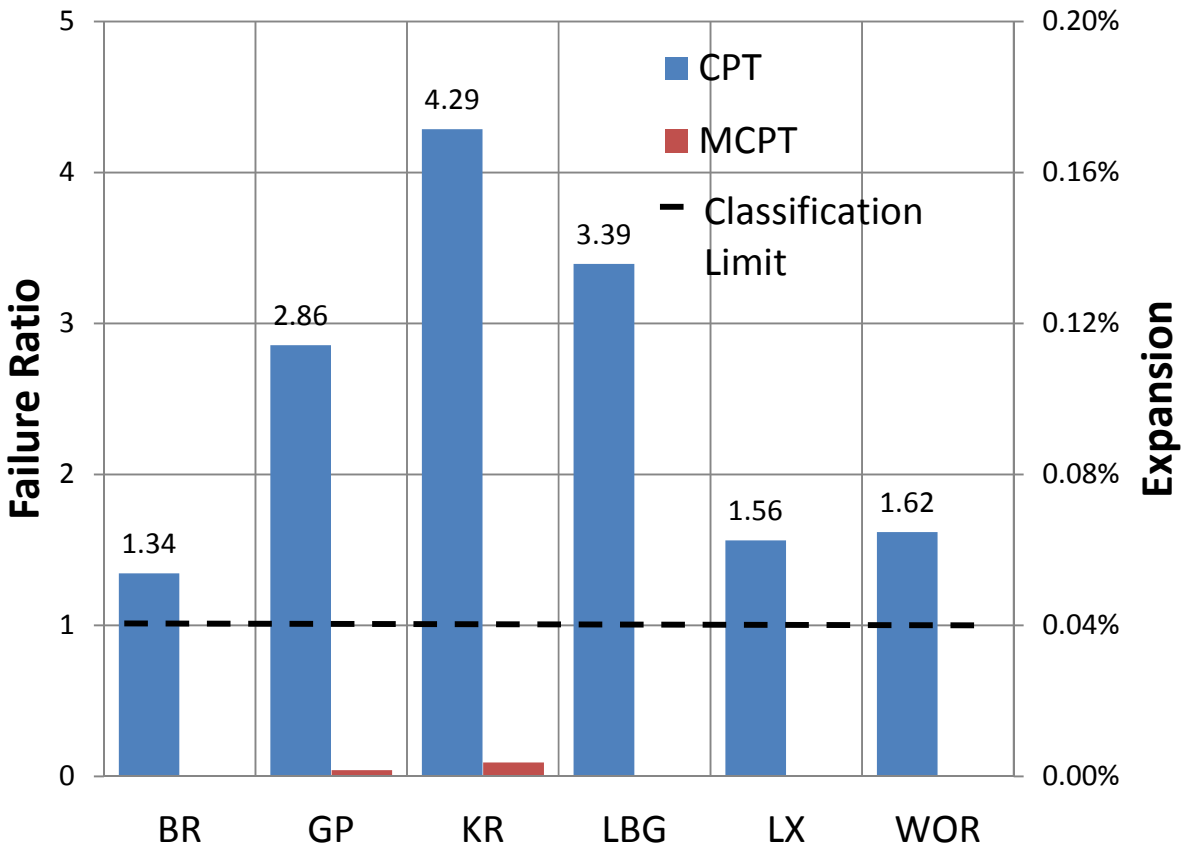

Figure 56. Comparison of CPT and MCPT test results.

7.2 MAMBT Test Results

The MAMBT was used to evaluate the effectiveness of 25 percent fly ash replacement on the reactivity of the eight Wyoming aggregates. Berube concluded that the reduced porosity associated with the addition of fly ash slows the infiltration of alkalis for a period of 14 days. After this time, the positive effects of the fly ash are negated by the chemistry of the storage environment (Berube et al. 1995). Testing in this study extended to 56 days to observe the effects of longer exposure periods. Reaction rates increased at approximately 14 days, supporting Berube's theory. A minimum of two batches were cast for each source. Batch average

expansions are shown throughout this section while individual specimen expansions are included in Appendix E. Common markers are used to indicate batches cast on the same day. Line styles, solid or dashed, indicate the common storage container of an individual batch.

Variations in expansion between unmitigated and mitigated AMBT specimens are shown in Figures 57 to 64. The unmitigated graph includes the 0.1 percent expansion limit separating nonreactive and moderately reactive aggregates, the 0.3 percent limit defining moderately reactive and highly reactive aggregates, and the 0.45 percent expansion limits used for to classify very highly reactive aggregate. Expansions for specimens using fly ash less than 0.01 percent at 14 days are mitigated. The mitigated graphs include the 0.01 percent expansion limit used to indicate successful mitigation. The limits are shown on the graphs by horizontal, dashed lines.

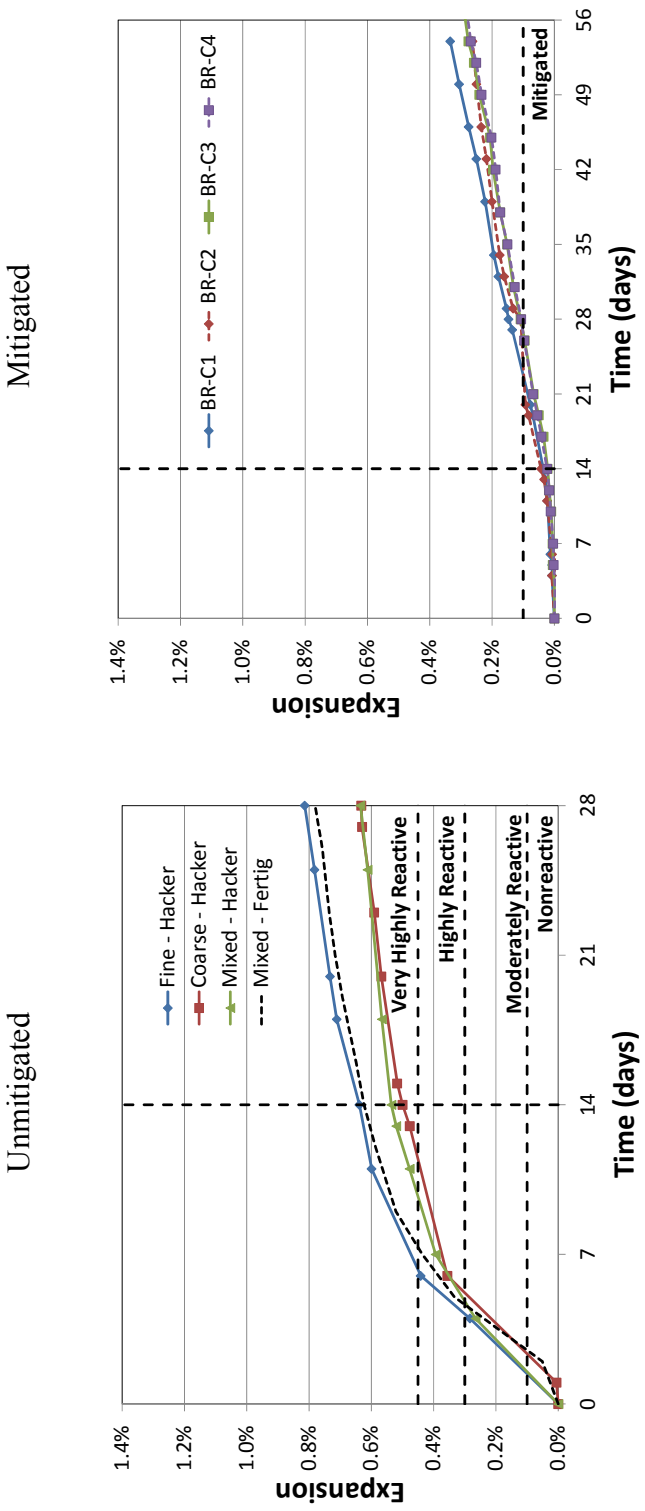

Figure 57. Comparison of unmitigated and mitigated Black Rock AMBT specimens.

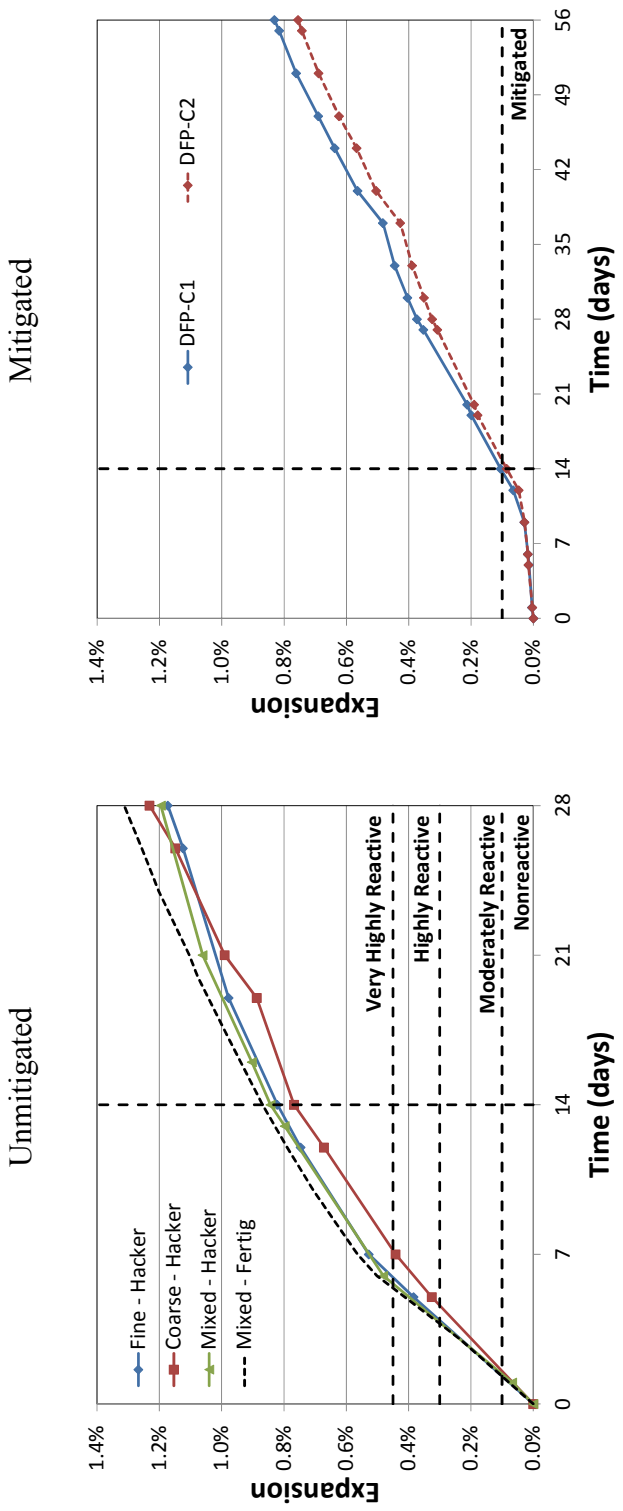

Figure 58. Comparison of unmitigated and mitigated Devries Farm AMBT specimens.

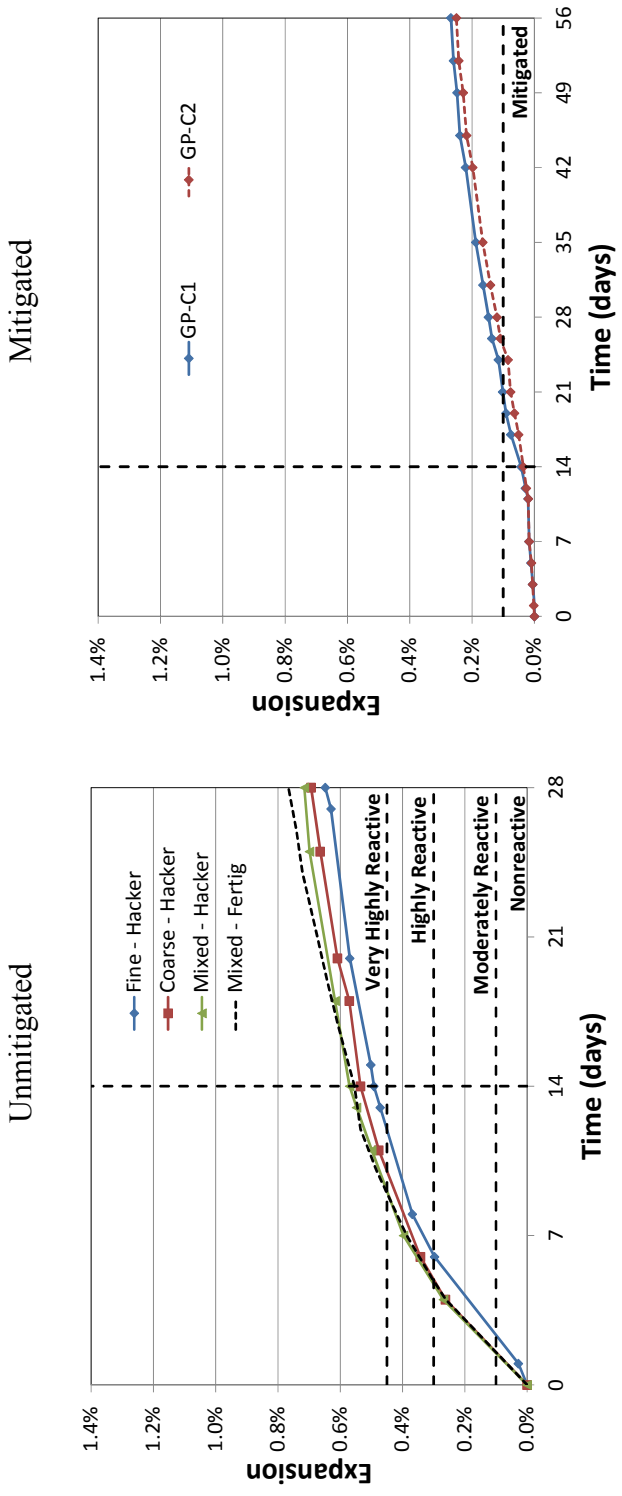

Figure 59. Comparison of unmitigated and mitigated Goton Pit AMBT specimens.

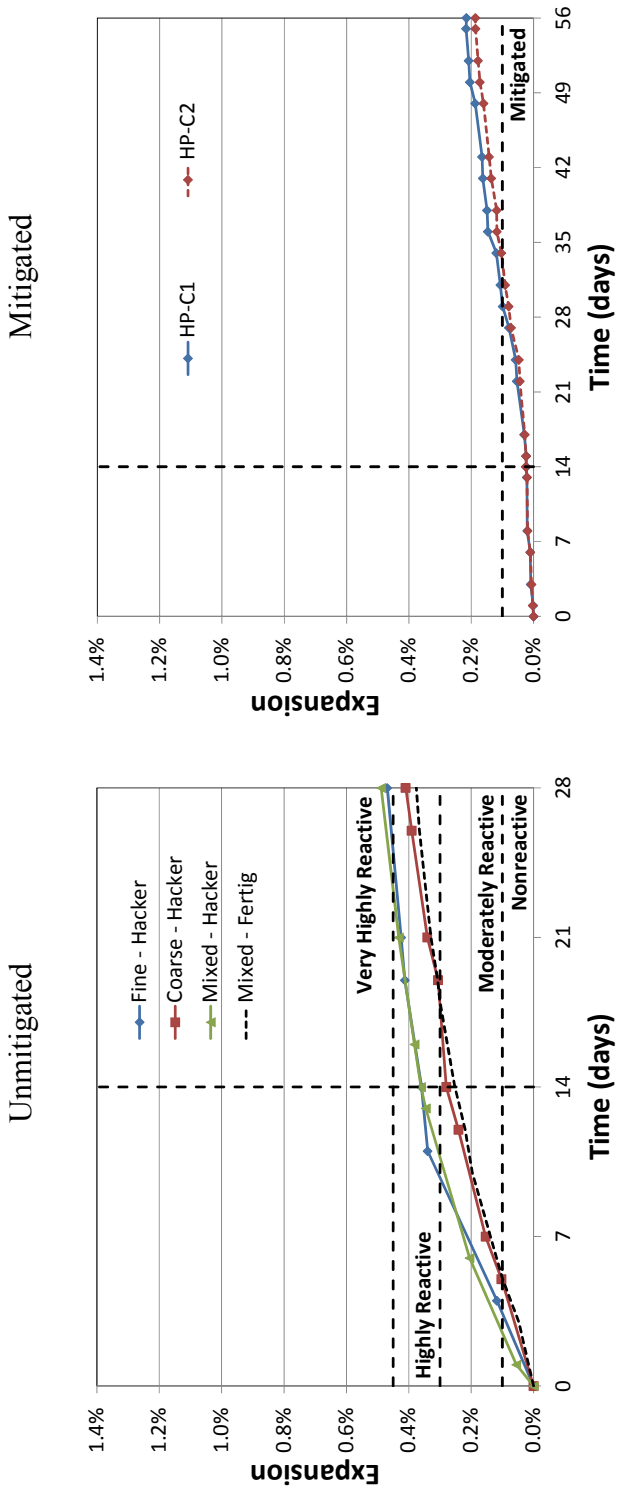

Figure 60. Comparison of unmitigated and mitigated Harris Pit AMBT specimens.

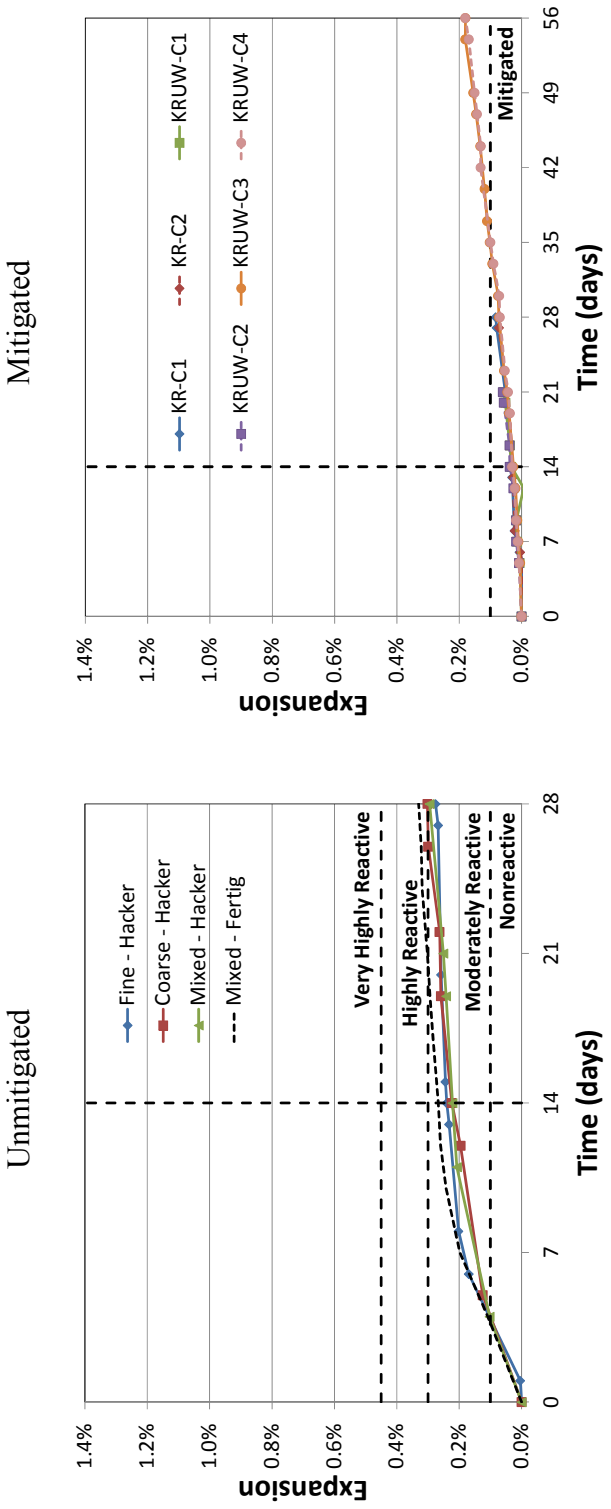

Figure 61. Comparison of unmitigated and mitigated Knife River AMBT specimens.

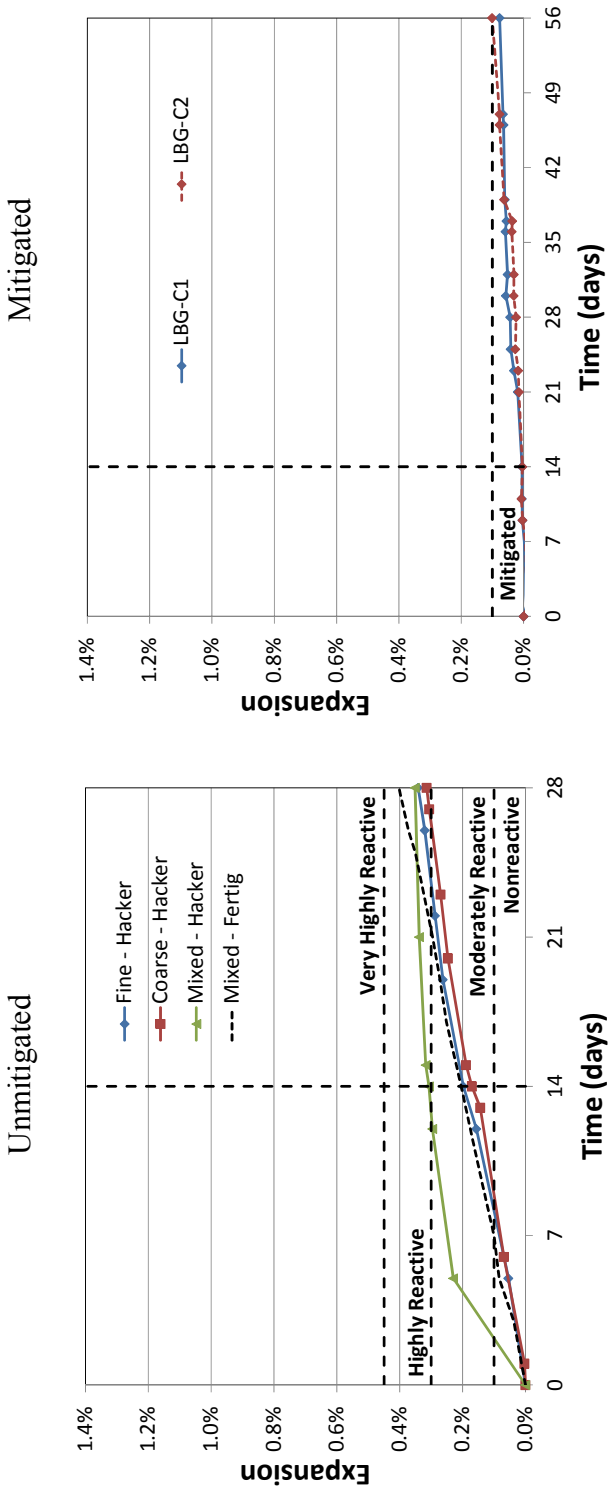

Figure 62. Comparison of unmitigated and mitigated Labarge AMBT specimens.

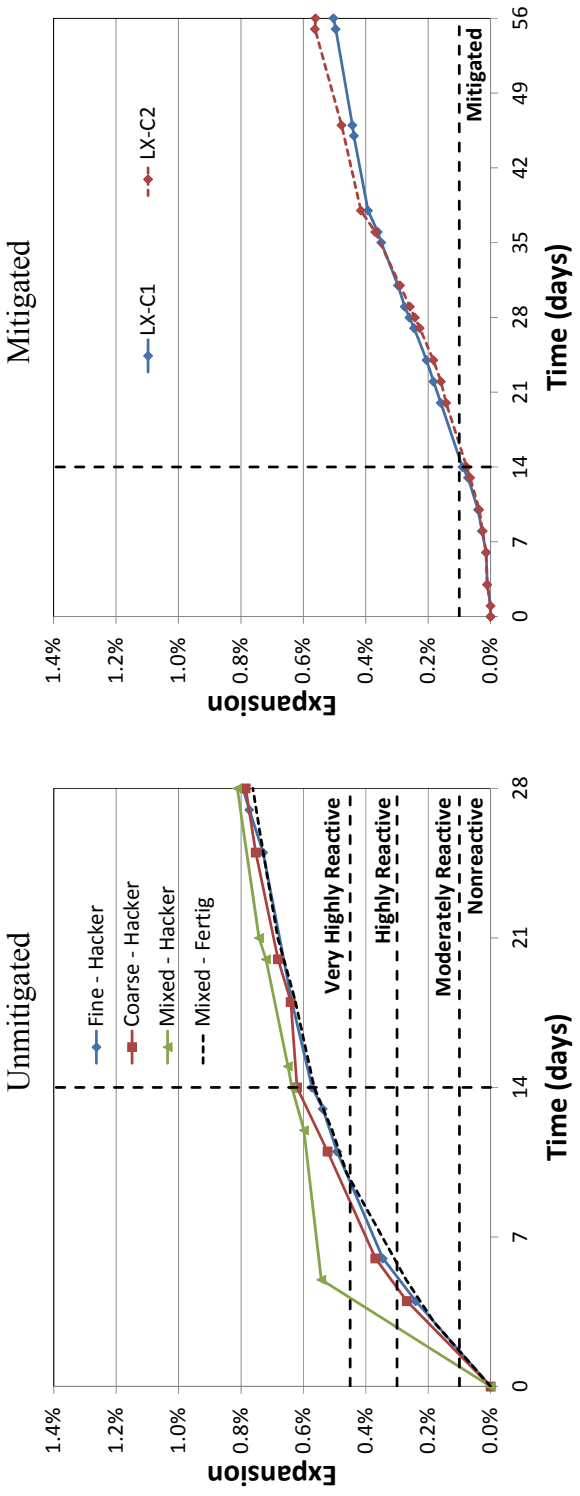

Figure 63. Comparison of unmitigated and mitigated Lamax AMBT specimens.

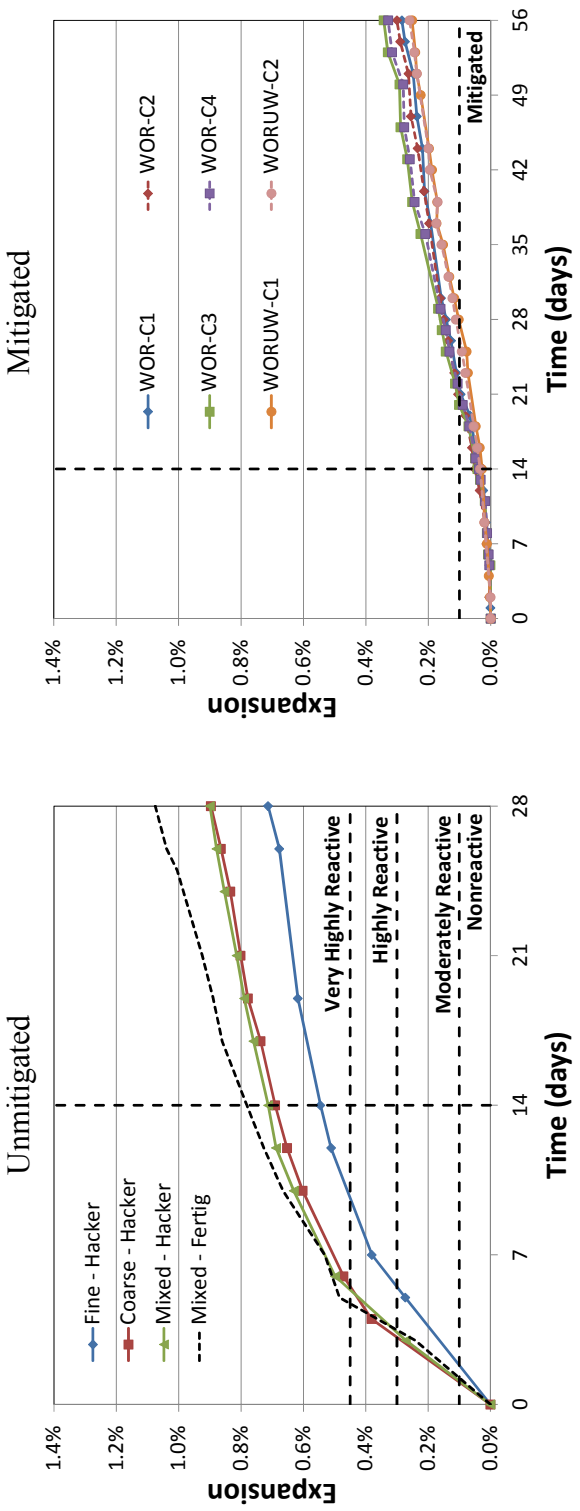

Figure 64. Comparison of unmitigated and mitigated Worland AMBT specimens.

Specimens experienced decreased expansion with the addition of 25 percent Class F fly ash. A summary of 14 day expansion data for the mitigated specimens is presented in Table 41. This table includes average expansion values on a pit basis as well as standard deviations, coefficients of variation, failure ratios and mitigation classification. Aggregates passing this test are labeled as having been mitigated by the 25 percent fly ash replacement.

Table 41. MAMBT test results.

Pit	Average Expansion	Standard Deviation	COV	Average Failure Ratio	Classification
BR	0.039%	0.009%	23.8%	0.39	Mitigated
DFP	0.095%	0.020%	20.6%	0.95	Mitigated
GP	0.039%	0.005%	11.9%	0.39	Mitigated
HP	0.024%	0.002%	9.5%	0.24	Mitigated
KR	0.029%	0.003%	10.9%	0.29	Mitigated
KRUW	0.033%	0.004%	11.7%	0.33	Mitigated
LBG	0.004%	0.002%	38.4%	0.04	Mitigated
LX	0.083%	0.010%	11.5%	0.83	Mitigated
WOR	0.042%	0.008%	19.9%	0.42	Mitigated
WORUW	0.039%	0.005%	15.3%	0.31	Mitigated

Differences in expansion are presented graphically in Figure 65. AMBT results are reported with the failure ratios compared to the mitigation classification limit, 0.1 percent expansion. All MAMBT test results are below the horizontal dashed line representing the mitigation limit. All aggregates show a distinct reduction in expansion with the addition of fly ash. The Devries Farm specimens continue to be the most expansive specimens in the AMBT testing conditions. This testing set revealed a tendency for increased expansion of Devries Farm aggregate in high alkali conditions.

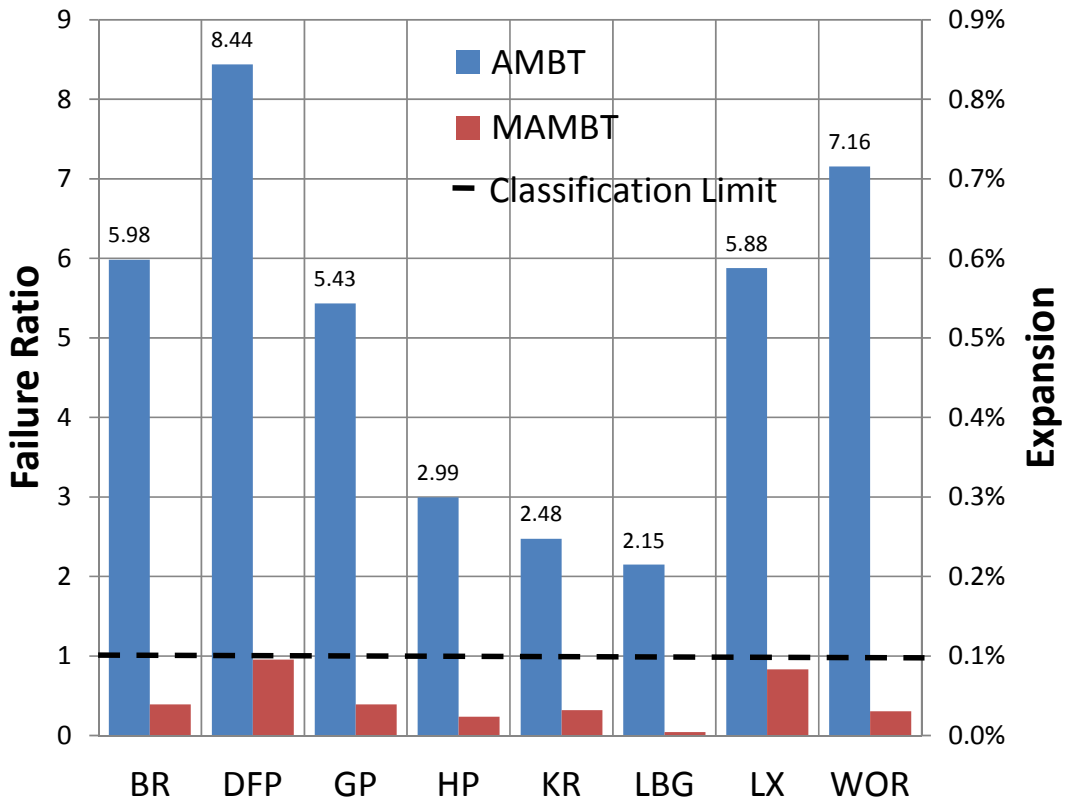

Figure 65. Comparison of AMBT and MAMBT test results.

7.3 Mitigation Summary

This section tabulates the results for all MCPT and MAMBT testing. All six reactive Wyoming aggregate sources were effectively mitigated using 25 percent Class F fly ash replacement. The two nonreactive aggregates tested showed no negative effects from the addition of fly ash; as shown in Table 42. This testing confirms that mitigation treatment currently used by the Wyoming Department of Transportation is effective. This research found that Class F fly ash with 0.967 percent CaO was sufficient to mitigate even the highly reactive Knife River aggregate.

Table 42. Mitigation failure ratios.

Pit	CPT	MCPT	AMBT	MAMBT	Mitigated?
BR	1.34	Negligible	5.98	0.39	Yes
DFP	0.64	-	8.44	0.95	Yes
GP	2.86	0.02	5.43	0.39	Yes
HP	0.26	-	2.99	0.24	Yes
KR	4.29	0.09	2.48	0.29	Yes
KRUW	-	-	-	0.33	Yes
LBG	3.39	Negligible	2.15	0.04	Yes
LX	1.56	Negligible	5.88	0.83	Yes
WOR	1.62	Negligible	7.18	0.42	Yes
WORUW	-	-	-	0.31	Yes

A goal of this research has been the determination of ways of economizing the use of fly ash. Economization of mitigation is evaluated in two parts: the classification of reactivity and initial evaluation of mitigation effectiveness. Mitigation levels based on reactivity would allow a smaller amount of fly ash to be used to mitigate a moderately reactive aggregate compared to a highly reactive aggregate. Having determined that the WYDOT standard mitigation strategy is effective for a range of reactivity levels, lower replacement mitigation levels may further reduce the amount of fly ash necessary for mitigation of less reactive aggregates. Testing may also be conducted to using Class C fly ash that is available throughout Wyoming.

8 Conclusions and Future work

8.1 Conclusions

Research was conducted in two parts: the classification of eight aggregate sources and the evaluation of mitigation measures to limit expansion. Eight Wyoming aggregate sources were evaluated for reactivity based on field exposure testing, petrographic analysis, the Concrete Prism Test (CPT), and the Accelerated Mortar Bar Test (AMBT). Unboosted field specimens were utilized to study natural field conditions; while boosted specimens accelerated the expansion to indicate longer-term performance. Petrographic analysis confirmed that ASR was present in the boosted field specimens tested despite the fact that it could not quantify the degree of reactivity. CPT became the most respected accelerated test although results were still time intensive. AMBT results, while conducted quickly, did not provide additional information for classification purposes due to the harshness of the test. While many methods exist for testing alkali-silica reactivity, each test balances accuracy and the time needed to conduct the test. CPT is therefore recommended as providing the best balance between these features.

Classifications are based largely on the results of field exposure and the CPT. The eight aggregates covered a range of reactivity, from non-expansive to highly expansive. Devries Farm and Harris Pit aggregates are classified as nonreactive. Black Rock, Lamax, and Worland are classified as moderately reactive. Goton Pit aggregate is classified as moderately/highly reactive due to an initial moderately reactive classification tempered by more expansive specimens. Knife River pit is classified as highly reactive. Labarge aggregate is classified as potentially reactive on the basis of high CPT results and five and a half years of field expansions. Additional field data

is desired to classify this behavior. These classifications are based on the assumption that each source is homogeneous. The authors recommend that design engineers use caution when considering the importance and service life expectations of a particular concrete application.

The analysis performed by DRP confirmed that petrography can be used as a tool in confirming the presence of ASR gel in damaged concrete. While the field blocks are still experiencing expansion, it was established that ASR gel is present in the six field blocks tested in this study.

Experimental classification work was also conducted on four aggregate sources using the Autoclaved Concrete Prism Test (ACPT) proposed by the University of Alabama (UA) and The University of Texas at Austin (UT). Results of this test were compared with both results from UA, UT and other ASR tests. The ACPT is still in the experimental stage and was not used for the classification of aggregates. To determine the potential of the ACPT, results from multiple research groups will be necessary to evaluate the repeatability of test results. While the ACPT requires additional repeatability testing before it may be used, the test shows promise.

Mitigation testing was conducted using the Mitigated Concrete Prism Test (MCPT) for all six reactive aggregates and the Mitigated Accelerated Mortar Bar Test (MAMBT) for all aggregates. Both tests were conducted using 25 percent Class F fly ash replacement from Craig, Colorado. Although all aggregates are mitigated using this strategy, it may be overly conservative for moderately reactive aggregates.

8.2 Future work

Many avenues for future investigation and testing should be conducted to add to the existing knowledge about ASR. These are broken into four areas: general ASR knowledge, field exposure testing, accelerated testing methods, and mitigation.

8.2.1 General ASR Knowledge

Additional information about field concrete that has been cast in projects such as buildings, bridges, and roadways should be collected to better define the problem. This information should be gathered into a database including aggregate source, cement used, mixture design, admixtures used, supplementary cementitious materials (SCMs) used, quantity of SCMs, and observed reactivity. The database may be used to provide information for the future use of given aggregate/cement/SCM combinations. While this is a time and labor intensive task, knowledge about additional aggregate reactivity and use would be beneficial to future applications. The collection of this information could be integrated as a part of quality assurance programs currently in place for Wyoming Department of Transportation projects.

8.2.2 Field Exposure Testing

Field exposure results become more useful with continued exposure and observation. With this in mind, continued field specimen measurement is highly recommended. Future work should also include the application of proposed field limits to additional field specimens, both at the University of Wyoming and at other institutions. This application will allow for the refinement of classification limits and more uniform definitions of field expansion across different testing

groups. Investigators should consider a single classification time or method to determine when the reaction is complete.

8.2.3 Accelerated Testing

Though it is often recommended, further investigation into the development of an improved short-duration testing method is needed. It is suggested that this begin with further study of the ACPT to determine the repeatability of the test on a larger scale. The number of aggregates and participating laboratories should also be expanded.

8.2.4 Mitigation

Having established that 25 percent Class F fly ash is effective as a blanket treatment for aggregates of varying reactivity, further research should be conducted to refine the mitigation levels necessary to limit reactivity while economizing the use of fly ash. This should be conducted by repeating MCPT and MAMBT tests with lower fly ash replacement levels. Testing using Class C fly ash, higher in CaO contents, could also be conducted to potentially expand the sources of effective fly ash. Most importantly, WYDOT should evaluate fly ash composition before use as a mitigating agent.

Bibliography

ACI Committee 221. (2008). *Report on Alkali-Aggregate Reactivity*. Farmington Hills: American Concrete Institute.

Aiqin, W., Chengzhi, Z., Mingshu, T., & Ningsheng, Z. (1999). "ASR in mortar bars containing silica glass in combination with high alkali and high fly ash contents." *Cement & Concrete Composites*, 375-381.

ASTM. (2001). Standard Test Method for Potential Alkali Reactivity of Aggregates, ASTM C1260. West Conshohocken.

ASTM. (2008). Standard Test Method for Determination of Length Change of Concrete Due to Alkali-Silica Reaction, ASTM C1293. West Conshohocken.

ASTM. (2008) Standard Test Method for Determination of Length Change of Concrete Due to Alkali-Silica Reaction, ASTM C1723. West Conshohocken.

ASTM. (2011). Standard Test Method for Determining the Potential Alkali-Silica Reactivity of Combinations of Cementitious Materials and Aggregate (Accelerated Mortar-Bar Method), ASTM C1567. West Conshohocken.

ASTM. (2012). Standard Specification for Coal Fly Ash and Raw or Calcined Natural Pozzolan for Use in Concrete, ASTM C618. West Conshohocken.

Berube, M.-A., Chouinard, D., Pigeon, M., Frenette, Boisvert, L., and Rivest, M. (2002). "Effectiveness of sealers in counteracting alkali-silica reaction in plain and air-entrained

laboratory concretes exposed to wetting and drying, freezing and thawing, and salt water." *NRC Research Press*.

Berube, M.A., Duchesne, J., and Chouinard, D. (1995). "Why the accelerated mortar bar test method ASTM C1260 is reliable for evaluating the effectiveness of supplementary cementing materials in suppressing expansion due to alkali-silica reactivity." *Cement, Concrete, and Aggregates*, 26-34.

Bleszynski, R., and Thomas, M. (1998). "Microstructural studies of alkali-silica reaction in fly ash concrete immersed in alkaline solutions." *Advanced Cement Based Materials*, 66-78.

Boddy, A. M., Hooton, R. D., and Thomas, M. D. (2000). "The effect of product form silica fume on its ability to control alkali-silica reaction." *Cement and Concrete Research*, 1139-1150.

Bournazel, J. P., and Moranville, M. (1997). "Durability of concrete: the crossroad between chemistry and mechanics." *Cement and Concrete Research*, 1543-1552.

Choktaweekarn, P., and Tangtermirikul, S. (2009). "A model for predicting the coefficient of thermal expansion of cementitious paste." *ScienceAsia*, 57-63.

Chrest, A. P. (1994). *Alkali-Aggregate Reactivity - A Summary.* PCI Committee on Durability.

Cornell, B. (2002). "Laboratory investigations of alkali silica reaction using the concrete prism test and its modifications." M.S. thesis, The University of Texas at Austin, Austin, TX.

Duchesne, J., and Berube, M.A. (2001). "Long-term effectiveness of supplementary cementing materials against alkali-silica reaction." *Cement and Concrete Research*, 1057-1063.

Fertig, R. J. (2010). Evaluation of ASR potential in Wyoming aggregates." M.S. thesis. University of Wyoming, Laramie, WY.

Fournier, B., Nkinamubanzi, P. C., Lu, Thomas, & Ideker. (2006). "Evaluating potential alkali-reactivity of concrete aggregates – How reliable are the current and new test methods?" IBRACON, Rio de Janeiro.

Fournier, B., Nkinamubanzi, P. C., and Chavrier, R. (2004). "Comparative field and laboratory investigations on the use of supplementary cementing materials to control alkali-silica reaction in concrete." ICON/CANMET, Ottawa.

Giannini, E. R., and Folliard, K. J. (2013). *A Rapid Test to Determine Alkali-Silica Reactivity of Aggregates Using Autoclaved Concrete Prisms*. Portland Cement Association.

Grattan-Bellew, P. (1997). "A Critical Review of Ultra-accelerated Tests for Alkali-Silica Reactivity." *Cement and Concrete Composites*, 403-414.

Hacker, D. P. (2014). "Evaluation of ASR potential in Wyoming aggregates and the stiffness damage test as a method for assessing expansion in ASR affected concrete." M.S. thesis, University of Wyoming, Laramie, WY.

Helmuth, R., Stark, D., Diamond, S., and Moranville-Regourd, M. (1993). *Alkali-Silica Reactivity: An Overview of Research.* Strategic Highway Research Program, Washington.

Hobbs, D. W. (1988). "Alkali-Silica Reaction in Concrete." *Technology & Engineering*.

Ichikawa. (2009). "Alkali-silica reaction, pessimum effects and pozzolanic effect." *Cement and Concrete Research*, 716-726.

Ideker, J., Drimalas, T., Bentivegna, A., Folliard, K., Fournier, B., and Thomas, M. (2012). “The Importance of Outdoor Exposure.” 14th ICAAR. Austin, TX.

Jones, A. (2011). “Evaluation of ASR potential in Wyoming aggregates and recycled concrete aggregate.” M.S. thesis, University of Wyoming, Laramie, WY.

Kosmatka, S. H., Kerkhoff, B., and Panarese, W. (2002). *Design and Control of Concrete Mixtures*. Portland Cement Association, Skokie, IL.

Lane, D. S. (1999). “Comparison of results for C 441 and C 1293 with implications of establishing criteria for ASR-resistant concrete.” *Cement, Concrete, and Aggregates*, 149-156.

Leeman, A., and Lothenbach, B. A. (2010). “Influence of superplasticizers on pore solution composition and on expansion of concrete due to alkali-silica reaction.” *Construction and Building Materials*.

Lu, D., Fournier, B., Grattan-Bellew, P. E., Xu, Z. and Tang, M. (2008). "Development of a universal accelerated test for alkali-silica and alkali-carbonate reactivity of concrete aggregates." *Materials and Structures,* 41(2).

Malvar, L. J., Cline, G. D., Burke, D. F., Rollings, R., Sherman, T., and Greene, J. L. (2002). “Alkali-Silica Reaction Mitigation: State of the Art and Recommendations.” *ACI Materials Journal*, 480-489.

Mindess, S., Young, J. F., and Darwin, D. (2003). *Concrete*. Upper Saddle River: Pearson Education, Inc.

Mo, X., Zhang, Y., Yu, C., Deng, M., Tang, M., Hunger, K. (2010). "Investigation of Alkali-Silica Reaction Inhibited by New Lithium Compound." *ACI Materials Journal*, 37-41.

Neville, A. (2012). *Properties of Concrete*. Prentice Hall.

Oberholster, R. E., and Davies, G. (1986). "An accelerated method for testing the potential alkali reactivity of siliceous aggregates." *Cement and Concrete Research*, 181-189.

Portland Cement Association. (2002). "Supplementary cementing materials for use in concrete." Portland Cement Association, Skokie, IL.

Pugh, J. S. (2003). "On the ability of accelerated test methods to assess potential for alkali-silica reaction." M.S. thesis. The University of Texas at Austin, Austin, TX.

Ramyar, K., Copuroglu, O., Andic, O., and Fraaij, A. (2004). "Comparison of alkali-silica reaction products of fly-ash- or lithium-salt-bearing mortar under long-term accelerated curing." *Cement and Concrete Research*, 1179-1183.

Rivard, P., Berube, M.-A., Ballivy, G., and Ollivier, J.-P. (2003). "Effect of drying-rewetting on the alkali concentration of the concrete pore solution." *Cement and Concrete Research*, 927-929.

Rivard, P., Berube, M.-A., Ollivier, J.-P., and Ballivy, G. (2003). "Alkali mass balance during the accelerated concrete prism test for alkali-aggregate reactivity." *Cement and Concrete Research*, 1147-1153.

Rothstein, D. (2011). *Petrographic investigation of test specimens from alkali-silica exposure tests using various Wyoming aggregate sources*. Boulder, Colorado.

Shafaatian, S. M., Akhavan, A., Maraghechi, H., and Rajabipour, F. (2013). "How does fly ash mitigate alkali-silica reaction (ASR) in accelerated mortar bar test (ASTM C1567)?" *Cement & Concrete Composites*, 143-153.

Shehata, M. H. (2000). "The effect of fly ash composition on the expansion of concrete due to alkali-silica reaction." *Cement and Concrete Research*, 1063-1072.

Shon, C.-S., Zollinger, D. G., and Sarkar, S. L. (2002). "Evaluation of modified ASTM C1260 accelerated mortar bar test for alkali-silica reactivity." *Cement and Concrete Research*, 1981-1987.

Stanton, T. E. (1940). "Expansion of concrete through reaction between cement and aggregate." *American Society of Civil Engineers Papers*, 1781-1810.

Swenson, E. G. (1958). "Cement-aggregate reaction in concrete of a Canadian bridge." *National Research Council Division of Building Research,* 1043-1056.

Thomas, M., Fournier, B., Folliard, K. J. (2012). "Selecting Measures to Prevent Deleterious Alkali-Silica Reaction in Concrete: Rationale for the AASHTO PP65 Prescriptive Approach." Federal Highway Administration, Springfield, VA.

Thomas, M. (2007). "Optimizing the Use of Fly Ash in Concrete." *Concrete*.

Thomas, M., Fournier, B., Folliard, K., Ideker, J., and Shehata, M. (2006). "Test methods for evaluating preventative measures for controlling expansion due to alkali-silica reaction in concrete." *Cement and Concrete Research*, 1842-1856.

Zhang, C., Wang, A., Tang, M., and Zhang, N. (1999). “Influence of dimension of test specimen on alkali-aggregate reactive expansion.” *ACI Materials Journal*, 204-207.

Appendix A: Classification Methods and Test Procedures

A.1 Large-Scale Field Exposure

Table 43. Other materials used in field specimens.

Specimen	*Water (lb)*	*NaOH (lb)*	*Air Ent. (lb)*	*Superplasticizer (lb)*	*Slump (in)*	*Air Content (%)*
BHC-1	57.5	0	0.2	2.2	3	4.5
BHC-2	57.5	0	0.2	2.32	5.5	6
BHC-3	53.1	0.68	0.15	2.8	7.5	4.1
BHP-1	61.25	0	0.25	0	5	7
BHP-2	58	0	0.25	0	6	6
BHP-3	56.5	0.68	0.16	2.18	6.5	4.2
DFP-1	57.5	0	0.25	0	3.5	5
DFP-2	58	0	0.25	0	4.5	7
DFP-3	57.5	0.68	0.24	2.74	4.5	5
GP-1	57.5	0	0.24	2.2	6.5	7.5
GP-2	53.4	0	0.2	2.2	4.5	4.5
GP-3	55.2	0.68	0.19	2.3	7	5.2
HPC-1	57.5	0	0.25	0	2.5	5
HPC-2	57.5	0	0.25	2.3	5.5	7
HPC-3	57.5	0.68	0.24	2.44	3.5	5
KR-1	57.5	0	0.2	2.26	7.5	6.6
KR-2	49	0	0.2	2.3	5	4.7
KR-3	55	0	0.25	2.1	3.5	5
KR-4	55	0.68	0.25	2.3	4	8
LBG-1	60.4	0	0.25	0	0.5	4
LBG-2	65	0	0.25	0	2	4
LBG-3	65	0.68	0.25	0	6	6
LX-1	57.5	0	0.25	3	6	8
LX-2	53.9	0	0.25	2.4	8.5	9
LX-3	57.5	0.68	0.24	2.47	7.5	7.4
WOR-1	63	0	0.25	0	5.5	4.5
WOR-2	60.2	0	0.25	0	5	6
WOR-3	57.5	0.68	0.15	2.3	5.5	5.8

BHC and BHP aggregates are collectively Black Rock (BR) aggregate.

A.1.1 Exposure Site

An outdoor exposure site, shown in Figure 66, was constructed on a bed of 101.6 mm (4 inch) minus rock to coarsely level the area and ensure proper drainage, and 19 mm (¾ inch) minus angular gravel was then placed on top of the rock for fine leveling. To date, a total of 28 field specimens have been transported to the site for outdoor exposure.

Figure 66. Outdoor exposure site.

Weather data has been logged daily from various weather stations at the University of Wyoming and the Laramie Airport to monitor temperature, relative humidity, and precipitation. This weather data may make future comparisons to other exposure site data more meaningful. Graphs of average daily maximum and minimum temperature, average daily relative humidity, and total monthly precipitation are shown in Figure 67, Figure 68, and Figure 69, respectively.

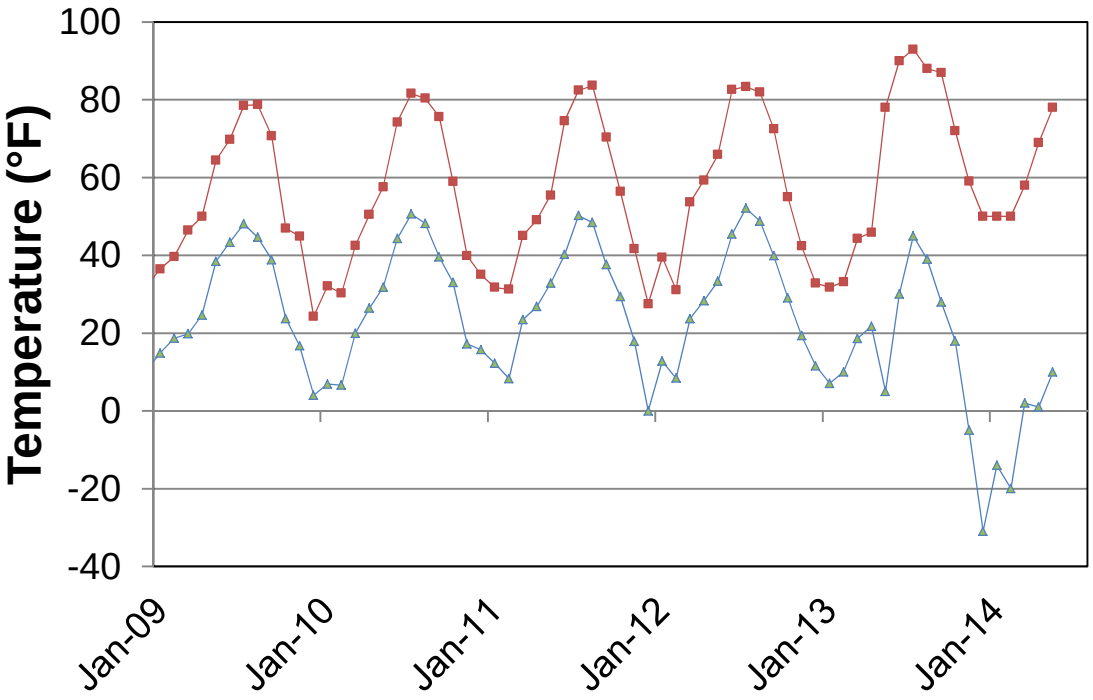

Figure 67. Average daily maximum and minimum temperatures in Laramie.

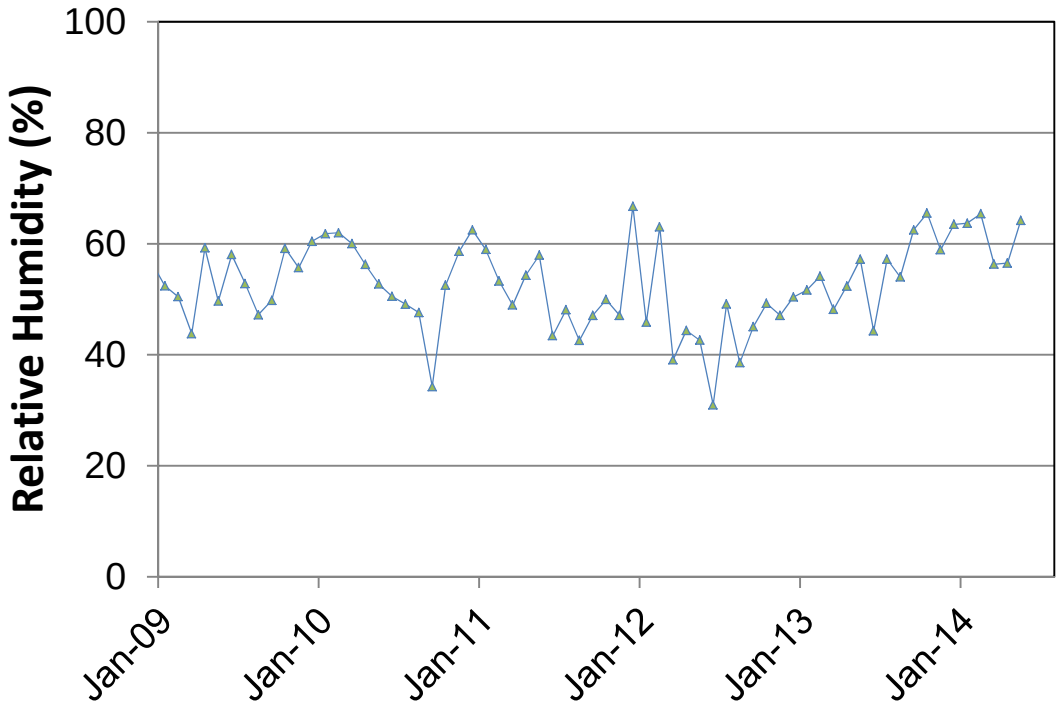

Figure 68. Average daily relative humidity in Laramie.

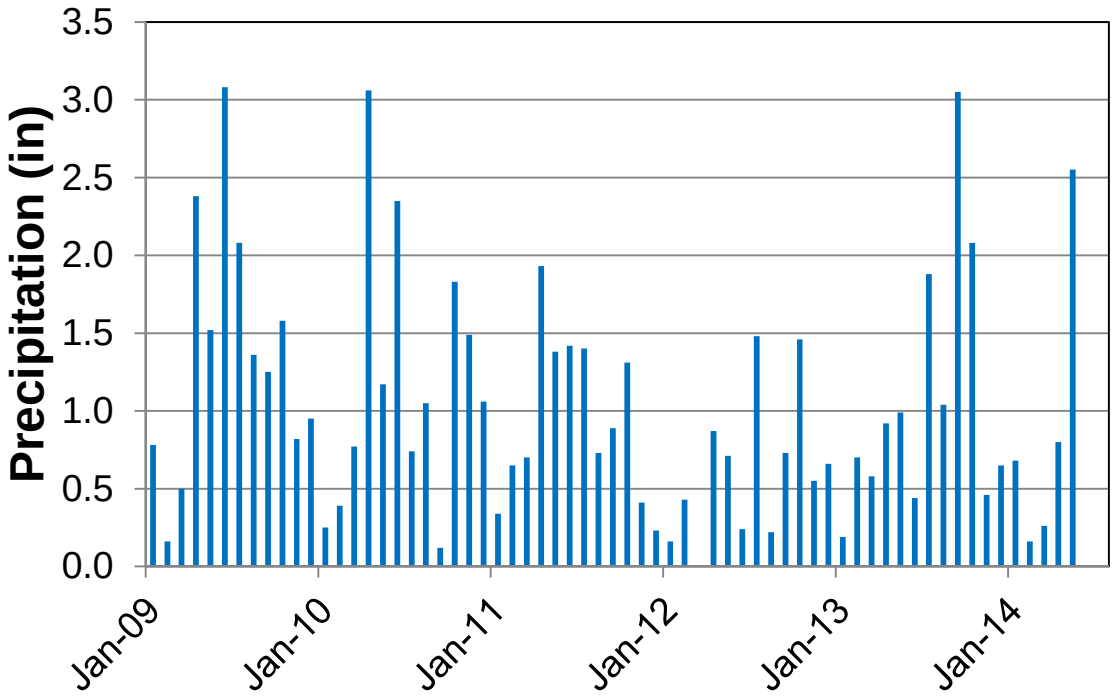

Figure 69. Total monthly precipitation in Laramie.

A.1.2 Casting

Forms for the 380 x 380 x 660 mm (15 x 15 x 26 inch) specimens were constructed using standard lumber and plywood. The bottom, sides, and ends were all constructed separately to be assembled at the time of casting which allowed for efficient construction and stripping of the forms. The inside corners and edges of the formwork were caulked to prevent moisture loss during curing, and a debonding agent was sprayed on the inside of the form. To secure the measurement studs into the concrete block, a threaded steel insert assembly was bolted to the inside of the form after the debonding agent was applied to ensure a good bond between the insert and the concrete. This assembly (Figure 70) consisted of the steel insert, a threaded rod, a wooden spacer, and a nut. The insert and the wooden spacer were placed on the inside of the

forms and the nut was placed on the outside as shown in Figure 71. Ten of these assemblies were installed in the forms: three on each side and two on each end.

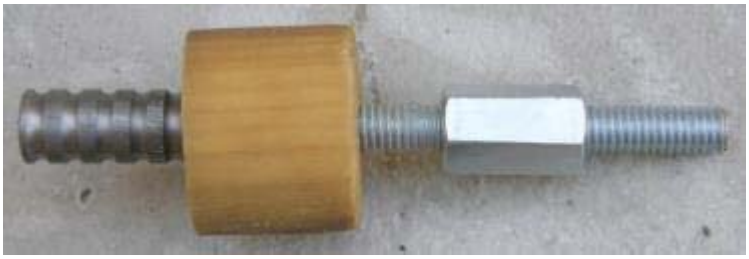

Figure 70. Threaded steel insert assembly.

a) b)

Figure 71. Insert assembly on a) the inside of the form and b) the outside of the form.

Before casting, all the required quantities of materials were measured and set aside. A gas powered concrete mixer was used to mix the concrete. The mixing procedure, shown below, was chosen.

1. Add half of the water to the mixer.
2. Add a small amount of fine aggregate and all of the coarse aggregate.
3. Start the mixer.
4. Add the cement, remaining fine aggregate, and remaining water steadily.
5. Mix for three minutes.

6. Stop the mixer for two minutes.
7. Mix for two minutes.

After measuring the slump according to ASTM C143 and measuring the air content using ASTM C231, the concrete was placed in the form in two layers. Each layer was consolidated using an internal concrete vibrator, paying special attention to ensure that the concrete was completely consolidated near the corners of the form and around the insert assemblies. When enough concrete had been placed in the form, the top was struck off flat and then finished with a magnesium float. An aluminum name plate, a steel lifting insert, and the top measurement pins (except for pins that were installed by drilling after the concrete cured) were installed in the concrete. The specimens were then covered with plastic to limit the moisture loss during curing. A field specimen after casting is shown in Figure 72 before measurement pins are installed and before the block is covered with plastic for curing.

Figure 72. Field specimen immediately after casting.

A.1.3 Measurement Stud Installation

To install the measurement studs on the top of the specimen, the merits of several different methods were analyzed. On the first group of blocks that were cast, holes were drilled in the top of the cured specimen and the measurement pins were installed with epoxy. A problem with this method was that it was difficult to drill the holes in the exact location that was needed and in a plane that was perpendicular to the surface of the block. In later specimens the top pins were cast into the wet concrete after measuring and marking out the appropriate locations for the studs. The setting out bar (Figure 73) included with the Demec mechanical strain gauge was used to confirm the accuracy of the measurement pin locations in the wet concrete. This method provided much better precision and ultimately made it easier to obtain reliable measurements.

Figure 73. Setting out bar.

To install the side measurement studs into the field specimens the studs were screwed into the threaded steel inserts that were cast into the block. The orientation of the stud was critical due to its effect on the location of the drilled offset hole. To control this orientation, a hex nut was screwed onto the stud before the stud was installed in the block. Once the stud was screwed into the threaded insert and the orientation of the offset hole was chosen, the hex nut was tightened against the block to lock the stud orientation in place. It was helpful to use a hollow socket when tightening the hex nut so the location of the offset hole could be monitored. An example of the installed measurement stud can be seen in Figure 74.

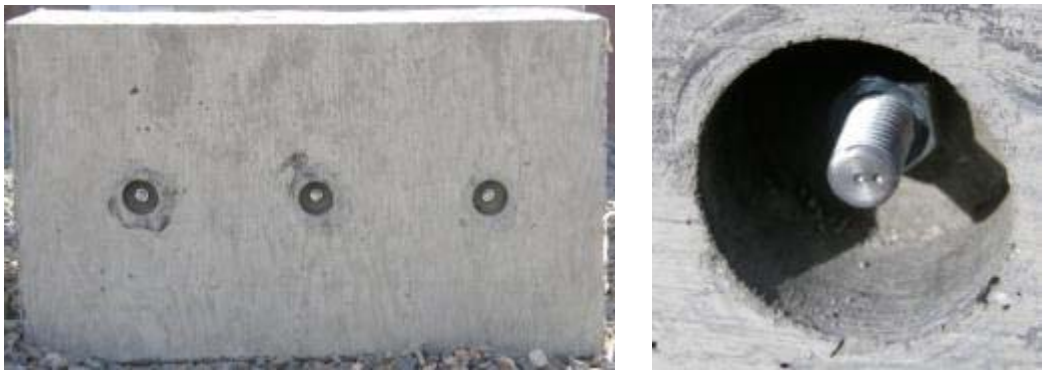

a) b)

Figure 74. Measurement studs - a) side view of field specimen and b) close up.

After the measurement studs were installed, pliable vinyl caps with pull tabs were placed over the studs to protect the measurement holes from corrosion. The pull tab made these caps easy to remove during measurement.

A.1.4 Labeling

Measurement studs were drilled with two holes to allow for variation in the field when locating the studs; one in the center and one offset approximately 2.5 mm (0.1 inch) using a milling machine. This allowed approximately 10.2 mm (0.4 inch) of tolerance, depending on the orientation of the measurement stud as shown in Figure 75.

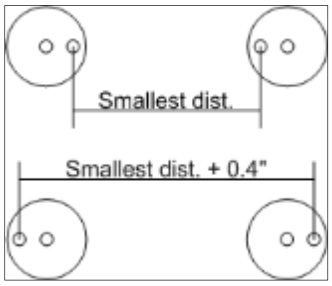

Figure 75. Tolerance gained from offset orientation.

Because of the offset hole, there are four possible measurements between any two pins. To document which measurement holes to use, a labeling method was developed using three letters. "M" stands for the middle hole, "O" refers to the outside hole, and "I" stands for the inside hole. A given measurement was described by a combination of two letters, which were written on the block in permanent marker as well as on the template for recording measurements. Due to the long-term exposure of the field specimens, marks written on the blocks have faded and disappeared. Figure 76 shows two example measurements using the labeling system where the left measurement is designated OM and the right measurement is designated IM.

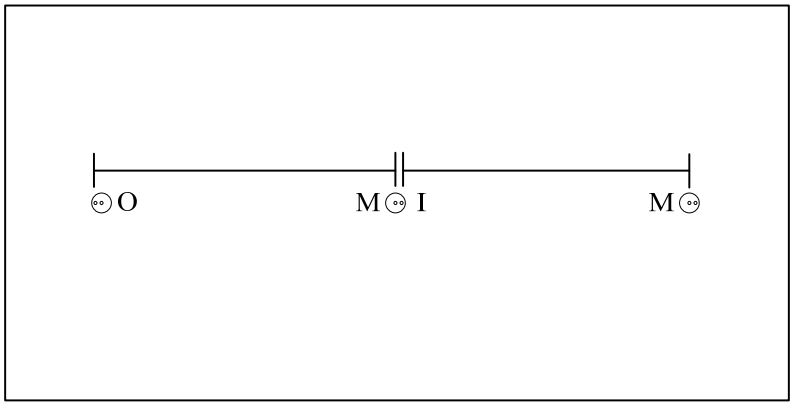

Figure 76. Using labeling system to measure side of block.

It was also important that the pivot point and fixed point of the measurement instrument were located in the same position for each respective measurement. For this reason, the orientation of the instrument was specified on the measurement recording sheet by the vertical line and an indicator arrow shown in Figure 77. The vertical line indicates placement of the pivot point of the strain instrument, and the arrow points toward the fixed point of the instrument.

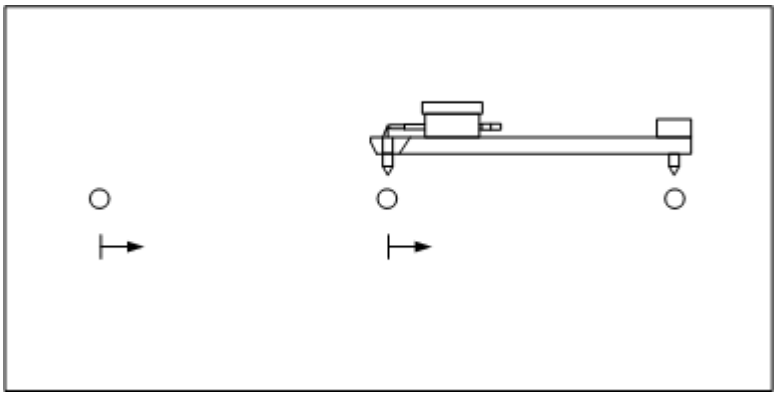

Figure 77. Orientation of strain gauge instrument based on indicator arrow.

A.2 Concrete Prism Test (CPT) – ASTM C1293

Table 44. Batch quantities for all aggregates used in CPT.

Aggregate Name	CA (lb)	FA (lb)
Black Rock	51.89	28.84
Devries Farm	51.28	28.11
Goton Pit	52.54	28.93
Harris Pit	51.58	29.53
Knife River	52.43	30.97
Labarge	52.48	29.57
Lamax	51.87	27.82
Worland	52.58	27.77

Table 45. Average compressive strength of concrete used in Fertig 2010 CPT.

Aggregate Name	Compressive Strength MPa (psi)	COV
Black Rock	28.9 (4193)	19.4%
Devries Farm	31.6 (4581)	4.0%
Goton Pit	29.1 (4214)	9.7%
Harris Pit	27.5 (3987)	8.6%
Knife River	30.8 (4465)	21.3%
Labarge	26.5 (3840)	10.8%
Lamax	32.1 (4653)	9.4%
Worland	26.5 (3840)	4.6%

Table 46. Average compressive strength of concrete used in Kimble CPT.

Aggregate Name	Compressive Strength MPa (psi)	COV
Black Rock	26.3 (3820)	17.4%

Table 47. Concrete mixture properties for all aggregates in Fertig 2010 CPT.

Aggregate Name	Slump (in)	Air (%)	Yield (ft^3)	Theoretical Yield (ft^3)
Black Rock	1	1.00%	0.751	0.758
Devries Farm	2	-0.44%	0.740	0.758
Goton Pit	1.5	-0.30%	0.741	0.758
Harris Pit	1.5	1.10%	0.752	0.758
Knife River	1.25	0.66%	0.748	0.758
Labarge	1.5	1.11%	0.751	0.758
Lamax	1	-0.09%	0.743	0.758
Worland	1.5	-0.01%	0.743	0.758

Table 48. Concrete mixture properties for all aggregates in Kimble CPT.

Aggregate Name	Slump (in)	Air (%)	Yield (ft^3)	Theoretical Yield (ft^3)
Black Rock	1.5	-	0.751	0.758

A.3 Autoclaved Concrete Prism Test (ACPT)

Table 49. Batch quantities for all aggregates used in ACPT.

Aggregate Name	Fraction Tested	CA kg (lb)	FA kg (lb)
Black Rock	Coarse	18.5 (40.7)	10.8 (23.7)
	Fine	18.6 (41.1)	10.3 (22.7)
Devries Farm	Coarse	18.8 (41.4)	9.8 (21.7)
	Fine	18.6 (41.1)	10.4 (23.0)
Goton Pit	Coarse	18.7 (41.2)	10.6 (23.3)
	Fine	18.7 (41.2)	10.5 (23.2)
Harris Pit	Coarse	18.4 (40.5)	10.9 (24.1)
	Fine	18.6 (41.1)	10.4 (22.9)
Knife River UW	Coarse	18.6 (41.1)	11.2 (24.8)
	Fine	18.6 (41.1)	10.6 (23.4)
Labarge	Coarse	18.7 (41.2)	10.8 (23.9)
	Fine	19.2 (42.4)	9.9 (21.9)
Lamax	Coarse	18.5 (40.7)	10.4 (22.9)
	Fine	19.2 (42.4)	9.8 (21.6)
Worland UW	Coarse	19.3 (42.5)	10.1 (22.2)
	Fine	18.6 (41.1)	10.4 (22.9)

Table 50. Average compressive strength of concrete used in ACPT 133 degree Celsius.

Aggregate Name	Fraction Tested	Tested Compressive Strength MPa (psi)	COV	Failure Ratio
Black Rock	Coarse	19.1 (2762)	2.1 %	0.92
	Fine	12.9 (1874) **	9.9%	3.37
Goton Pit	Coarse	18.6 (2690) *	-	1.08
	Fine	22.2 (3218)	2.3%	3.50
Harris Pit	Fine	16.2 (2354)	1.0%	1.11
	Fine	17.3 (2515)	3.7%	2.39
Knife River UW	Coarse	16.4 (2375) *	-	0.75
	Coarse	14.9 (2158) *	-	0.85
	Fine	15.5 (2246)	9.1%	1.93

** Two cylinders were tested. * One cylinder was tested.

Table 51. Average compressive strength of concrete used in ACPT 130 degree Celsius.

Aggregate Name	Fraction Tested	Tested Compressive Strength MPa (psi)	COV	Failure Ratio
Black Rock	Coarse	19.6 (2836)**	0.8%	0.78
	Fine	21.9 (3179)	1.1%	3.81
Goton Pit	Coarse	14.7 (2133)	NA	1.13
	Coarse	14.9 (2156)	16.0%	1.26
	Fine	26.3 (3817)	3.3%	2.16
	Fine	18.5 (2682)	2.9%	3.41
Harris Pit	Coarse	14.7 (2127)	6.0%	0.83
	Fine	18.7 (2716)	3.6%	2.33
Knife River UW	Coarse	22.8 (3307)	2.6%	0.79
	Fine	17.0 (2458)	0.8%	2.48

** Two cylinders were tested.

Appendix B: Mitigation Test Methods and Procedures

B.1 Mitigated Concrete Prism Test (MCPT) – ASTM C1293

Table 52. Batch quantities for all aggregates used in MCPT.

Aggregate Name	CA kg (lb)	FA kg (lb)
Black Rock	23.5 (51.9)	10.7 (23.5)
Goton Pit	23.8 (52.5)	10.6 (23.4)
Knife River	23.8 (52.4)	11.6 (25.5)
Labarge	23.8 (52.5)	10.9 (24.1)
Lamax	23.5 (51.9)	10.2 (22.4)
Worland	23.9 (52.6)	7.9 (17.4)

Table 53. Average compressive strength of concrete used in MCPT.

Aggregate Name	Tested Compressive Strength MPa (psi)	COV
Black Rock	23.1 (3344)	20.8%
	26.3 (3820)	17.4%
Goton Pit	23.1 (3357)	17.4%
Knife River	32.0 (4641)	7.5%
Labarge	26.6 (3857)	2.7%
	25.4 (3682)	7.4%
Lamax	25.7 (3728)	3.8%
Worland	21.5 (3121)**	11.4%

Four specimens tested unless otherwise noted.
** Two cylinders were tested.

Appendix C: Materials and Equipment

September 25, 2008

Jennifer Tanner
University of Wyoming
1000 E. University Ave.
Laramie, WY 82070
RE: WAL # 08803

ANALYTICAL REPORT
Three cement samples were analyzed for total alkalies per ASTM C114.

SAMPLE ID	Na2O	K2O	Total as Na20
#1	.21	.76	.71
#2	.19	.76	.69
#3	.22	.76	.72

Figure 78. 2008 Holcim cement analysis. (Data sheet reproduced for clarity.)

July 8, 2013

Jennifer Tanner
University of Wyoming
1000 E. University Ave.
Laramie, WY 82070
WAL #130650-1
Sample ID: Holcim 2013 Cement
P.O.#

CHEMICAL ANALYSIS
Wt%, as Rec'd Basis

Silicon Dioxide	SiO_2	20.09	
Aluminum Oxide	Al_2O_3	4.68	
Iron Oxide	Fe_2O_3	3.34	
Calcium Oxide	CaO	62.10	
Magnesium Oxide	MgO	1.42	
Sodium Oxide	Na_2O	0.14	
Potassium Oxide	K_2O	0.87	
Total Alkalies as Na_2O			0.71
Titanium Dioxide	TiO_2	0.20	
Manganic Oxide	Mn_2O_3	0.26	
Phosphorus Pentoxide	P_2O_5	0.19	
Strontium Oxide	SrO	0.22	
Barium Oxide	BaO	0.05	
Sulfur Trioxide	SO_3	3.70	
Loss on Ignition		2.76	
Total		100.00	
Insoluble Reside		0.32	
Tricalcium Silicate	C_3S	53.35	
Tricalcium Aluminate	C_3A	6.75	
Dicalcium Silicate	C_2S	17.35	
Tetracalcium Aluminoferrite	C_4AF	10.17	

*TiO_2 and P_2O_3 not included in Al_2O_2
*No correction has been made for the possible use of limestone.
Analysis per ASTM C 114

Figure 79. 2013 Holcim cement analysis. (Data sheet reproduced for clarity.)

June 05, 2012

Jennifer Tanner
University of Wyoming – Civil and Architectural Engineering
1000 E. University Ave.
Dept. 3295
Laramie, WY 820712000

Denver Division #: 120517-1
Sample ID: Craig Fly Ash
P.O.#

CHEMICAL ANALYSIS
WT%, DRY BASIS

Silicon Dioxide, SiO_2	54.40	
Aluminum Oxide, Al_2O_3	23.48	
Iron Oxide, Fe_2O_3	4.28	
Total ($SiO_2 + AL_20_3 + Fe_2O_3$)		82.16
Calcium Oxide, CaO	9.67	
Magnesium Oxide, MgO	2.15	
Sodium Oxide, Na_2O	0.70	
Potassium Oxide, K_2O	1.09	
Titanium Dioxide, TiO_2	0.85	.71
Manganese Dioxide, MnO_2	0.05	
Phosphorus Pentoxide, P_2O_5	1.24	
Strontium Oxide, SrO	0.29	
Barium Oxide, BaO	0.51	
Sulfur Trioxide, SO_3	0.40	
Loss on Ignition (750°C)	0.89	
Total	100.00	
Moisture (105°C), as Received	0.05	

Analysis per ASTM C 311

Figure 80. Fly ash analysis. (Data sheet reproduced for clarity.)

Appendix D: Classification Test Results

D.1 Field Exposure Test Results

Individual field exposure expansion results are included by aggregate source.

D.1.1 Black Rock

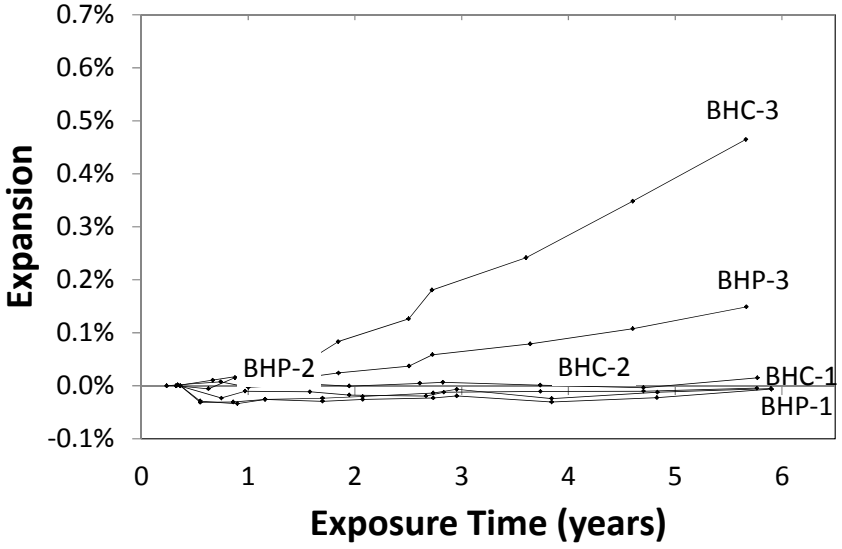

Figure 81. Field exposure results for Black Rock.

D.1.2 Devries Farm

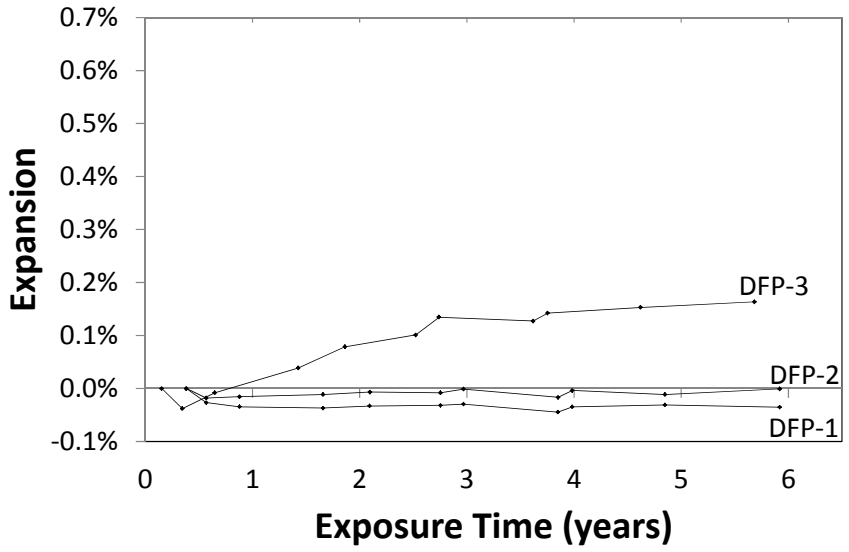

Figure 82. Field exposure results for Devries Farm.

D.1.3 Goton Pit

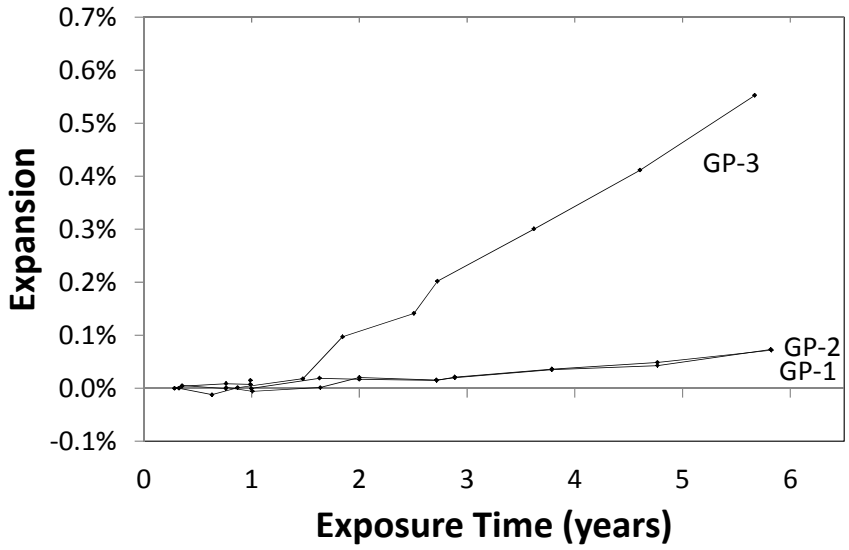

Figure 83. Field exposure results for Goton Pit.

D.1.4 Harris Pit

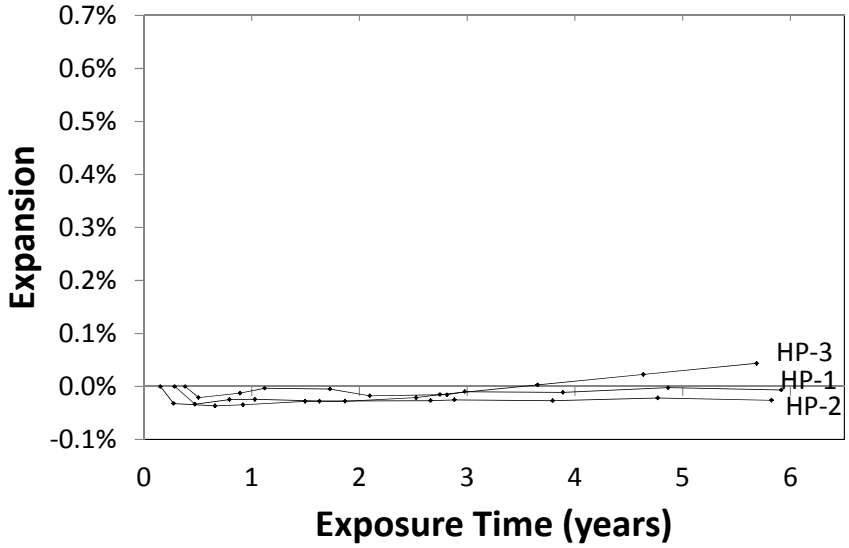

Figure 84. Field exposure results for Harris Pit.

D.1.5 Knife River

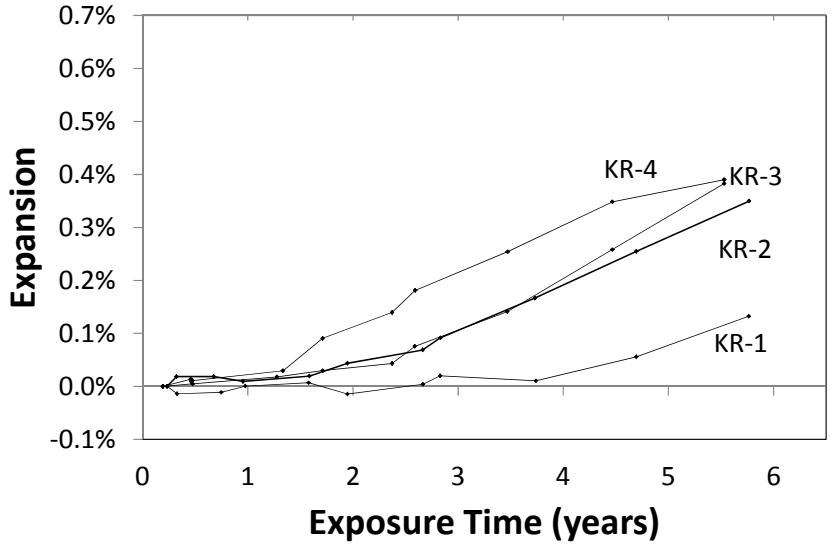

Figure 85. Field exposure results for Knife River.

D.1.6 Labarge

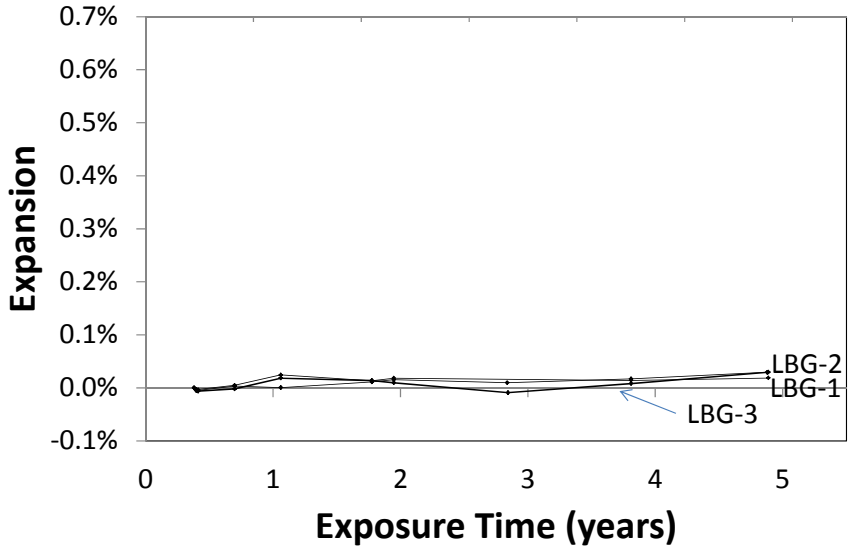

Figure 86. Field exposure results for Labarge.

D.1.7 Lamax

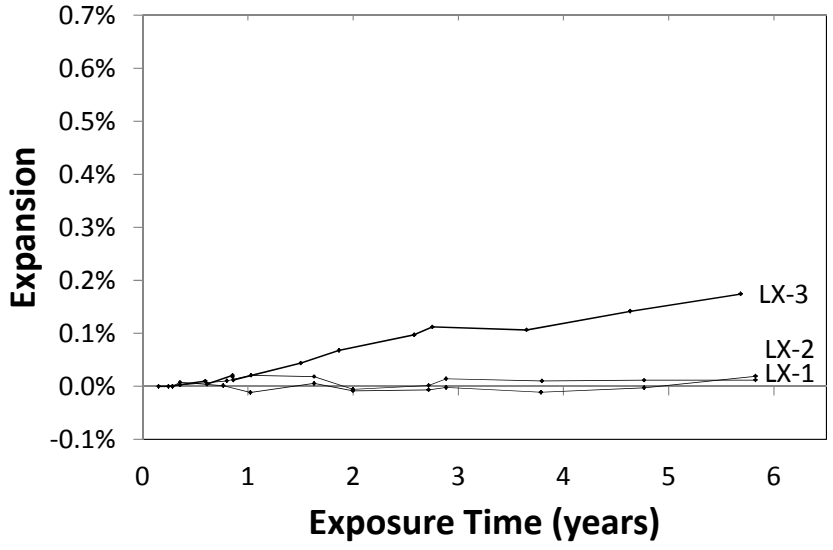

Figure 87. Field exposure results for Lamax.

D.1.8 Worland

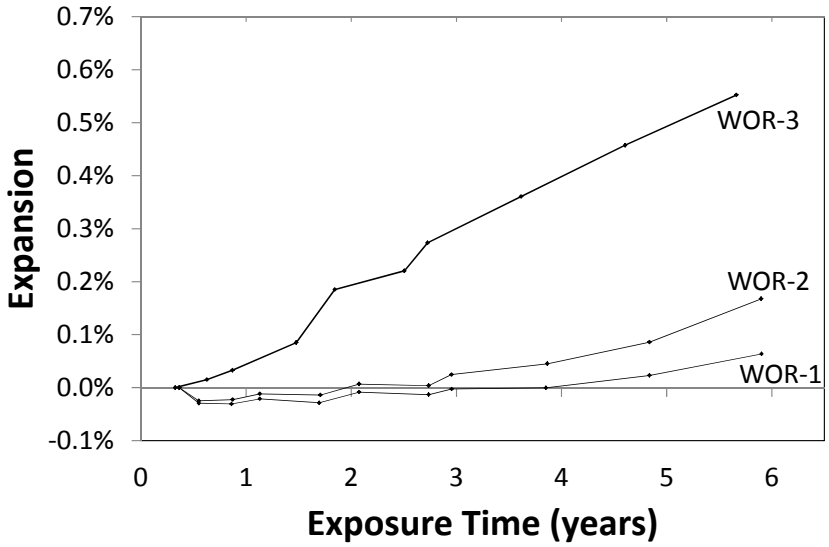

Figure 88. Field exposure results for Worland.

D.2 AMBT Results

Table 54. ASTM C1260 test results.

Pit	Average Expansion (%)	Failure Ratio	Classification
BR	Coarse: 0.500	MR: 5.00 HR: 1.67 VHR: 1.11	Very Highly Reactive
	Fine: 0.638	MR: 6.38 HR: 2.13 VHR: 1.42	Very Highly Reactive
	Mixed: 0.607	MR: 6.07 HR: 2.02 VHR: 1.35	Very Highly Reactive
DFP	Coarse: 0.768	MR: 7.68 HR: 2.56 VHR: 1.71	Very Highly Reactive
	Fine: 0.821	MR: 8.21 HR: 2.74 VHR: 1.82	Very Highly Reactive
	Mixed: 0.864	MR: 8.64 HR: 2.88 VHR: 1.92	Very Highly Reactive
GP	Coarse: 0.535	MR: 5.35 HR: 1.78 VHR: 1.19	Very Highly Reactive
	Fine: 0.492	MR: 4.92 HR: 1.64 VHR: 1.09	Very Highly Reactive
	Mixed: 0.558	MR: 5.58 HR: 1.86 VHR: 1.24	Very Highly Reactive
HP	Coarse: 0.280	MR: 2.80 HR: 0.93 VHR: 0.63	Moderately Reactive

HP	Fine: 0.359	MR: 3.59 HR: 1.20 VHR: 0.80	Highly Reactive
	Mixed: 0.279	MR: 2.79 HR: 0.93 VHR: 0.62	Moderately Reactive
KR	Coarse: 0.224	MR: 2.24 HR: 0.75 VHR: 0.50	Moderately Reactive
	Fine: 0.240	MR: 2.40 HR: 0.80 VHR: 0.53	Moderately Reactive
	Mixed: 0.255	MR: 2.55 HR: 0.85 VHR: 0.57	Moderately Reactive
LBG	Coarse: 0.170	MR: 1.70 HR: 0.57 VHR: 0.38	Moderately Reactive
	Fine: 0.198	MR: 1.98 HR: 0.66 VHR: 0.44	Moderately Reactive
	Mixed: 0.230	MR: 2.30 HR: 0.77 VHR: 0.51	Moderately Reactive
LX	Coarse: 0.620	MR: 6.20 HR: 2.07 VHR: 1.38	Very Highly Reactive
	Fine: 0.572	MR: 5.72 HR: 1.91 VHR: 1.27	Very Highly Reactive
	Mixed: 0.583	MR: 5.83 HR: 1.94 VHR: 1.30	Very Highly Reactive
WOR	Coarse: 0.691	MR: 6.91 HR: 2.30 VHR: 1.53	Very Highly Reactive
	Fine: 0.545	MR: 5.45 HR: 1.82 VHR: 1.21	Very Highly Reactive
	Mixed: 0.764	MR: 7.64 HR: 2.55 VHR: 1.70	Very Highly Reactive

D.3 ACPT Results

Table 55. ACPT test results.

Coarse Agg.	Fine Agg.	Testing School	Autoclave Temp °C	Specimen Percent Expansion 1	2	3	4	Average Expansion	Std Dev	COV	Failure Ratio (R)	Interlab Std Dev
BR	BK	UA	133 (271.4)	0.110%	0.106%	0.112%	-	0.11%	0.00%	2.79%	1.37	0.0196%
BR	BK	UW	133 (271.4)	0.074%	0.072%	0.079%	0.068%	0.07%	0.00%	0.04922	0.92	
BR	BK	UW	130 (266)	0.066%	0.058%	0.061%	0.063%	0.06%	0.00%	6.52%	0.78	NA
BK	BR	UA	133 (271.4)	0.368%	0.363%	0.354%	-	0.36%	0.01%	1.96%	4.52	0.0395%
BK	BR	UW	133 (271.4)	0.268%	0.285%	0.267%	0.259%	0.27%	0.01%	3.75%	3.37	
BK	BR	UW	130 (266)	0.302%	0.323%	0.305%	0.289%	0.30%	0.01%	3.73%	3.81	NA
GP	BK	UA	133 (271.4)	0.121%	0.126%	0.133%	-	0.13%	0.01%	4.76%	1.58	0.0213%
GP	BK	UA	133 (271.4)	0.124%	0.110%	0.137%	-	0.12%	0.01%	10.92%	1.55	
GP	BK	UW	133 (271.4)	0.082%	0.084%	0.089%	0.091%	0.09%	0.00%	4.17%	1.08	
GP	BK	UW	130 (266)	0.091%	0.093%	0.086%	-	0.09%	0.00%	4.01%	1.13	NA
GP	BK	UW	130 (266)	0.105%	0.095%	0.100%	0.104%	0.10%	0.00%	4.50%	1.26	NA
BK	GP	UA	133 (271.4)	0.360%	0.380%	0.359%	-	0.37%	0.01%	3.23%	4.58	0.0704%
BK	GP	UW	133 (271.4)	0.280%	0.293%	0.282%	0.264%	0.28%	0.01%	2.50%	3.50	
BK	GP	UW	130 (266)	0.137%	0.180%	0.168%	0.205%	0.17%	0.02%	12.86%	2.16	NA
BK	GP	UW	130 (266)	0.281%	0.280%	0.268%	0.263%	0.27%	0.01%	3.26%	3.41	NA
HP	BK	UA	133 (271.4)	0.066%	0.063%	0.065%	-	0.06%	0.00%	2.36%	0.81	0.01%
HP	BK	UW	133 (271.4)	0.051%	-	-	-	0.05%	-	-	0.64	
HP	BK	UW	130 (266)	0.066%	0.067%	0.067%	-	0.07%	0.00%	0.87%	0.83	NA
BK	HP	UA	133 (271.4)	0.268%	0.282%	0.281%	-	0.28%	0.01%	2.82%	3.46	0.0462%
BK	HP	UW	130 (266)	0.177%	0.201%	0.186%	0.180%	0.19%	0.01%	5.74%	2.33	NA
KR UW	BK	UA	133 (271.4)	0.106%	0.067%	0.078%	-	0.08%	0.02%	24.03%	1.05	0.0141%
KR UW	BK	UW	133 (271.4)	0.064%	0.056%	-	-	0.06%	0.01%	9.43%	0.75	
KR UW	BK	UW	133 (271.4)	0.068%	0.066%	0.070%	0.069%	0.07%	0.00%	2.50%	0.85	
KR UW	BK	UW	130 (266)	0.068%	0.066%	0.055%	0.064%	0.06%	0.01%	11.07%	0.79	NA
BK	KR UW	UA	133 (271.4)	0.320%	0.350%	0.338%	-	0.34%	0.02%	4.49%	1.68	0.0978%
BK	KR UW	UW	133 (271.4)	0.148%	0.163%	0.150%	0.155%	0.15%	0.01%	5.29%	0.77	

D.2 Petrography Observations

This appendix section contains the observations and conclusions of the petrographic analysis performed by DRP Consulting Inc. in September 2013. The petrography was conducted on six Wyoming aggregates cored from field specimens.

D.2.1 Black Rock

Aggregate Description

The coarse aggregate is a crushed river gravel with a 19 mm (¾ in.) nominal top size. The aggregate is siliceous in composition and consists primarily of igneous rocks with minor amounts of metamorphic and sedimentary rocks. The rock types consists of, in approximate order of decreasing abundance, rhyolite, andesite, quartzite, limestone, minor amounts of various intermediate volcanic rocks and rare fragments of vesicular basalt and granitic to dioritic rocks. The fine aggregate is a natural river sand composed of rock types similar to those observed in the coarse aggregate, suggesting they are derived from a common geologic source.

8.2.4.1.1 Observations Relevant to ASR

No evidence of ASR was observed in the core. No deposits of gel were observed and no microcracks associated with reactive aggregates were observed. No significant reaction rims were observed and no internal microcracking of coarse or fine aggregate particles was observed. After the exposure test exudations were observed at eight (8) distinct sites on the polished surface. SEM/EDS analysis confirmed the gel composition was consistent with ASR. The gel exudation that was observed after the elevated T/RH exposure test is shown in Figure 89 and 90.

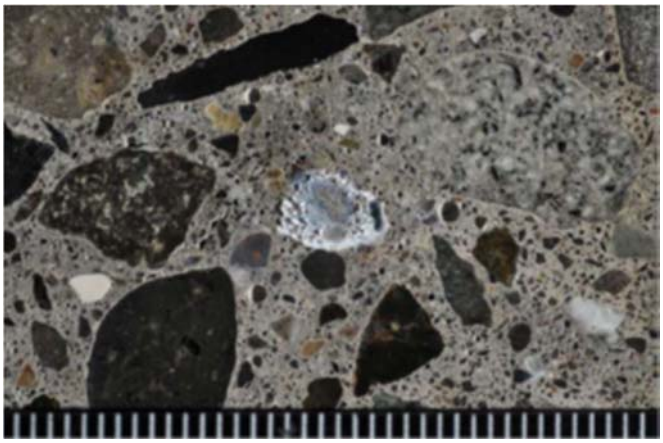

Figure 89. Photograph of the polished surface of Black Rock core.

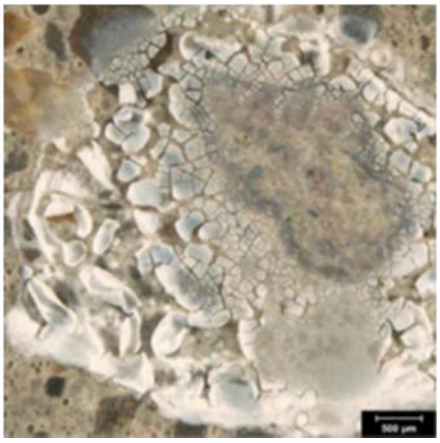

Figure 90. Reflected light photomicrograph of the polished surface of Black Rock core.

D.2.2 Goton Pit

Aggregate Description

The coarse aggregate is a crushed river gravel with a 19 mm (¾ in.) nominal top size. The gradation is somewhat uneven with few particles sitting on the 12.5-19 mm (½-¾ in.) sieves. The aggregate consists of a mixture of siliceous rocks that are mostly igneous but metamorphic and sedimentary rocks are present as a minor component. The rock types include, in approximate

order of decreasing abundance, rhyolite, granite, quartzite, andesite and occasional particles of chert, which appear to replace limestones. The fine aggregate is a natural river sand that consists primarily of siliceous volcanic rocks and granitic rocks similar to those in the coarse aggregate, indicating derivation from a common geologic source.

Observations Relevant to ASR

Evidence of negligible ASR was observed in the core, based on reaction rims observed commonly on particles of rhyolite, andesite, chert and quartzite. No deposits of gel were observed and no microcracks associated with reactive aggregates were observed. After the exposure test exudations were observed at thirty-six (36) distinct sites on the polished surface. SEM/EDS analysis confirmed the gel composition was consistent with ASR. The gel exudation that was observed after the elevated T/RH exposure test is shown in Figure 91 and 92.

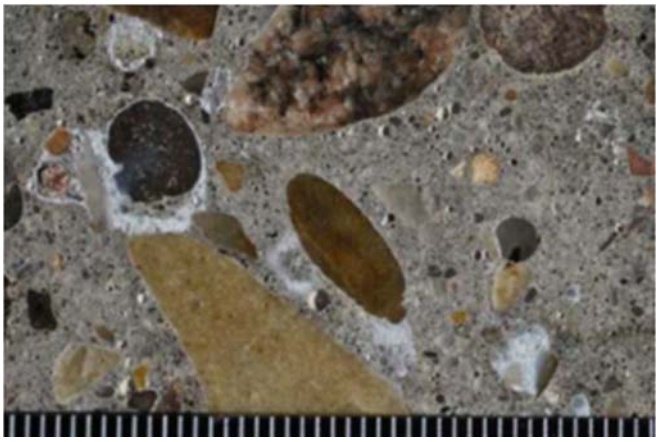

Figure 91. Photograph of the polished surface of Goton Pit core.

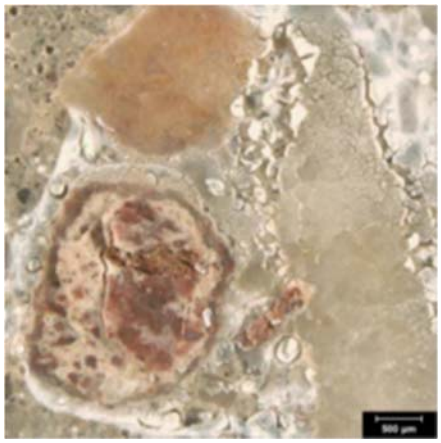

Figure 92. Reflected light photomicrograph of the polished surface of Goton Pit core.

D.2.3 Knife River

Aggregate Description

The coarse aggregate is a crushed river gravel with a 19 mm (¾ in.) nominal top size that shows minor gap grading but even distribution. The aggregate consists of a mixture of siliceous igneous rocks that consist primarily of granitic rocks with minor amounts of rhyolite. Occasional granite particles show well-developed foliations defined by aligned biotite and occasional particles show evidence of hydrothermal alteration and retrograde metamorphism. The sand is a natural river sand that consists of a blend of siliceous igneous rocks similar to those observed in the coarse aggregate, indicating derivation from a common geologic source.

Observations Relevant to ASR

Evidence of negligible ASR was observed in the core, based on reaction rims observed commonly on particles of rhyolite in the coarse and fine aggregate. No deposits of gel were observed and no microcracks associated with reactive aggregates were observed. After the exposure test exudations were observed at sixteen (16) distinct sites on the polished surface.

SEM/EDS analysis confirmed the gel composition was consistent with ASR. The gel exudation that was observed after the elevated T/RH exposure test is shown in Figure 93 and 94.

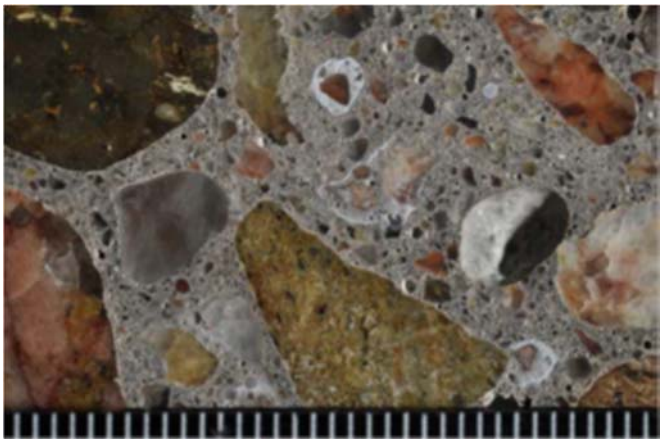

Figure 93. Photograph of the polished surface of Knife River core.

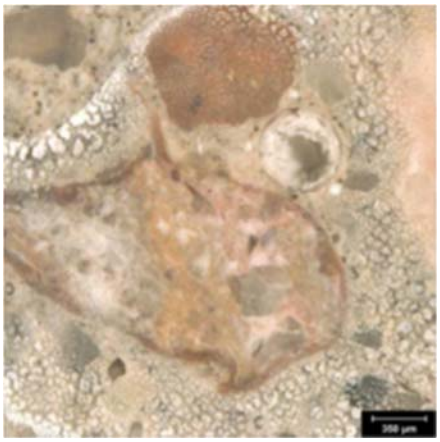

Figure 94. Reflected light photomicrograph of the polished surface of Knife River core.

D.2.4 Labarge Pit

Aggregate Description

The coarse aggregate is a crushed river gravel with a 19 mm (¾ in.) nominal top size but most particles are 12.5 mm (½ in.) or smaller and the core has a fairly high sand content. The

aggregate is siliceous and consists of a mixture of granitic rocks and quartzite. The granitic rocks range widely in color and texture whereas most of the quartzites are arenitic. Minor components present in the aggregate include basalt, diabase, and rhyolite. The sand is a natural river sand that consists of granitic rocks and quartzite with minor amounts of siliceous volcanic rocks.

Observations Relevant to ASR

Evidence of negligible ASR was observed in the core, based on reaction rims observed commonly on particles of quartzite in the coarse aggregate and particles of siliceous volcanic rocks and rare granite particles in the fine aggregate. No deposits of gel were observed and no microcracks associated with reactive aggregates were observed. After the exposure test exudations were observed at thirty three (33) distinct sites on the polished surface. SEM/EDS analysis confirmed the gel composition was consistent with ASR. The gel exudation that was observed after the elevated T/RH exposure test is shown in Figure 95 and 96.

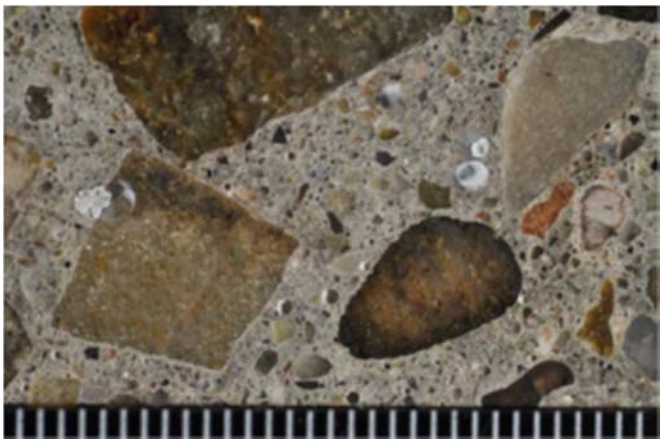

Figure 95. Photograph of the polished surface of Labarge core.

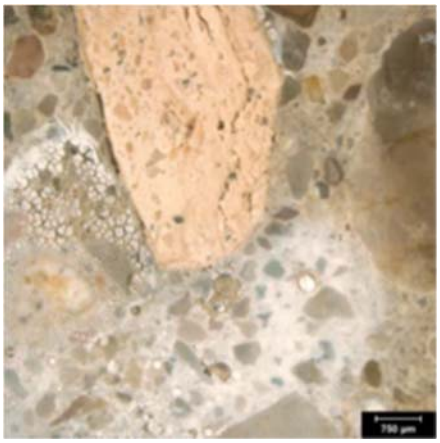

Figure 96. Reflected light photomicrograph of the polished surface of Labarge core.

D.2.5 Lamax Pit

Aggregate Description

The coarse aggregate is a crushed river gravel with 19 mm (¾ in.) nominal top size. The gradation is even with tight particle packing. The coarse aggregate is siliceous and consists primarily of igneous rocks that are plutonic and volcanic as well as metasedimentary and sedimentary rocks. The rock types include, in approximate order of decreasing abundance, rhyolite, andesite, quartzite, granite, limestone and dioritic rocks. The fine aggregate is a natural river sand that consists of rocks that are similar to those observed in the coarse aggregate, indicating derivation from a common geologic source.

Observations Relevant to ASR

Evidence of negligible ASR was observed in the core, based on reaction rims observed occasionally on particles of siliceous volcanic rocks in the fine aggregate. No deposits of gel were observed and no microcracks associated with reactive aggregates were observed. After the exposure test exudations were observed at thirty-five (35) distinct sites on the polished surface.

SEM/EDS analysis confirmed the gel composition was consistent with ASR. A black gel rimmed a mortar fragment; the SEM/EDX analysis of this material is consistent with ASR gel but the silicon peak is lower than observed in other exudations. The gel exudation that was observed after the elevated T/RH exposure test is shown in Figure 97 and 98.

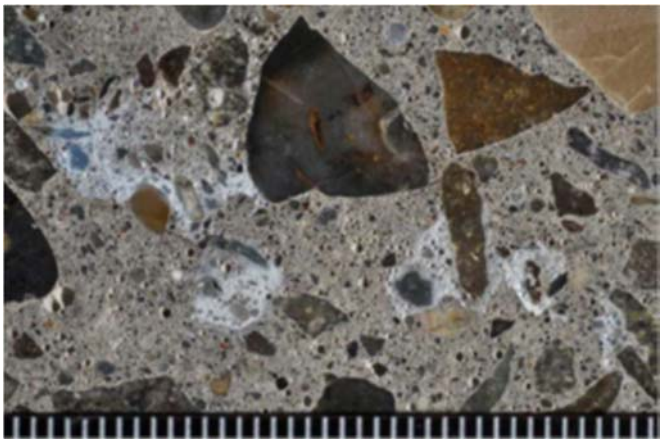

Figure 97. Photograph of the polished surface of Lamax core.

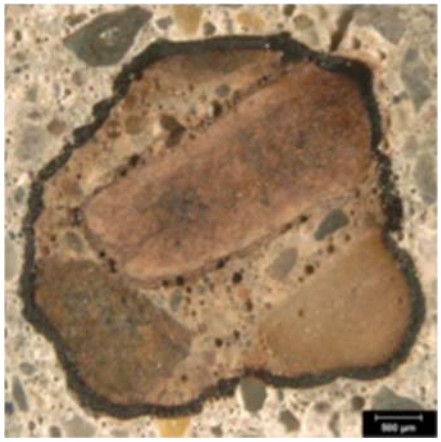

Figure 98. Reflected light photomicrograph of the polished surface of Lamax core.

D.2.6 Worland

Aggregate Description

The coarse aggregate is a crushed river gravel with 19 mm (¾ in.) nominal top size. The gradation is somewhat uneven with high sand content. The coarse aggregate is siliceous and consists primarily of siliceous igneous and metasedimentary rocks and minor carbonate sedimentary rocks. The rock types include, in approximate order of decreasing abundance, rhyolite, quartzite andesite, granite, and limestone. The fine aggregate is a natural river sand that consists of rocks that are similar to those observed in the coarse aggregate, indicating derivation from a common geologic source.

Observations Relevant to ASR

Evidence of negligible ASR was observed in the core, based on reaction rims observed on particles of rhyolite and quartzite in the coarse aggregate and on particles of siliceous volcanic rocks in the fine aggregate. No deposits of gel were observed and no microcracks associated with reactive aggregates were observed. After the exposure test exudations were observed at nineteen (19) distinct sites on the polished surface. SEM/EDS analysis confirmed the gel composition was consistent with ASR. The gel exudation that was observed after the elevated T/RH exposure test is shown in Figure 99 and 100.

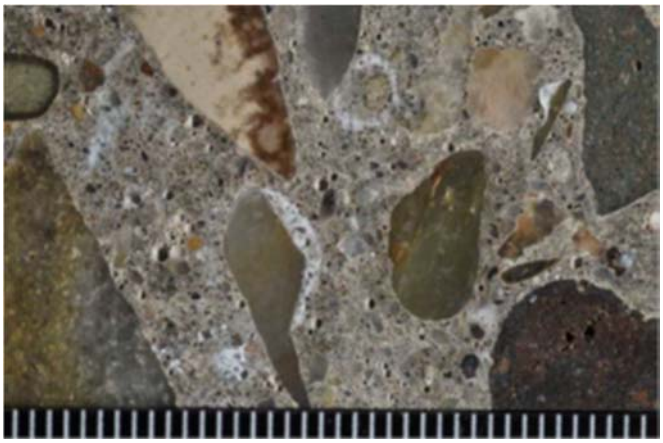

Figure 99. Photograph of the polished surface of Worland core.

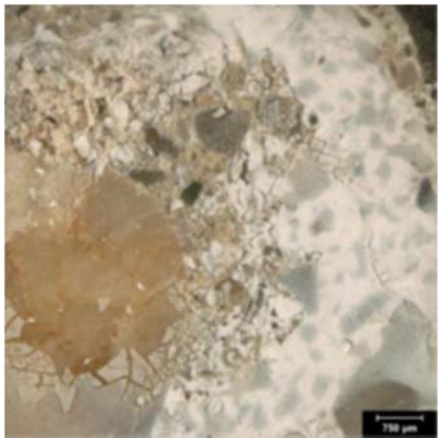

Figure 100. Reflected light photomicrograph of the polished surface of Worland core.

D.2.6 Summary of petrographic study

Table 56 summarizes the results of the present investigation.

Table 56. Summary of Results.

Aggregate	Rating	Exudation Sites
BR	None	8
GP	Negligible	36
KR	Negligible	16
LBG	Negligible	33
LAX	Negligible	35
WOR	Negligible	19

These findings indicate that the concrete represented by the cores shows no evidence of significant ASR after several years of exposure to Laramie, Wyoming field conditions. The only evidence of ASR that was observed from standard optical petrographic examination of the cores involved the presence of reaction rims on various aggregate particles. No deposits of gel, microcracks associated with reactive aggregates, or other evidence of ASR was observed in any core after the optical petrographic examination. However, after the polished slabs from the cores were exposed to elevated T/RH conditions, each of them produced exudations of ASR gel. This indicates that ASR is present in the cores, but has not progressed to a point where microcracking and gel deposits have formed in microcracks or voids.

Appendix E: Regression Analysis

Regression Analysis: Autoclave Coarse versus AMBT Coarse

Analysis of Variance

Source	DF	Adj. SS	Adj. MS	F-Value	F-Value
Regression	1	11.933	11.9335	28.88	0.000
AMBT Coarse	1	11.933	11.9335	28.88	0.000
Error	9	3.719	0.4132		
Total	10	15.652			

Model Summary

S	R-sq	R-sq(adj)	R-sq(pred)
.642806	74.24%	73.60%	73.65%

Coefficients

Term	Coef	SE Coef	T-Value	P-Value	VIF
AMBT Coarse	0.2530	0.0471	5.37	0.000	1.00

Regression Equation

Autoclave Coarse = 0.2530 AMBT Coarse

Fits and Diagnostics for Unusual Observations

Obs	Autoclave Coarse	Fit	Resid	Std Resid	
5	1.875	2.226	-0.351	-0.71	X

X Unusual X

Figure 101. Regression Analysis for Autoclave failure ratios versus AMBT failure ratios for coarse aggregate.

Regression Analysis: Autoclave Fine versus AMBT Fine

Analysis of Variance

Source	DF	Adj. SS	Adj. MS	F-Value	F-Value
Regression	1	82.860	82.86	43.27	0.001
AMBT Fine	1	82.860	82.860	43.27	0.001
Error	5	9.575	1.915		
Total	6	92.434			

Model Summary

S	R-sq	R-sq(adj)	R-sq(pred)
1.38381	89.64%	87.57%	80.82%

Coefficients

Term	Coef	SE Coef	T-Value	P-Value	VIF
AMBT Fine	0.787	0.120	6.58	0.001	1.00

Regression Equation

Autoclave Fine = 0.787 AMBT Fine

Fits and Diagnostics for Unusual Observations

Figure 102. Regression Analysis for Autoclave failure ratios versus AMBT failure ratios for fine aggregate.

Regression Analysis: Autoclave Coarse versus CPT Coarse

Analysis of Variance

Source	DF	Adj. SS	Adj. MS	F-Value	F-Value
Regression	1	12.478	12.4777	35.37	0.000
CPT Coarse	1	12.478	12.4777	35.37	0.000
Error	9	3.175	0.3527		
Total	10	15.652			

Model Summary

S	R-sq	R-sq(adj)	R-sq(pred)
0.593909	79.72%	77.46%	75.01%

Coefficients

Term	Coef	SE Coef	T-Value	P-Value	VIF
CPT Coarse	0.3018	0.0507	5.95	0.000	1.00

Regression Equation

Autoclave Coarse = 0.3018 CPT Coarse

Fits and Diagnostics for Unusual Observations

Obs	Autoclave Coarse	Fit	Resid	Std Resid	
10	1.563	2.113	-0.550	-1.16	X

X Unusual X

Figure 103. Regression Analysis for Autoclave failure ratios versus CPT failure ratios for coarse aggregate.

Regression Analysis: Autoclave Coarse versus CPT Fine

Analysis of Variance

Source	DF	Adj. SS	Adj. MS	F-Value	F-Value
Regression	1	78.10	78.100	27.24	0.003
CPT Fine	1	78.10	78.100	27.24	0.003
Error	5	14.33	2.867		
Total	6	92.43			

Model Summary

S	R-sq	R-sq(adj)	R-sq(pred)
1.69317	84.49%	81.39%	80.53%

Coefficients

Term	Coef	SE Coef	T-Value	P-Value	VIF
CPT Fine	0.621	0.119	5.22	0.003	1.00

Regression Equation

Autoclave Fine = 0.621 CPT Fine

Fits and Diagnostics for Unusual Observations

Obs	Autoclave Coarse	Fit	Resid	Std Resid	
5	7.130	7.610	-0.480	-0.56	X

X Unusual X

Figure 104. Regression Analysis for Autoclave failure ratios versus CPT failure ratios for fine aggregate.

Appendix F: Mitigation Test Results

F.1 MAMBT Test Results

Table 57. MAMBT results for individual test specimens.

		Expansion							Average
		Specimen			Batch	Pit	Standard	COV	Failure
Pit	Casting	1	2	3	Average	Average	Deviation		Ratio
BR	1	0.037%	0.040%	0.029%	0.035%	0.039%	0.0093%	23.8%	0.39
	2	0.056%	0.033%	0.039%	0.043%				
DFP	1	0.134%	0.092%	0.089%	0.105%	0.095%	0.0196%	20.6%	0.95
	2	0.091%	0.088%	0.078%	0.086%				
GP	1	0.043%	0.038%	0.046%	0.042%	0.039%	0.0046%	11.9%	0.39
	2	0.038%	0.035%	0.034%	0.036%				
HP	1	0.020%	0.024%	0.024%	0.023%	0.024%	0.0023%	9.5%	0.24
	2	0.027%	0.024%	0.023%	0.025%				
KR	1	0.031%	0.027%	0.032%	0.030%	0.029%	0.0032%	10.9%	0.29
	2	0.029%	0.032%	0.024%	0.028%				
KR-UW	1	0.033%	0.035%	0.030%	0.033%	0.033%	0.0038%	11.7%	0.33
	2	0.037%	0.040%	0.036%	0.038%				
	3	0.034%	0.034%	0.027%	0.032%				
	4	0.030%	0.031%	0.028%	0.030%				
LBG	1	0.007%	0.003%	0.004%	0.005%	0.004%	0.0016%	38.4%	0.04
	2	0.005%	0.003%	0.003%	0.004%				
LM	1	0.091%	0.091%	0.088%	0.090%	0.083%	0.0096%	11.5%	0.83
	2	0.084%	0.079%	0.066%	0.076%				
WOR	1	0.032%	0.036%	0.041%	0.036%	0.042%	0.0083%	19.9%	0.42
	2	0.045%	0.054%	0.053%	0.051%				
	3	0.052%	0.041%	0.034%	0.042%				
	4	0.043%	0.039%	0.029%	0.037%				
WOR-UW	1	0.027%	0.028%	0.028%	0.028%	0.031%	0.0047%	15.3%	0.31
	2	0.039%	0.033%	0.028%	0.033%				

F.1.1 Black Rock

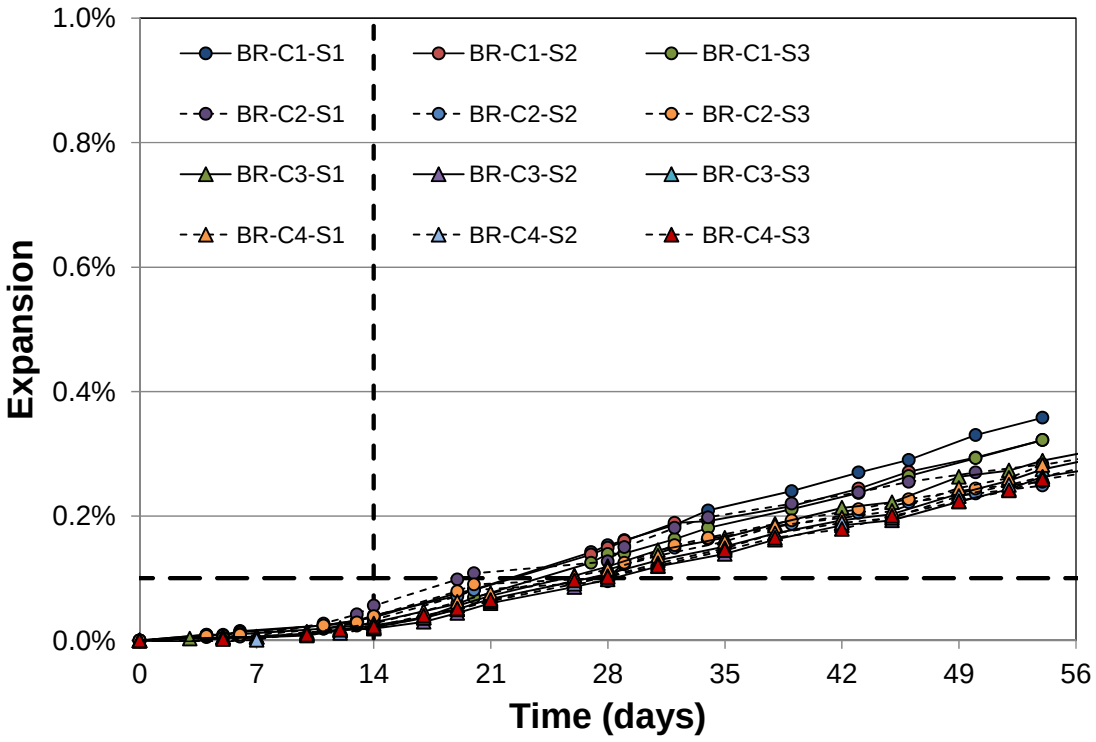

Figure 105. Individual MAMBT specimen results for Black Rock.

F.1.2 Devries Farm

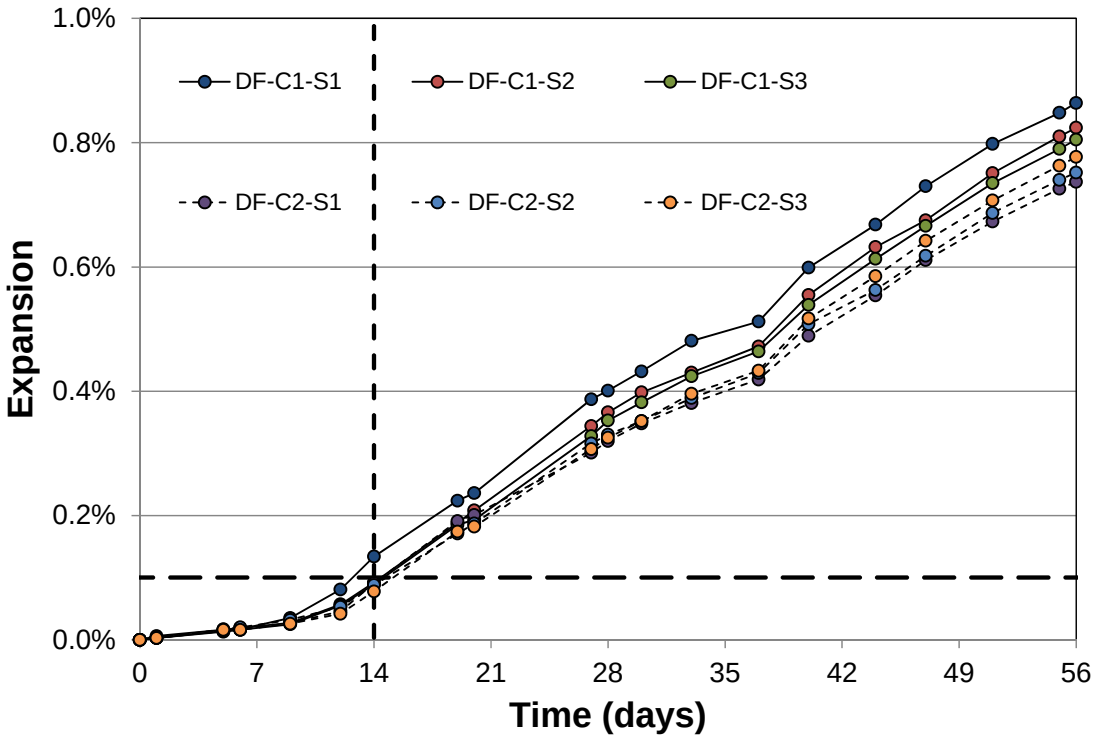

Figure 106. Individual MAMBT specimen results for Devries Farm.

F.1.3 Goton Pit

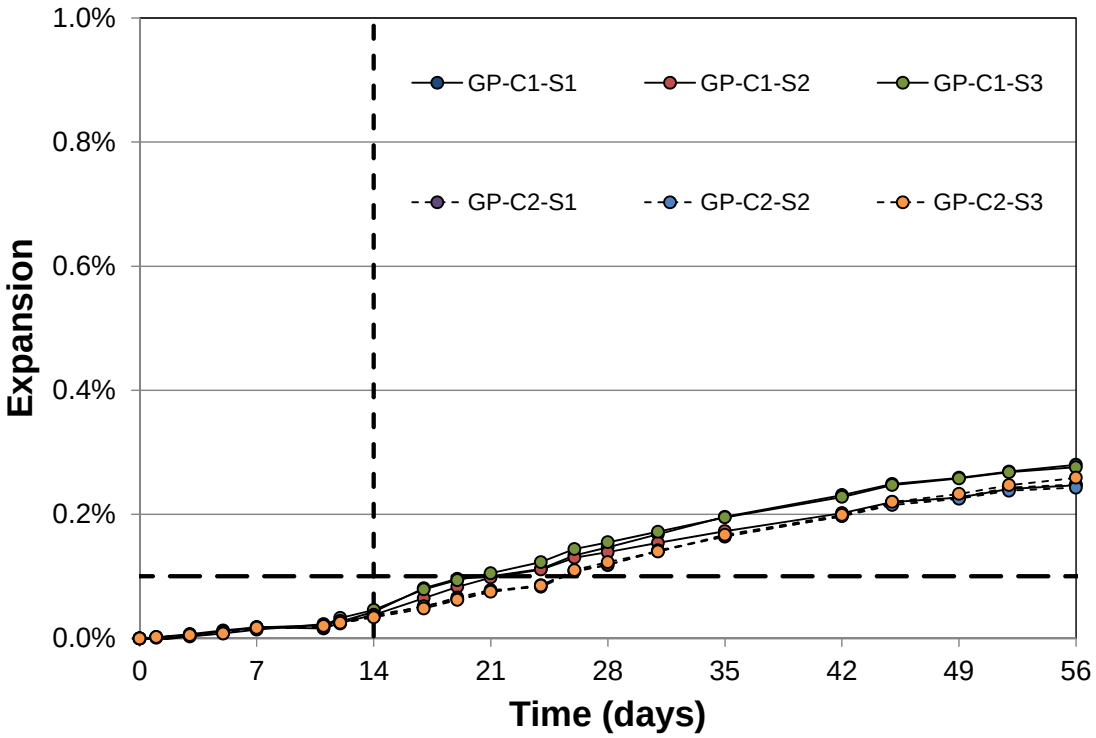

Figure 107. Individual MAMBT specimen results for Goton Pit.

F.1.4 Harris Pit

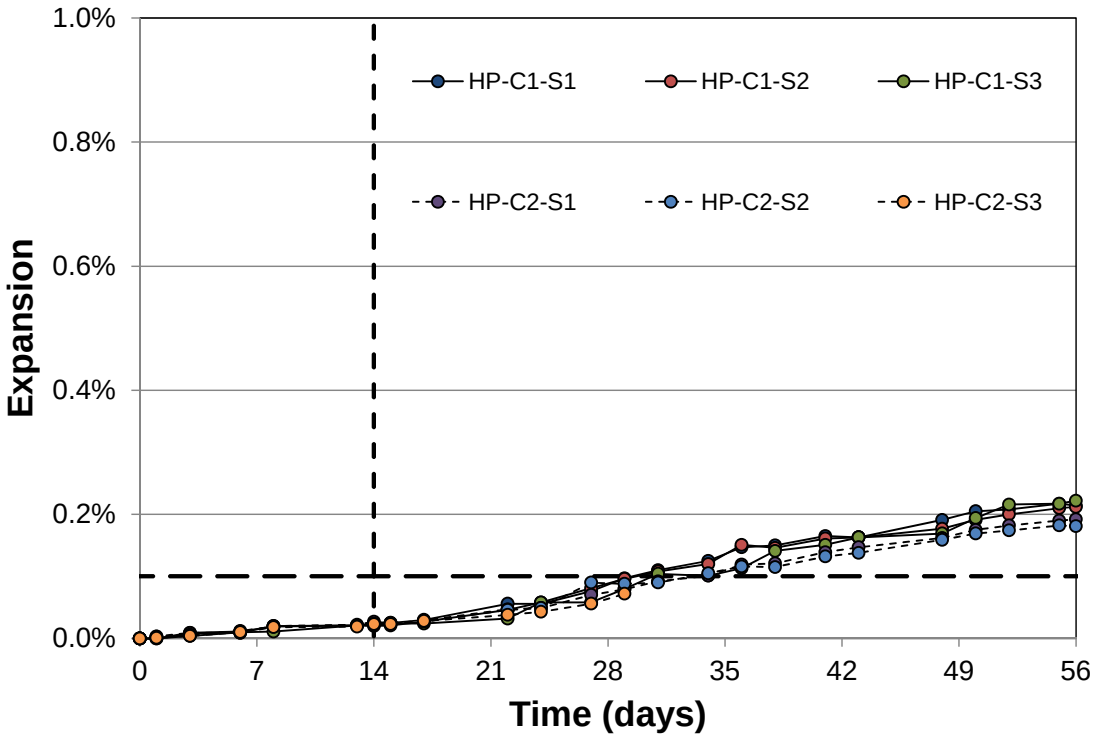

Figure 108. Individual MAMBT specimen results for Harris Pit.

F.1.5 Knife River

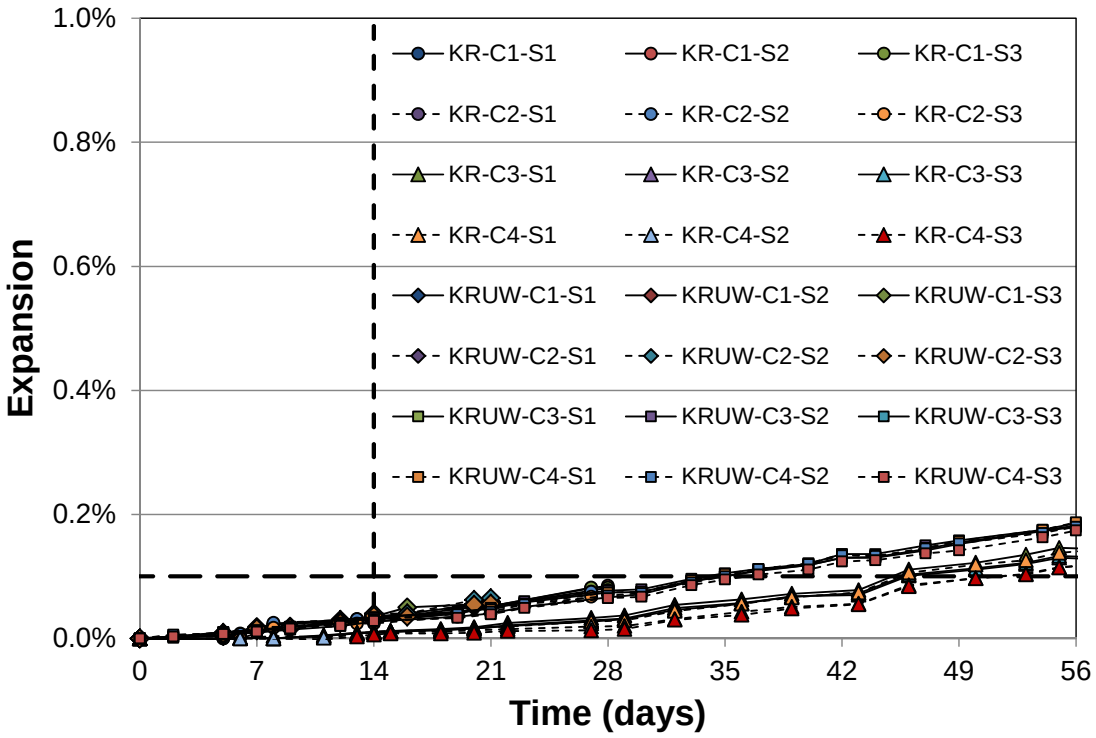

Figure 109. Individual MAMBT specimen results for Knife River.

F.1.6 Labarge

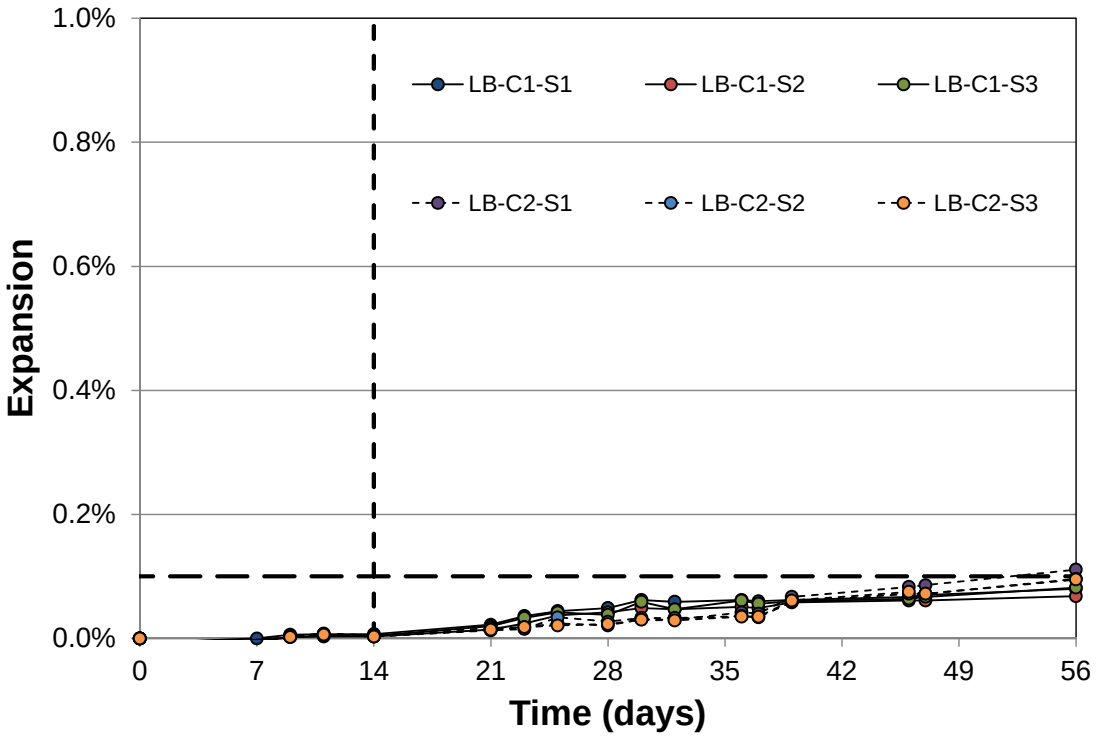

Figure 110. Individual MAMBT specimen results for Labarge.

F.1.7 Lamax

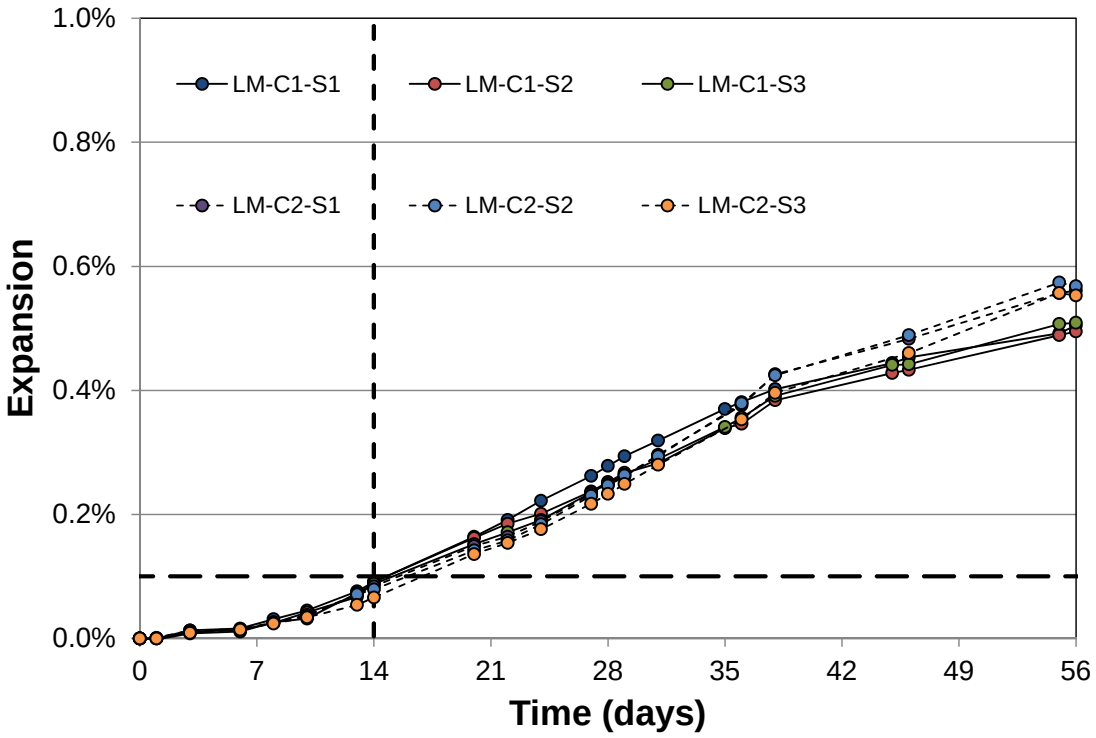

Figure 111. Individual MAMBT specimen results for Lamax.

F.1.8 Worland

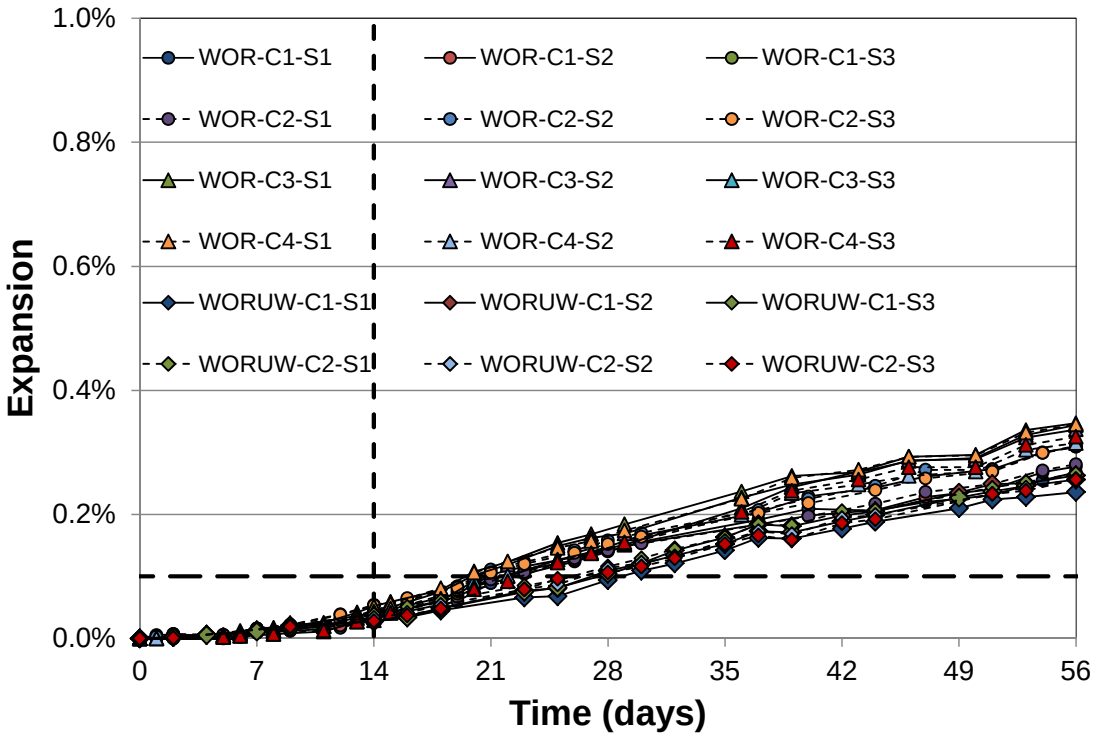

Figure 112. Individual MAMBT specimen results for Worland.